12-2022

Multiple Objective Function Optimization and Trade Space Analysis

Yifan Xu
yxu5@clemson.edu

MULTIPLE OBJECTIVE FUNCTION OPTIMIZATION AND TRADE SPACE ANALYSIS

A Thesis
Presented to
the Graduate School of
Clemson University

In Partial Fulfillment
of the Requirements for the Degree
Master of Science
Mechanical Engineering

---

by
Yifan Xu
December 2022

Accepted by:
Dr. John R. Wagner, Committee Chair
Dr. Cameron Turner
Dr. Todd Schweisinger

ABSTRACT

Optimization can assist in obtaining the best possible solution to a design problem by varying related variables under given constraints. It can be applied in many practical applications, including engineering, during the design process. The design time can be further reduced by the application of automated optimization methods. Since the required resource and desired benefit can be translated to a function of variables, optimization can be viewed as the process of finding the variable values to reach the function maxima or minima. A Multiple Objective Optimization (MOO) problem is when there is more than one desired function that needs to be minimized concurrently. In MOO, Pareto Solutions are defined as the set of solutions that are not worse than any single solution of all objective functions simultaneously. In other words, MOO is a process of applying algorithms to find Pareto solutions to a certain problem. Using Tradespace analysis, we can further identify the optimal Pareto Solution with the highest utility at a fixed cost. The combination of MOO and tradespace analysis can evaluate hundreds of designs simultaneously to select the optimal one.

Mechanical system design is the process of devising a procedure to accomplish the given task, for which a design engineer's role is to optimize resource consumption. With recent advancements in multi-functional systems, the complexity of machines has been increasing. This presents a great challenge for design engineers, who must contend with optimizing systems with several functions in tandem. It is thus essential to develop methods that can simplify the design process. Tower clocks, as a classical type of machine, were extensively used for public time display during the period when watches and home clocks

were rare. These mechanical movements once played essential roles in society and industry. They could be found at churches, courthouses, and universities/schools to visually and auditorily record the passage of time for residents and students. They were also used to regulate railroad schedules and workforce hours for the emerging industrial sector. Although mainly used for decorative purposes today, the components of such movement, including the assembled gears, escapement, and pendulum with weight drive, provide insight into optimization and tradespace analysis problems.

In this research, computational methods plus experimental observations were used to investigate the optimal designs of the E. Howard Clock Model 00 - a movement was manufactured by E. Howard Clock Company. First, A computer-aided-design (CAD) model of this movement was created using the SolidWorks® software package to illustrate the working principle of the pendulum clock and facilitate engineering optimization studies. Next, the mathematical model of this clock was developed and simulated to explore the operation behaviors and conversion of potential-to-kinetic energy. The experimental process to validate this model was also described in detail. After that, A Single Objective Optimization (SOO) algorithm (i.e., simulated annealing) was applied to the model to optimize the pendulum subsystem for accuracy, quality factor, and mass. Numerical results show the desired quality factor can be achieved by varying the pendulum length and bob radius/thickness. Compared to the original, the optimized design added 15% to the mass of the pendulum while maintaining the clock's accuracy. Tradeoffs between quality factor, pendulum properties, and period were investigated and discussed with representative experimental and computational results. Lastly, two Multiple Objective Optimization

(MOO) approaches (i.e., Multi-objective Genetic Algorithm (MOGA-II) and Multi-objective Simulated Annealing (MOSA) were applied to the developed mathematic model. The optimal movement designs in terms of pendulum mass and time accuracy were further explored for a range of clock periods. Numerical results demonstrated a 0.7% increase in the quality factor and a 0.56% reduction in the mass while maintaining the designed period by modifying the above-mentioned pendulum's parameters. More importantly, these changes can provide material cost savings in a mass production scenario. Overall, this study highlighted the optimization design engineers have considered for decades which can now be visualized using computer tools for greater insight. This methodology has the potential to be applied in the designing of other complex systems as well.

ACKNOWLEDGMENTS

I would like to thank my advisor, Dr. John Wagner, for his guidance, patience, and sincere interest in my research. I would like to acknowledge Mr. David Moline for sharing his experiences with the pendulum clock and MATLAB Skills. I also thank Dr. Cameron Turner and Dr. Todd Schweisinger serving as my committee member. Last but not least, I would like to thank my group colleague Zaker Syed.

TABLE OF CONTENTS

Page

LIST OF TABLES

LIST OF FIGURES

List of Figures (Continued)

List of Figures (Continued)

Figure Page

List of Figures (Continued)

Figure Page

NOMENCLATURE LIST

A	Surface area of the bob (m^2)
a_i/b_i	Fit Parameters in tradespace analysis
B	Damping coefficient of pendulum (N/rad/s)
B_{E2}	Viscous damping coefficient of escape wheel (N/rad/s)
C_D	Drag coefficient
C_{ir}	Bob shape iron price for (€/kg)
C_o	Pendulum shape oak price (€/m)
D_{ij}	Diameter as gear j^{th} on arbor i^{th} (m)
E	Elite set in MOGA-II
E_i	Quantized energy in MOSA (J)
E_{loss}	Energy loss during one swing period
E_{p_i}	Quantized energy for solution i in MOSA (J)
E_{loss}	Energy loss during one swing period
F_{ai}	Air resistance acting on pendulum (N)
$f(\bar{x})$	Objective function for single objective optimization problem
$f(\bar{x}_i)$	Objective function for single objective optimization problem with design variables $\bar{x}_i$
$f_{\mathrm{i}}(\bar{x}_i)$	Objective functions for MOO
f_0	Frequency of pendulum (Hz)
g	Gravity (m/s^2)

$g_j(x)$	Equality constraints for SOO
$h_k(x)$	Inequality constraints for SOO
$g_j(\bar{x})$	Equality constraints for MOO
$h_k(\bar{x})$	Inequality constraints for MOO
h	Thickness of the bob (m)
In_i	Individual in MOGA-II
J	Pendulum moment of inertial (Kg·m^2)
J_{E2}	Escape wheel moment of inertia (N·m2)
k_B	Boltzmann constant (J/K)
k_i	Scaling factor
L	Length of pendulum rod (m)
l_{min}	Minimum perturbation length in MOSA
l_{per}	Perturbation length parameter in MOSA
l_i	Initial perturbation length in MOSA
M	Hanging weight mass (kg)
m	Pendulum rod and bob mass (kg)
m_L	Lower limit for pendulum mass keeps the system stable
m_u	Upper limit for pendulum mass keeps the system stable
N	Current iteration number in MOSA
N_{hot}	Hot iteration number

N_{ij}	Number of teeth as j[th] gear on i[th] arbor
N_{in}	Number of population in first generation for MOGA-II
N_{it}	Iteration number stop criteria for MOGA-II
N_{MO}	Number of solution were created in MOSA
N_{tot}	Total iteration number for MOSA
P / P'/P"	A Generation in MOGA-II
P_{acc_i}	Chance MOSA solution will be replaced by perturbation pair
P_{f1}	Distance from the pallet to the pivot (m)
P_i	MOSA solution
P_i'	Perturbation pair of solution P_i in MOSA
Q	Quality factor
Q_{des}	Desired quality factor for optimization
R	Bob radius (m)
R_t	Train ratio
r	Pendulum rod radius (m)
r_{A4}	Radius of winding drum (m)
r_{E2}	Radius of escape wheel (m)
r_a	Random number created between 0 and 1
r_i	Ranking i[th] solution in MOSA
s_i	Relational digital variables
T	Period (s)

T_{ij}	Torque of teeth as j[th] gear on i[th] arbor (Nm)
T_A	Escapement anchor toque (Nm)
T_{A1}	Input torque (Nm)
T_{A4}	Torque of winding drum (Nm)
T_a	Simulated annealing temperature (^oC)
T_{des}	Pendulum desire period (s)
T_e	Escape wheel torque (Nm)
T_{end}	End temperature for simulated annealing (^oC)
T_{F2}	Impulsive torque (Nm)
T_i	Initial temperature of simulated annealing (^oC)
T_w	Hanging weight torque (Nm)
T_1	Current temperature of simulated annealing (^oC)
U_{tot}	Total utility
v_m	Single attribute utility for mass
$v_{\Delta t}$	Single attribute utility for period difference
v_Q	Single attribute utility for quality factor
W	Weight of hanging weight (kg)
w_m	Utility weighing for mass
$w_{\Delta t}$	Utility weighing for period difference
w_Q	Utility weighing for quality factor
x_i	Design variables

$x_{i,in}$	Initial guess for design variables x_i
$x_{i,L}$	Lower limit for design variables x_i
$x_{i,U}$	Upper limit for design variables x_i
$x_{p,i}$	Design variables of Pareto solution
x_{st}	Step size of design variables in optimization
$\bar{x}$	Design variable vector
$\bar{x}_f$	Design variable set with optimized values
$\bar{x}_{in}$	Design variable set with initial values
$\bar{x}_p$	Pareto solution design variable vector
y_{ext}	Vertical drop of hanging weight (m)
θ	Pendulum angular angle (rad)
θ_e	Amplitude of pendulum swing (rad)
θ_{ij}	Angular rotation as gear j^{th} on arbor i^{th} (rad)
θ_{E2}	Angular rotation of escapement wheel (rad)
τ	Time constant (s)
ω_{E2}	Escape wheel angular speed (rad/s)
ξ_i	Angular limits for impulse, hold (rad)
δ	Angle enclosed by line between escape wheel center
ρ_{ai}	Density of air (kg/m^3)
ρ_i	Iron density (kg/m^3)
ρ_w	Wood density (kg/m^3)

ΔE_i	Energy between two MOSA solutions (J)

Subscript

o	E. Howard clock initial parameters

CHAPTER ONE

INTRODUCTION

The successful and efficient creation of a complex industrial or consumer product requires the application of design and optimization methods in the development process. This chapter describes their importance by introducing formulation of them and how optimization may accelerate the engineering design process. In addition, the idea of tradespace analysis which serves as an additional method to select optimized designs, is also presented. The pendulum clock, a historically important mechanical system, is discussed in this chapter. Computer-aided-design (CAD) models of some pendulum clock crucial components are shown for visual representation. Next, this research's experimental activities, including the methods and equipment, are presented. Finally, the objectives and approaches of this thesis are presented in bullet points.

1.1 Engineering Design

Engineering design is the process of devising a system, component, or process to meet specific needs. It is a decision-making process and could be complex where knowledge from multiple disciplines such as science, mathematics, and engineering are applied. In many cases, engineering design is an iterative process. If additional refinements prove beneficial in bringing the design closer to the requirement, such improvements should be applied to the result of a previous design and repeat the design process. Generally Speaking, engineer design includes the following steps- setting objectives, analysis,

construction, testing, and evaluation. Furthermore, this decision process must consider realistic constraints such as economic factors, durability, and ethics (Haik et al., 2015).

Engineering design is an essential step in the product development process, as the design is the first thing people look at for a product. A good design will make consumers more inclined to buy the product. On the other hand, a poor design may fail to achieve the desired goal or even cause catastrophic consequences. For example, the Chornobyl disaster led to 56 deaths and 6.6 million people being exposed to radiation due to the critical design flaws of the nuclear power plant (Hatch et al., 2005).

Engineering design has three broad categories - adaptive design, development design and new design. Adaptive design is the minor modification of existing designs, e.g., changing a product's dimension or material for a particular use. Development design also builds off of a current design, but has significantly more changes, thereby altering the final product dramatically. Finally new designs are novel ideas, born from imagination and creativity, given form. The first automobiles and airplanes are two examples of this approach.

Although design methodologies explore possible products, engineers face several challenges during application. Firstly, growing system complexity makes development difficult. For example, the design of any automobile requires multidisciplinary knowledge of interdependent systems and components. This correlated complexity dramatically increases the workload of engineers. Next, the heterogeneity of the information coming from different sources (e.g., simulation versus experimental data) complicates the process. The inherent uncertainties of which may hinder the designs from achieving desired goals.

For example, conflicting needs and opinions of individuals from the same products makes it impossible to satisfy everyone. Thus, a formulation of the engineering design process is necessary as a guide to meet desired goals (Pahl et al., 2007).

The minimum phases of a robust design process is shown in Figure 1.1: Identification of the design tasks, conceptual design, embodiment design, and detail design. Engineering design starts with listing the customer's needs and expectations for a given product. Next, the design engineers make the decisions of either modifying/improving an existing or creating a new product. This step focuses on gathering information about existing designs that may be similar. The design engineers then define goals that are to be delivered by design. The relationship between the product's input and output defines the overall function. Customers set product requirements, and the function stage converts such requirements into engineering terminology, which the design can directly apply. Specification - a step to gather factors that relate to the design's final performance is the last step of the task identification phase. A specification is composed of a metric and a value. For example, "the average cost of manufacturing" is the metric, while "less than 5,000 dollars" is the metric's value. In this manner, vague objectives and constraints are also defined in the specification.

The conceptual design phase starts with the conceptualization stage, where new design ideas are generated mind; creativity is the crucial factor. It is possible to have multiple designs fulfill the requirement. In such cases, methods for evaluating the different devices are required. Pugh's evaluation matrix and decision matrix are approaches that are commonly used for alternative comparison. The basic idea for them are similar, which

includes the following steps: 1. Choose the comparison criteria, 2. Select the alternatives to be compared, and 3. Generate scores. At the end of the conceptualization stage, the design with the highest scores is chosen.

The embodiment design phase creates product drawings and prototypes to present the information. Layout drawings, assembly drawings, and detail drawings were used to communicate the design idea between designers. Afterward, the drawings are required to transfer to the hardware to test the design's performance. And a comprehensive or focused prototype is constructed at this stage. A comprehensive prototype is a model with identical scale and operation to the final product, while a focused prototype only concentrates on the part of the product elements. At the end of embodiment design, a potential design is chosen.

After the last design has been completed, the detail design phase begins. A complete analysis is conducted in the detail design. Factors such as safety cost and aesthetics are checked to ensure they fulfill the requirements. The last step in engineering design is the experiment; a model of the final product is constructed at this stage. Various experiments are conducted on the model to test whether the performance meets the requirement.

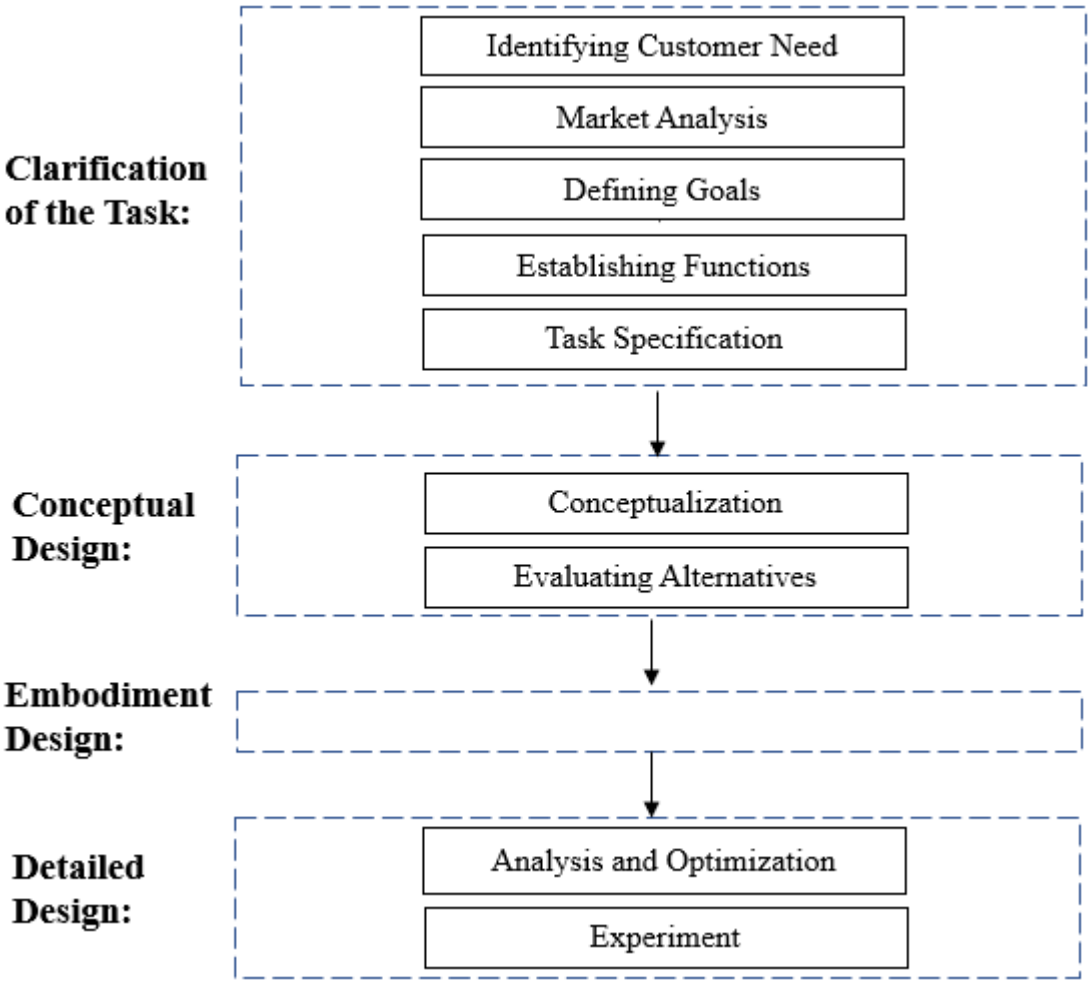

Figure 1.1：Engineering design process map

With the development of computer packages, CAD plays an increasingly important role in engineering design. By applying computational technology, the overall product development process may be shortened, lowering product costs (Chang., 2016). For example, in the traditional design-build-test process, product performance can only be evaluated in lengthy, expensive physical tests. However, with the product model represented in CAD, the product's performance can be analyzed in the early design stage.

And the cost of tests may reduce significantly by applying simulation tools. In this research, hundreds of designs were created and evaluated with a computational model.

1.2 Optimization

Optimization is a process of achieving the best result by changing the related variables, usually under certain constraints. It can be applied in many areas such as manufacturing, physics, and economics. For example, as the principle of minimum energy states, particles always migrate to the optimized location for a closed system to minimize the internal energy. Another example is when buying an airfare, people may consider the ticket price and the flight length to make an optimized decision. For the latter example, people make such a decision out of their instinct without realizing the optimization concept (Martins et al., 2021).

In order to minimize the required resource or maximize the desired benefit, engineers are supposed to make various decisions, especially in the design phase. Since, in many cases, the required resource and desired benefit can be translated to a function of certain variables, optimization can be viewed as the process of finding the value of such variables that reach the maximum or minimum value of a function $f(y)$.

Optimization is crucial in modern engineering design, as it accelerates the design cycle and may obtain better results. Traditionally, design is an iterative process of evaluating and changing current design by engineers until its performance meets the requirement. By involving in optimization, the whole process can be automated. The design is change driven by the applied optimization algorithm until the stop criterion is reached, which could be optimality conditions or iteration number.

The formulation of a design optimization problem is vital in the design process as it helps the engineer better understand the problem. A poor problem formulation maybe leads to an unacceptable or unrealistic solution. The formulation of the design optimization problem includes the decide which parameters in the system could be changed, what the objective of the question needs to be minimized, and what constraints need to be satisfied. Figures 1.2 shows the procedure of design optimization problem formulation. Reformulation, for example, adding constraints, may is required if the optimization result is not satisfied (Baldick., 2021).

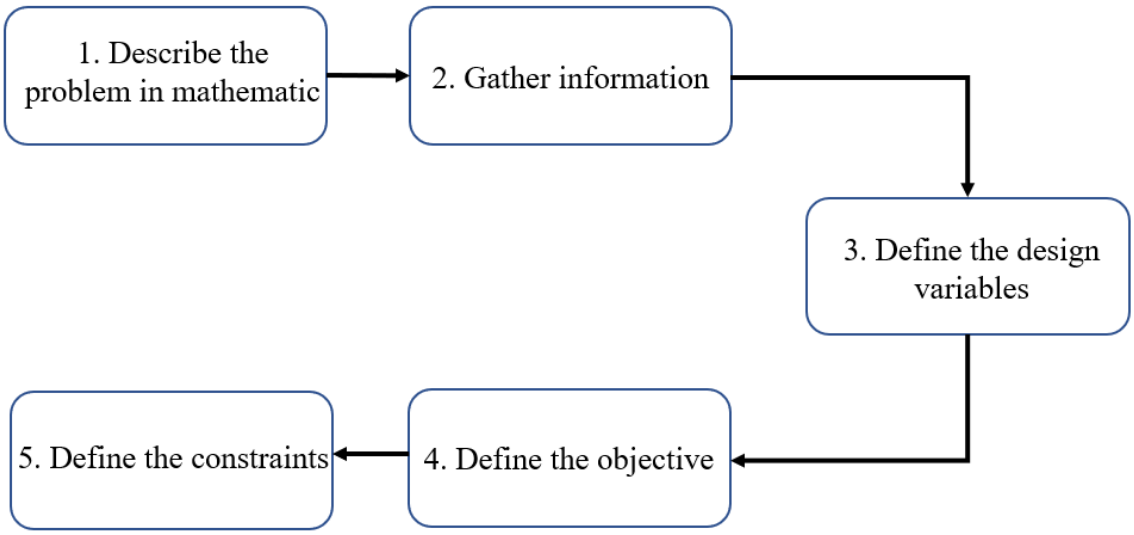

Figure 1.2： Process of optimization problems formulation

The first step is to understand and describe the design problems, including the goal and requirements of the problem. The next step is to gather information on the optimization problem. For example, the inputs and outputs of the problem should be identified at this stage.

The third step is to identify the design variables, which are usually represented by the vector: y = $[x_1, x_2, \ldots, x_n]$. The design variables are required to be independent of each other, and the number of variables n determines the dimension of the problem. An n-dimensional design space was formed by taking each design variable, x_i, as a coordinate axis. And each point in the design space is a design point that is a potential solution to the design problem. In some cases, the design variable's initial values could be the best guess of the engineers or existing good designs.

The next step of optimization is to define the objective function; in this manner, different designs can be evaluated and compared. During this step, engineers are supposed to express their design aim mathematically. The objective function must be a function of the elements of the design variables to be maximized or minimized. For example, an aircraft's weight or the building's cost could be minimized as an objective function. Some optimization problems have more than one objective function, called multi-objective optimization (MOO) problems. Tradeoffs exist between different objective functions.

The design variables were usually under specific requirements in engineering problems called design constraints. The constraints can be physical or other limitations that must be satisfied to obtain acceptable solutions. Constraints include equality constraints and inequality constraints. An equality constraint is called when the constraint function is equal to a value; otherwise, it is an inequality constraint. A feasible region is formed in design space by the design variables that satisfy all the constraints.

Selecting an appropriate optimization method to solve a given optimization problem is essential. There is no single algorithm that can effectively solve all the

optimization problems. The identification of optimization problem classification is required to select an appropriate algorithm. There are many ways to classify optimization problems. For example, the design variables can be continuous, discrete, or even a mix of these two; as mentioned earlier, based on the number of objective functions, the optimization problem can be classified as single and multi-objective optimization problem. A part of the classifications of optimization problems is summarized in figure 1.3. The various techniques are available for the solution of different types of optimization problems (Martins et al., 2021). For example, the differential calculus method can be applied if the optimization problem is unconstrained. However, the most suitable optimization method for real design problems may not be obvious in advance. Therefore, the engineer may run optimization with different algorithms to compare effectiveness. And in this thesis, several optimization methods have been applied to explore the same problem, and results were presented and compared.

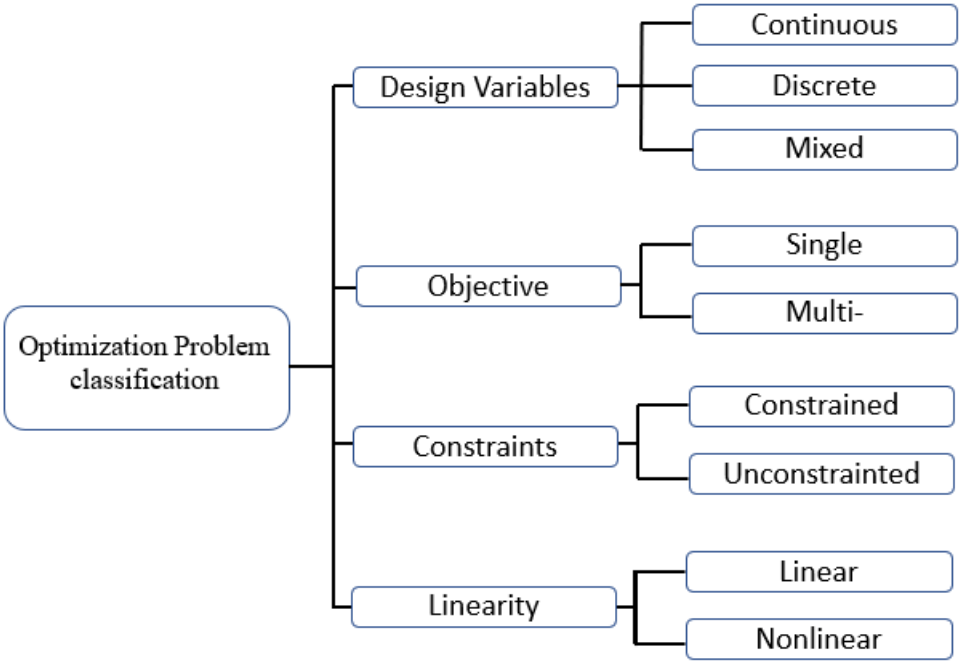

Figure 1.3: Partial classification of optimization problems

1.3 Tradespace Analysis

In some cases, the optimal solutions to an optimization problem are still too many to analyze, and tradespace analysis is applied to narrow down the potential solutions further. Tradespace is the space of possible design options with a given set of design variables. The goal of tradespace analysis is to use the design maker's preference to evaluate various designs (Spero et al., 2014). Models are developed to simulate the attributes of a design based on its user's preferences and further guide the design choice. These choices are then varied systematically to create a tradespace. Based on the designer's preference assign weight functions to each attribute, a single utility function can be obtained by summing the product of each attribute and its weighting function. The utility is a dimensionless factor ranging from zero (minimal acceptable) to one (most desirable) is calculated for each design to evaluate their relative gratification by allocating the resources of an attribute. A

cost model to assess designs' expenses is required to enable a utility-cost plot to be created to help find the highest utility for a fixed cost.

The non-dominated designs, also known as Pareto solutions, are desired for the tradespace analysis. In this case, the non-dominated design is defined as no other single design in the tradespace that is both cheaper and has a higher utility than it. In many cases, the Pareto solutions are not unique; thus, a Pareto frontier characterized by the set formed by Pareto solutions can be obtained.

1.4 CAD Model of the Clock

Mechanical pendulum clocks (e.g., street and tower clocks) reigned as the world's time-keeping standard for centuries and were recognized for their durability and accuracy. Traditionally, they served the commerce and public activities of the local populace. But in later years, these were replaced with their electronic counterparts (i.e., digital and atomic clocks) due to rapid globalization, which required synchronizing times over long distances. Even so, pendulum clocks are still used for decorative purposes today. The Boston, MA based E. Howard Clock Company manufactured a variety of large movements, including the Model 00. These time-only movement-powered single and twin dial street clocks used an anchor escapement which is the experimental subject of this thesis. The system components of this movement, especially the escapement mechanism, provide insight into advanced design optimization problems.

In this research, the CAD model of the E. Howard Clock Model 00 was built using the SolidWorks™ software package. The dimensions of various system parameters were carefully measured using a caliper and other laboratory tools. Each component was

constructed individually and assembled into the three-dimensional virtual model. Some core subsystem and components is shown in Figure 1.4. Such a CAD model lets us visually illustrate the pendulum clock's working principle. More importantly, it helps us better define optimization problems, for example, the geometry constraints of the pendulum. Furthermore, a two-dimensional schematic diagram of E. Howard Model 00 clock time train was also created in Inventor™ to illustrate the arbors and gears.

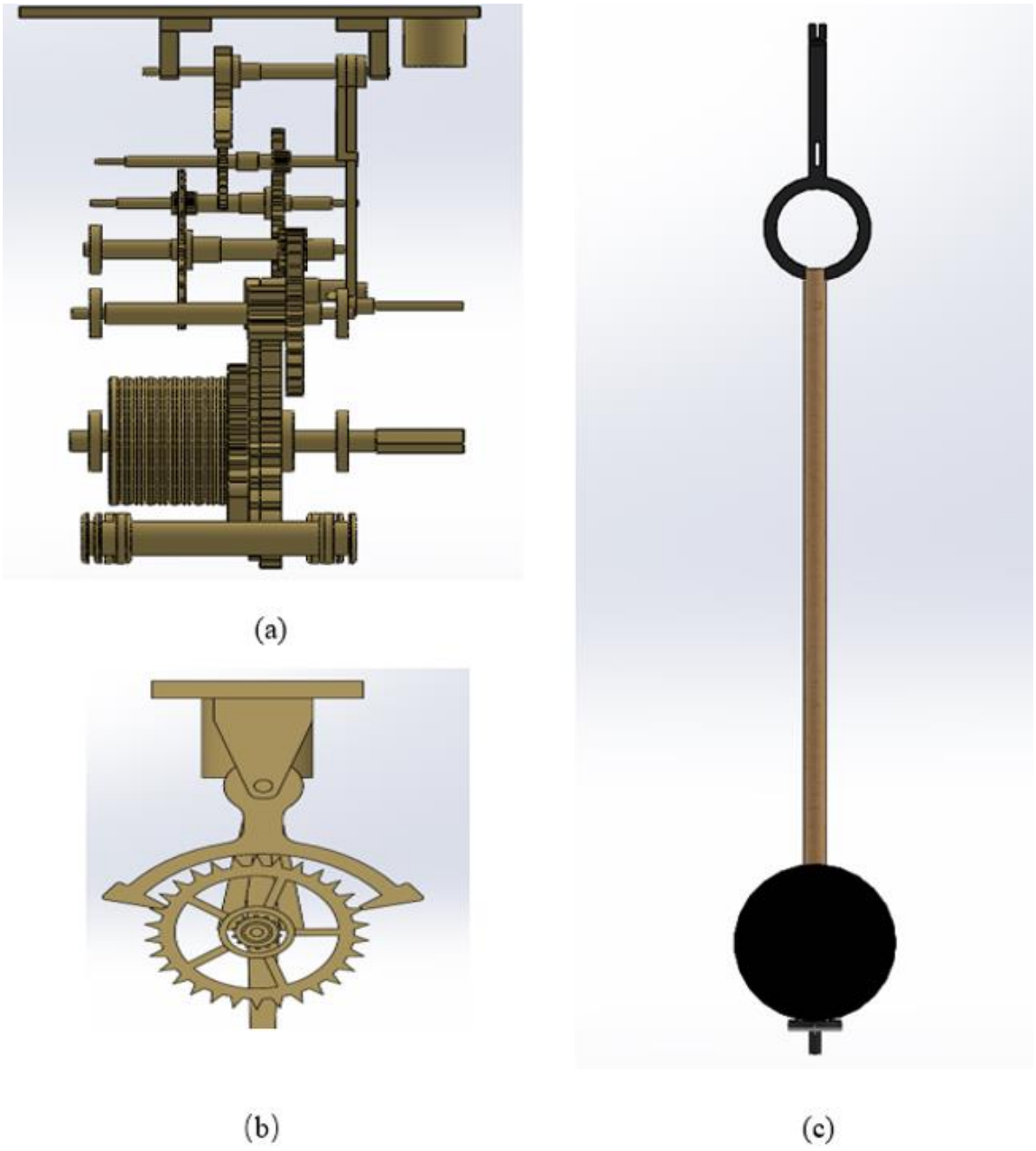

Figure 1.4: Computer-aided-design model for E. Howard Model 00 movement subsystem and components: (a) Gear train, and (b) Escapement subsystem, and (c) Pendulum subsystem. (Supplemental models can be found in Appendix F)

1.5 Experimental testing

To study the operation and performance of the clock, the motion of three moving components: the escape wheel, crutch, and pendulum, was recorded and analyzed. Three small cube-shaped high flux magnets were attached to the pendulum, the escape wheel pivot and crutch pivot, and using epoxy putty and a drop of adhesive. High-resolution magnetic field angular position sensors (Honeywell APS00B) were mounted on long thin wood sticks with attached soldered wires and placed near the rotating shafts with center alignment for optimal magnetic field sensing (refer to Figure 1.5). The sensor creates an analog output voltage proportional to the magnetic flux passing over its surface. A pair of linear amplifiers - Analog Devices AD623, raised the output voltage for each channel with a gain of 25 or 30 were used to amplify the magnetic signal. The analog signals were first supplied to the National Instrument ELVIS^{TM} data acquisition system and then converted to the digital signal through analog-to-digital converters. The host computer executed LabView for real-time data logging and Matlab™ for post-processing, including 4th order, low pass Butterworth 250 Hz filter.

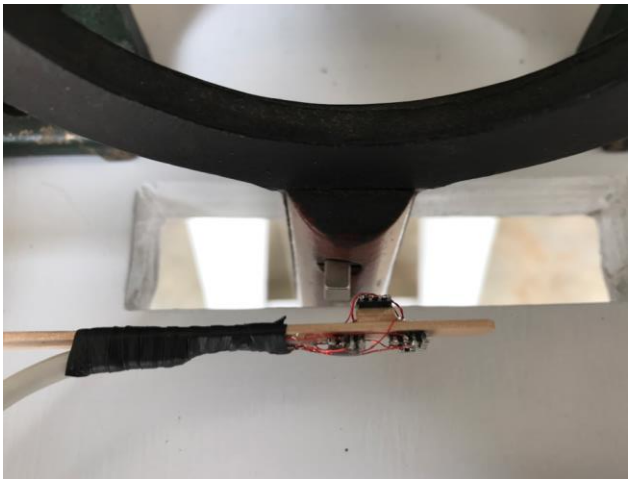

(a)

(b)

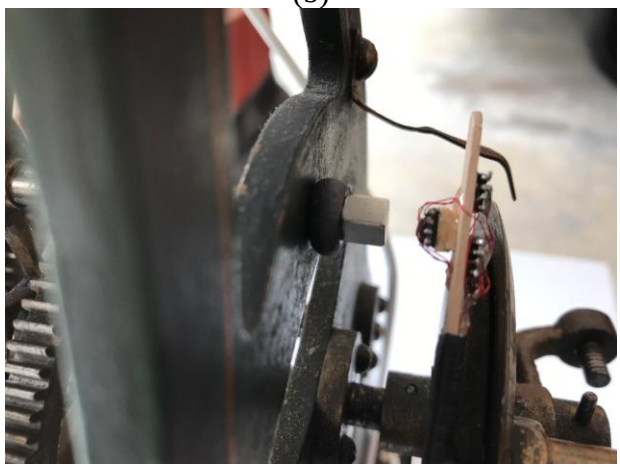

(c)

Figure 1.5: Experimental measurement of the (a) pendulum (b) escape wheel crutch arbor (c) crutch pivot angular motion with magnet, sensor, and amplifier.

1.6 Dissertation Objectives and Approaches

This research intends to achieve the following research objectives:

1. Gain expertise with optimization and tradespace analysis methods including Pareto Space.
2. Explore the application of these design tools to a classical mechanical system to demonstrate what can be accomplished by students in an undergraduate or graduate level course.
3. Collect experimental data on a historic street clock to benchmark the performance and share with horology community.

To reach the above goals the following research approaches have been applied

1. Review the history and design of the street clock and introduce the working principle of the pendulum clock base on the E. Howard Model 00 movement.
2. Determine the correspondence between Quality Factor and clock's accuracy through literature search
3. Create a three-dimensional CAD model for the E. Howard pendulum clock to facilitate the illustration of design.
4. Experimentally test the motion behavior of several movement's components.
5. Experimentally determine the Quality Factor of E. Howard movement under free response.
6. Develop a mathematical model for the pendulum system to simulate the free response of the pendulum. Evaluate the Quality Factor of different conceptual pendulum designs with this model.

7. Develop a mathematical model for the escapement subsystem to evaluate the period of the pendulums with different designs.
8. Conduct experiments to validate the above two models.
9. Design an SOO algorithm to obtain one pendulum design that can achieve the optimum accuracy quality factor and mass combination.
10. Design appropriate MOO optimization algorithms to explore the optimum parameters for the pendulum clock in terms of clock's mass, accuracy, and period.
11. Exam the efficiency of different MOO algorithms by comparing their optimization results
12. Use tradespace analysis to identify further the optimal solution with the highest utility at a fixed cost.

1.7 Thesis Organization

The document is organized into five chapters. Chapter One introduces the background of this study. The techniques used in this thesis are discussed in a general way. Chapter Two reviews the history of the pendulum clock and emphasizes the important role it played in the era of the rise of industrialization. The design and working principle of the pendulum clock is discussed in detail, and several experimentally determined parameters, especially Quality Factor, are also presented in this chapter.

A mathematic model that represents the pendulum clock's pendulum subsystem is developed in Chapter Three. The experimental process that validates this model is included. The principle of the simulated annealing algorithm applied to explore the

optimized design of the pendulum clock in this chapter is discussed in detail. The optimized design and original design of E. Howard Model 00 is compared in this chapter.

Chapter Four starts by introducing the Quality Factor and how it relates to the accuracy of the clocks. Another mathematic model that represents the escapement subsystem is developed as well. Afterward, the general form of MOO is given, and two MOO algorithm applied in this chapter is discussed thoroughly. The idea of tradesapce analysis is presented. Finally, the optimized designs of the pendulum clock that are determined through MOO and tradespace analysis are presented. The conclusion that includes research summary and further work recommendation is the given in Chapter Five. Lastly, the appendices provide the supplemental information to support the research are given.

CHAPTER TWO

E. HOWARD STREET CLOCK MOVEMENT MODEL 00 – HISTORY, DESIGN AND TEST DATA

The presence of a street clock in a city is unusual today, although they were prevalent a century ago for public time display and accompanying advertisement of the sponsoring business. Tower clocks with bells were installed in churches, court houses, and universities/schools to visually and auditorily note the passage of time for residents and students. The E. Howard Clock Company of Boston, MA manufactured a variety of large movements including the Model 00. This time only movement powered single and twin dial street clocks using an anchor escapement. In this article, the design and quality factor of the Model 00 clock will be experimentally explored to provide insight into the general operation and performance.

2.1 Introduction

In the mid-19th century, the transformation of the United States from rural-agricultural to urban-industrial was slowly underway along with territory growth as the western states opened. Railroads were growing and passenger plus freight volume increasing as commerce flourished. To regulate the railroad schedules and help the emerging plants with fixed workforce hours, the availability of standard time and dependable clocks and watches were requirements (Bartky., 1989). The synchronization of clocks with a known time in a defined geographic region, or time zone, required the public display of time so that individuals and companies could set their time pieces. The large dials, typically 3 or 4 feet

in diameter, on street and tower clocks provided a much-needed visual display of the time with accompanying hour strike with attached bell in some instances.

Jewelry stores may also have had high precision clocks inside, or street clocks out front, so that customers and others could set their watches. An E. Howard Clock Company (Boston, MA) two dial street clock was erected in 1878 outside the Eli Hertzberg Jewelry Company in San Antonio, TX (Mrini., 2019). The clock has moved locations over the years but remains a treasured "timepiece for generations of San Antonians" (quote from an inscription on a clock informational plaque) as shown in Figure 2.1.

Figure 2.1: E. Howard & Company street clock from 1878 that resided in front of Hertzberg Jewelry Company in San Antonio before relocation to N. St. Mary's and Houston streets

(used with permission from Richard Marini)

Edward Howard (1813-1904) was involved in a number of clockmaking business ventures that included watches, clocks, and tower clocks with partners. The E. Howard & Company (Boston, MA), under other names and ownership, manufactured tower clocks beginning in 1843 through 1964 (Shelley., 1999). The 4,000 tower clocks produced included weight driven models with time and possibly strike trains to sound bells. The painted cast iron structural frames and polished steel arbors with brass and steel wheels created a decorative appearance for these elegant movements. The company catalogs list street and tower clocks for various applications including single, dual, and four dial displays for sidewalks, brackets, church steeples, and court houses (Howard., 1890). Eventually, the hand cranked weights could be automatically rewound or clock hands driven directly with electric motors.

In this article, the design and performance of a circa 1912 serial #3494 Model 00 movement shown in Figure 2.2 will be investigated. Paul Middents reported that the E. Howard Model 00 first appeared in the 1912 catalog and was also used in Joseph Mayer (Seattle, WA) produced twin dial street clocks (Middents., 2014). This movement was also listed as driving clock hands for single 3 feet (weather exposed) and 4 feet (weather protected) diameter dials (Ly., 1995). Robert Shaw discussed the restoration of a similar E. Howard Model 00 movement in a two-dial street clock located in Hamilton, Bermuda that featured a 90 pound weight in a triple compound style (Shaw., 2016). These movements were widely manufactured and installed in the early 20th Century for public time displays with operational examples of interest remaining today to the horology community.

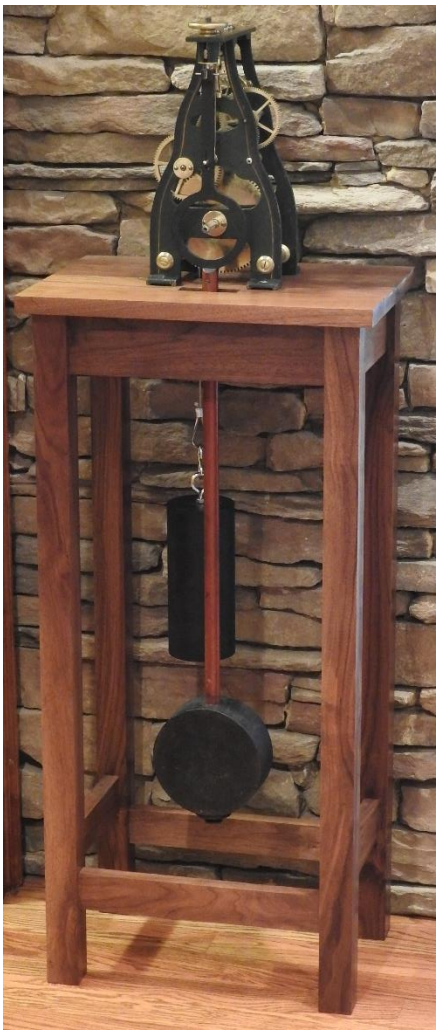

Figure 2.2: Tower clock on stand with attached weight and pendulum plus bob

2.2 Clock Design and Operation

The time-only clock movement design will be explored in terms of the configuration, components, and parameter values. The clock features six arbors between two parallel plates as shown in Figure 2.3. An external weight of w= 30 pounds (it should be much heavier per catalog data but adequate to run this movement without hands) is suspended on

a cable that wraps about the winding drum to provide the input torque, $T_{A1} = \frac{1}{2} D_{A4} W$. Similarly, the vertical drop of this weight can be expressed as $y_{ext} = \left(\frac{1}{2}\right) D_{A4} \theta_{A1}$. A series of four meshed gears (pinions, gears) reduce this input torque that is eventually presented to arbor pinion E2 which interacts with the escape wheel. The relationship between the input and output torques and rotational angles can be expressed as

$$T_{E2} = \left(\frac{1}{R_t}\right) T_{A1} \text{ and } \theta_{E2} = (R_t)\theta_{A1} \tag{2.1}$$

where the train ratio becomes $R_t = \left(\frac{N_{B1}}{N_{A1}}\right)\left(\frac{N_{C1}}{N_{B2}}\right)\left(\frac{N_{D1}}{N_{C2}}\right)\left(\frac{N_{E1}}{N_{D2}}\right)$ (2.2)

The summary of wheel teeth and diameters is listed in Table 2.1. The substitution of values results in a train ratio of 1,333.33: 1. For the time display, the train ratio is 22.20:1 which offers a rather high torque to accommodate the larger hands and accompanying load. Accordingly, the thickness of the mechanical components is large to help ensure the strength and longevity of the wheel teeth.

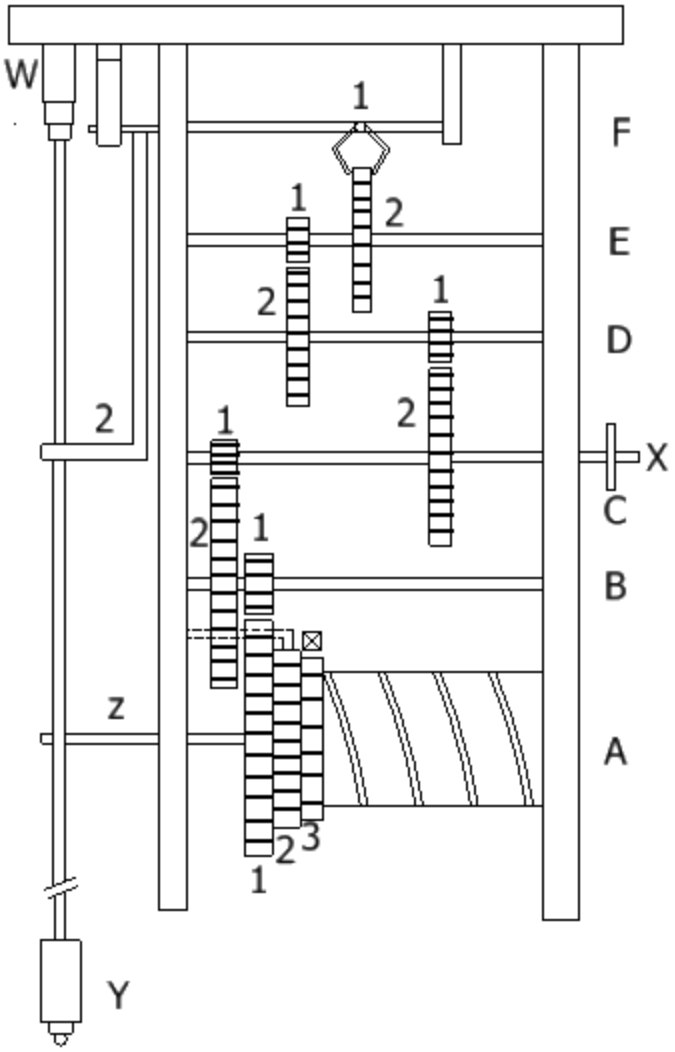

Figure 2.3: Schematic diagram of E. Howard Model 00 clock movement time train

The clock features an anchor escapement with two adjustable pallets, F_1, engaging with the escape wheel, E_2. The escapement divides the time train rotational motion into fixed time intervals (beat of 1 second) during motion of the pendulum (period of 2 seconds) acting through the attached crutch. The pendulum swings approximately $\theta = \pm 2°$. The E. Howard pendulum bob is a short circular cylinder or thick disk weighing approximately 25 pounds. The pendulum bob's larger diameter is turned on its edge in contrast to other tower

clocks which feature a tall vertical circular cylinder of narrow diameter. This is notable, given the aerodynamic resistance of the bob which effects the overall clock performance as measured by the quality factor.

Arbor	Gear	Symbol	Description	No. Teeth	Diameter (inches)	Thickness (inches)
A	1	A1	Great wheel	90	6.087	0.455
A	2	A2	Wheel & safety pawl	100	5.730	0.200
A	3	A3	Wheel with ratchet	40	3.820	0.400
A	4	A4	Winding drum		3.000	
B	1	B1	Input pinion	18	1.264	0.680
B	2	B2	Arbor B wheel	80	3.900	0.284
C	1	C1	Input pinion	18	0.945	0.485
C	2	C2	Arbor C wheel	96	3.723	0.258
D	1	D1	Input pinion	12	0.515	0.440
D	2	D2	Arbor D wheel	90	3.500	0.210
E	1	E1	Input pinion	12	0.515	0.335
E	2	E2	Escape wheel	30	2.410	0.150
F	1	F1	Verge			
F	2	F2	Crutch			
W			Suspension spring			
X			Time display shaft			
Y			Pendulum rod, bob			

Table 2.1: Summary of E. Howard Model 00 clock component parameters

A computer-aided-design (CAD) model of the E. Howard Clock Model 00 was created during this investigation using the SolidWorks™ software package to support future engineering optimization studies (refer to Figure 2.4). The dimensions for each component were carefully gathered and assembled into the three-dimensional virtual model. The animation of the 3D model will enable the clock's operation to be explored for different designs including gear thickness, pendulum bob profile (horizontal vs vertical cylinders), and arbor layout changes.

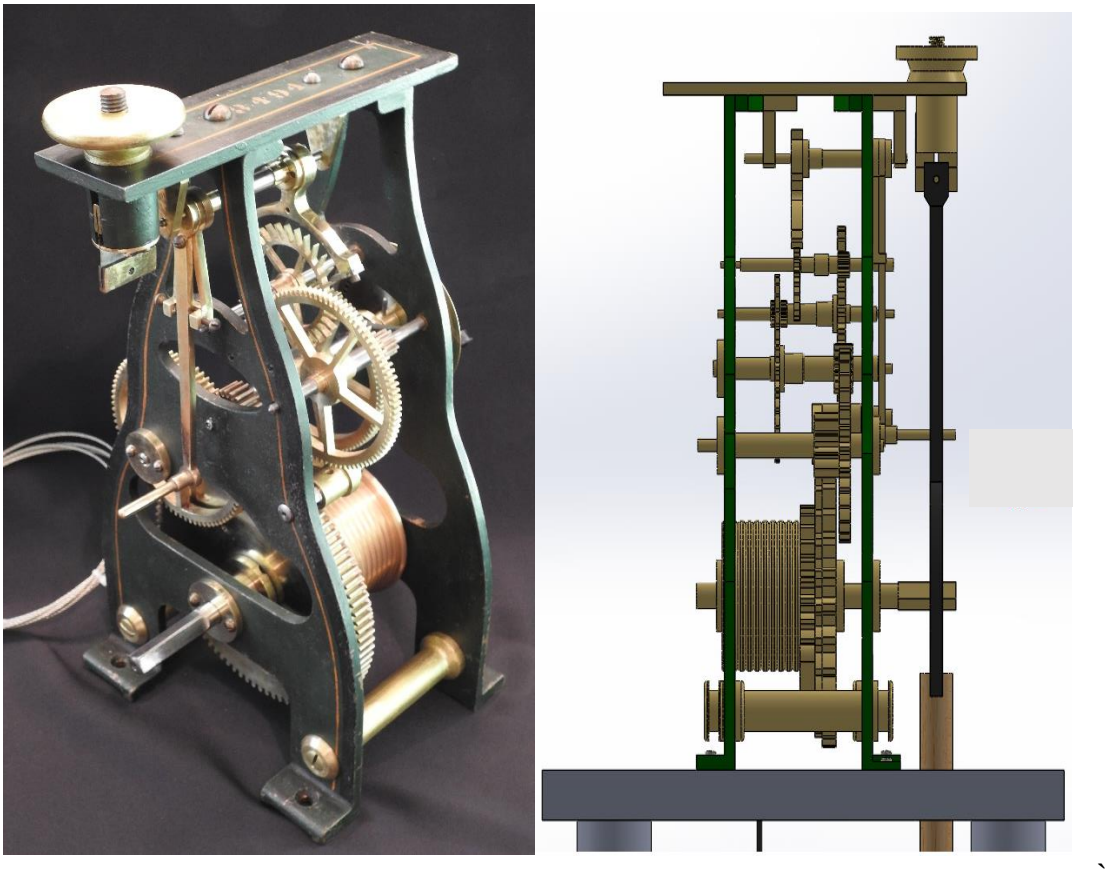

Figure 2.4: E. Howard clock movement and corresponding three-dimensional computer-aided-design (CAD) model for virtual engineering design studies

2.3 Quality Factor

The quality factor, Q, of a pendulum system in horology corresponds to the logarithmic decay of the underdamped mechanical oscillator. Simply put, it is a measure of how "long" a pendulum will swing back-and-forth when given an initial condition (displacement) and released with the crutch removed so that only frictional effects of the suspension spring and aerodynamic forces act on the pendulum rod and bob to dissipate the initial stored energy. The expression for the quality factor can be stated as

$$Q = 2\pi \frac{E_{store}}{E_{loss}} \quad (2.3)$$

A minimum amount of energy is absorbed/released continually by the suspension spring which will not be considered. An inverse relationship exists between the quality factor value and the energy loss rate. Typically, clock pendulums demonstrate higher Q values (3,000-15,000) as they will oscillate for an extended time before coming to rest (Rawlings., 1993).

To calculate the quality factor, the pendulum's damping ratio, B, or the exponential time constant, τ, may be determined by measuring either the logarithmic decrement (Palm III., 2007) and/or the free response motion decay (Nawrodt et al., 2006) based on

$$Q = \frac{1}{2B} = \frac{\tau\omega_n}{2} \quad (2.4)$$

One time constant corresponds to a 63.2% change between the initial and final steady-state values of the pendulum's transient response.

To collect experimental data, analog sensors were attached to the clock and connected to a National Instruments data acquisition board with LabView™ software. In Figure 2.5, a portion of the pendulum's angle response is graphed when subjected to an initial displacement of 2.12° from a vertical zero angle. The pendulum oscillates with gradual decay due to aerodynamic drag and suspension spring losses and eventually comes to rest. The time constant can be identified as the elapsed time when the pendulum motion decays by 0.632 * 2.12° or 1.34° such that the oscillation amplitude envelope passes through 2.12° - 1.34° = 0.78°. Using the collected test data, a time constant of τ = 5,599 seconds was measured. The period of the E. Howard movement is T = 2.0 seconds and $f_0 = 0.5$ (Hz).

The quality factor is calculated as Q = 8,795 which falls within the expected range for this pendulum street clock.

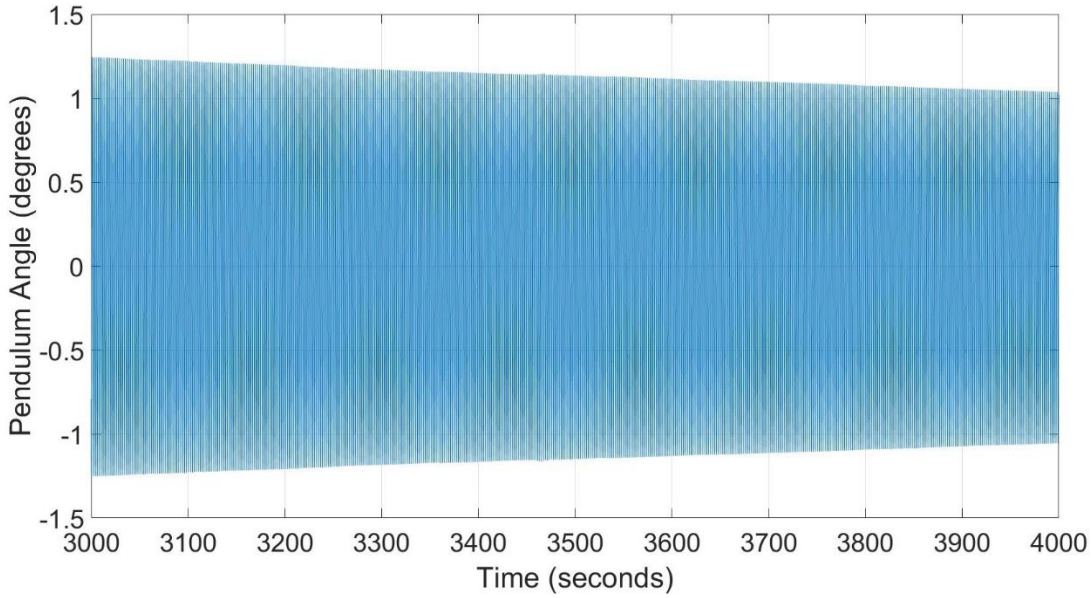

Figure 2.5: Quality factor determination by free response of clock pendulum; pendulum angular position verses time for a select portion of the total decay time.

The normal operation of the clock movement was further investigated for the escape wheel, crutch, and pendulum angles. Three small magnets were mounted at the ends of the escape wheel and the crutch arbors, and on the pendulum rod at the center of rotation near the suspension spring guide at the bottom of the adjustable upper mount. Non-contacting magnetic sensors were mounted near each of these magnets to measure the angular motion of the three components. A slightly more than two second long portion of the collected data is plotted in Figure 2.7 verses time. The graphs show the complete start and finish of one period of the pendulum oscillation and the lock, impulse and drop cycles on each of the two pallets.

When examining the escape wheel data, before 55.0 seconds an escape wheel tooth drops and lands on a pallet, stopping the rotation, though the tooth does bounce about 0.3°. It remains there and recoils slightly (about 0.1°) as the pallet slides under it until the start of an impulse after 55.8 seconds. As this impulse end, the change in angular slope indicates the drop onto the other pallet, again with a slight bounce. On this pallet there is a very slight recoil until the next impulse begins before 56.75 seconds. Upon dropping, the tooth again bounces, this time about 0.4°.

During this time interval, the pendulum is moving smoothly in sinusoidal motion. The crutch would follow the same oscillatory motion, except that it is connected to the pendulum rod via a pin in a slot that is slightly larger than the pin. Thus, the crutch can shift within this slot as observed by the periodic discontinuity in the crutch angle per Figure 2.6. It is believed that the motion during this shift may be described as follows. During the impulse, the escape tooth contact force on the impulse face of the pallet pushes the crutch and pendulum, via the crutch, through a vertical (zero angle) position. However, when the impulse ends and the drop begins, gravity is the predominant force on the crutch. The pendulum continues rising by its own momentum, but the crutch slows quickly and would start to fall back towards vertical except that the still rising pendulum closes the gap, overtaking the crutch, and starts pushing the crutch. The transition from crutch pushing the pendulum to pendulum pushing the crutch takes about 50 milliseconds. The crutch is then pushed by the pendulum to the maximum angle. When the pendulum starts swinging back towards vertical, gravity acts to keep the crutch in contact with the pendulum. The next impulse starts before the two reach vertical and the cycle is repeated.

Even in this short duration of the E. Howard clock movement operation, one can observe that the mechanical behavior is not quite symmetric. The difference in recoil has already been noted. The time between the alternating drops is not quite symmetric either, varying in this case by 0.05 seconds. While this might suggest the clock is slightly out of beat (which is adjusted by screws on the crutch), it is also possible that select teeth on the escape wheel are the root cause. This is not a new movement, after all, but nevertheless it demonstrates what may happen in the motion of a large pendulum street clock.

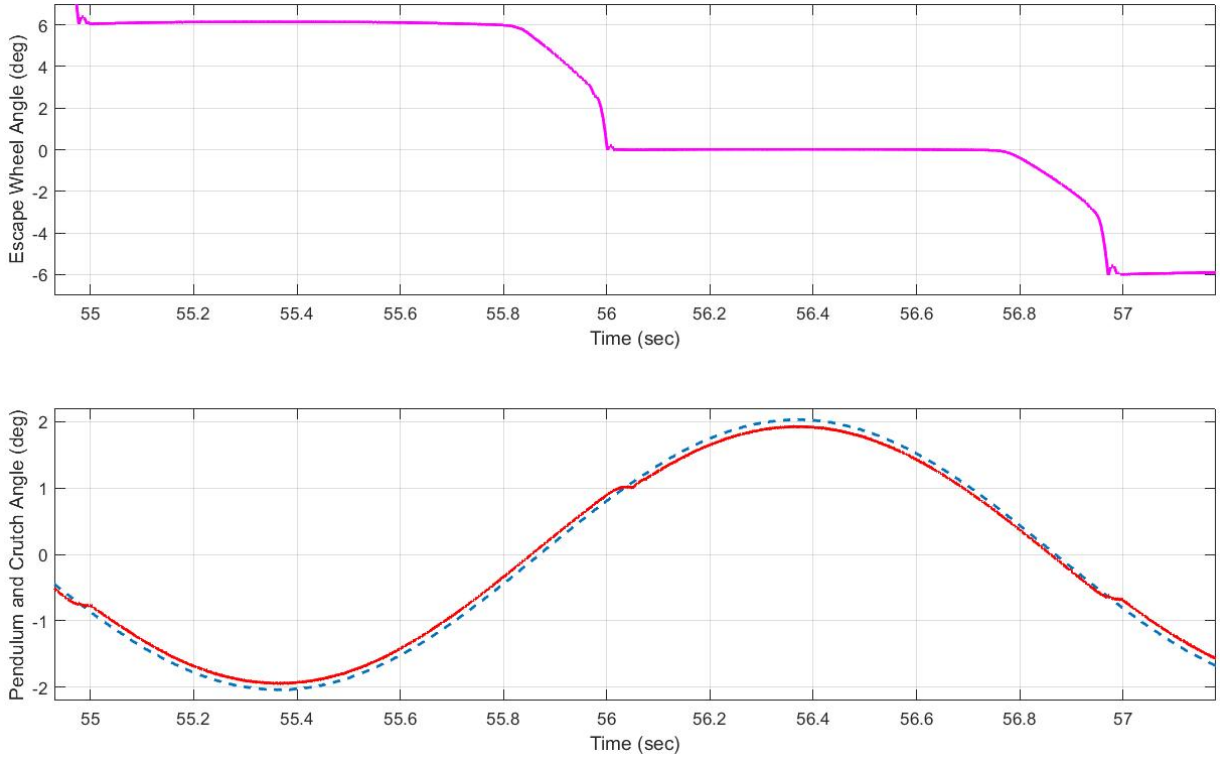

Figure 2.6: Angles of escape wheel (magenta), crutch (red) and pendulum (dashed blue) versus time from experimental data collected on the E. Howard Model 00 with three installed magnetic sensors and data acquisition system.

2.4 Conclusion

Street and tower clocks displayed public time in small towns and large cities across the United States during the late 19th and early 20th centuries. The ability for individuals to set pocket watches and household clocks from these public clocks enabled society to begin adopting uniform time for factory shifts, commerce, transportation, and many other aspects of everyday life. The E. Howard model 00 movement features a robust design with heavy duty arbors, pinions, gears and end plates that has enabled their continued operation for many decades with regular maintenance. Although many of these large clocks were manufactured, few installations and examples remain of these horological achievements due to their destruction in urban modernization efforts. Those that remain are a vivid testimony of a by-gone era when artistic flair, science of time keeping, large scale clock design, manufacturing excellence, and need for public time all intersected to create a truly unique solution that spread across the country for everyday citizens.

CHAPTER THREE

MODELING AND DESIGN OF A MECHANICAL MOVEMENT – A SIMULATED ANNEALING OPTIMIZATION STUDY

The mechanical pendulum clock reigned as the world's time standard for centuries and was recognized for its durability and accuracy. Although these movements have been displaced by electronic and atomic clocks, the assembled gears, escapement, and pendulum with weight drive provide an insightful optimization problem. In this paper, a mathematic model of an E. Howard pendulum street clock has been developed and simulated to explore the general operation and conversion of potential-to-kinetic energy. A simulated annealing optimization method has been applied to this model to determine the optimal design of the pendulum subsystem in terms of the combination of accuracy quality factor and mass. Numerical results show that the desired quality factor can be achieved without a change in the clock's period by adding 15% to the pendulum bob. Tradeoffs between the three design variables are investigated and discussed with representative experimental and computer results.

3.1 Introduction

Mechanical clocks and watches embodied the emerging scientific advances and artistic trends between the 15^{th} to 20^{th} centuries (Denny., 2002) as humankind created devices to mark the passage of time. The introduction of electric motors, quartz crystals, and atomic (electromagnetic radiation) into clocks has largely moved the mechanical ones into a historical position. Large clocks, commonly known as tower and street clocks, were

essential in providing visual time displays to help communities coordinate their daily work schedules and leisure activities (Matthews., 2000). The pendulum clock movement with escapement contains a feedback control system to maintain the constant swing period of pendulum which is crucial for accuracy (Bernstein., 2002). Further, clock mechanics illustrate fundamental engineering concepts and offer a platform for case study (Wagner et al., 2008).

The mechanical pendulum clock, created in 1657 by Christian Huygens, was studied by Galileo Galilei around 1582 (Baker et al., 2008). The movement converts potential energy from the hanging weight into periodic oscillations of a point mass pendulum through reduction gears and escapement. The Graham deadbeat escapement engages in a symmetric manner with the multi-toothed escape wheel through dual pallets to discretize rotational motion into pendulum swing (Penman., 2002). A thin steel suspension spring holds the pendulum in a vertical fashion while the crutch, connected to the escapement, provides impulse forces based on the escapement. The dial time display (minutes, hours) is often taken from the second set of wheels in the gear train with a 12:1 ratio for the hours. The weight is wound approximately every 8 days using a removable hand crank. A screw adjustment on the pendulum allows small changes to the overall length to adjust the clocks period for accuracy. A classic pendulum clock movement is the E. Howard Model 00 from 1905 shown in Figure 2.4.

Several important characteristics of pendulum clocks are the time accuracy, the Quality Factor, and the mass. The clock period should be fine-tuned by adjusting the pendulum length nut and then repeatable in day-to-day operation to avoid error growth which leads

to inaccurate time displays. On the other hand, the Quality Factor denotes the energy loss due to friction and aerodynamic forces as the pendulum swings back-and-forth. This quantity essentially represents how well the clock can convert potential energy into kinetic energy. Finally, the amount of stock metal used in the construction of the gear train, weight, and pendulum. An optimization problem can be formulated to evaluate these interactions. Engineering optimization focuses on determining the optimal and practical solutions to complex design problems under certain constrains. These constrains may include geometry cost and other service requirements. The optimization maximizes the performance and minimizes the cost at the same time.

In this paper, a select number of design variables will be optimized for a mechanical pendulum clock to improve the accuracy and Quality Factor while reducing the weight based on a verified mathematical model. The remainder of the paper is organized as follows. Section 3.2 provides a nonlinear mathematical model of the mechanical movement with escapement description for time keeping behavior with validation. The quality factor associated with the pendulum's free response is presented in Section 3.3. In Section 3.4, the optimization of the clock weight and accuracy will be stated followed by a case study in Section 3.5. The pendulum rod and bob are designed for weight and accuracy while satisfying the quality factor. The conclusion is contained in Section 3.6.

3.2 Mechanical Clock Mathematical Model

A lumped parameter model of a mechanical clock movement has been derived which features the external weight, gear train, escapement, and pendulum. The escapement regulates the rotational torque available through the gear train to impulse the pendulum on a periodic basis. The escape wheel rotational motion, $\theta_{E2} = \int \omega_{E2} dt$, can be described as

$$J_{E2} \frac{d\omega_{E2}}{dt} + B_{E2}\omega_{E2} = T_e - T_{F2} \tag{3.1}$$

where J_{E2} and B_{E2} are moment of inertia and vicious damping coefficient of the escape wheel. The applied torque acting through the gear train on the wheel is denoted as T_{E2}. The variable T_{F2} represents the impulsive torque that arises every half-period due to the escape wheel and crutch drive torque.

The gear train consists of four meshed gear interfaces that help to reduce the applied torque from the suspended weight and increase the available rotations as shown in Figure 2.3. For this system, the train ratio can be expressed in equation 2.2

The hanging weight, W, that acts on the drum (winding wheel) provides the power required to operate the movement with that torque expressed as $T_{A4} = r_{A4}W$. The gear train relationship enables the escape wheel torque to be expressed as $T_{E2} = R_t T_{A4}$.

The pendulum angular rotation, θ_Y, can be written by considering the pendulum bob to be a point mass as

$$J\ddot{\Theta} + B\dot{\Theta} + mgL\sin\Theta + F_{ai}L = T_{F2} \tag{3.2}$$

where B is the damping coefficient, J is the pendulum's moment of inertia, and m is the total mass of the pendulum rod and bob. The parameter L denotes the length of the pendulum rod from the suspension spring to the center of the bob (Schwartz et al., 2001).

An aerodynamic drag force, F_{ai}, primarily acts on the pendulum bob to dissipate energy as it swings through the air. This force considers the drag coefficient, C_D, surface area of the bob (and rod) acted on by the air, A, air density, ρ_{ai}, and translational velocity of the bob, $l\dot{\theta}_Y$, so that

$$F_{ai} = \frac{1}{2} C_D A \rho_{ai} (L\dot{\theta})^2 \tag{3.3}$$

Let ξ_1 and ξ_2 denotes the angle of the pendulum engages and disengages the escapement. If one considers the motion of pendulum to be symmetric, then T_{F2} can be calculate as

$$T_{F2}(\theta) = \begin{cases} T_{E2}\left(\frac{P_{f1}}{r_{E2}}\right) tan\delta & \begin{cases} -\xi_1 < \theta_Y < \xi_2, \frac{d\theta}{dt} < 0 \\ -\xi_2 < \theta_Y < \xi_1, \frac{d\theta}{dt} > 0 \end{cases} \\ 0 & \{otherwise \end{cases} \tag{3.4}$$

where r_{E2} is the radius of escape wheel, P_{f1} is the distance from the pallet to the pivot, and δ denotes the angle enclosed by the line between the center of the escapement wheel and the contact point of the impulse face (Kesteven, 1978).

3. 3 Metrics – Quality Factor & Accuracy

To evaluate the performance of a mechanical clock, several measures can be applied including utilization of the available energy in keeping time and accuracy. The quality factor, Q, is a dimensionless parameter defined as the ratio of the energy stored in the system to the energy loss due to resistance in one period (Nawrodt et al., 2008) or equation (2.3).

For a pendulum system, a higher Q value is desired as it corresponds to a lower rate of energy loss which makes the system more stable and accurate (Feinstein, 2005). A pendulum clock has a Q value of 10,000 or more in air. For an oscillator system, the quality factor can be calculated as

$$Q = \pi f_0 \tau \tag{3.5}$$

where f_0 is the system's natural frequency and τ is the exponential time constant (Nagourney et al., 2017). For small pendulum swing, the period, $T = 1/f_0$, can be expressed as

$$T = 2\pi\sqrt{L/g} \tag{3.6a}$$

so that

$$Q = \frac{\tau}{2}\sqrt{\frac{g}{L}} \tag{3.6b}$$

The accuracy of the clock movement depends primarily on the pendulum length, L, symmetrical operation of the escapement (equal impulse forces acting on the pendulum), aerodynamic drag of the pendulum and pendulum bob, and friction in the mechanical parts.

3.4 Experimental Testing & Model Validation

To validate the dynamic mathematical model, the performance of the clock movement was experimentally investigated. Honeywell high resolution magnetic field angular position sensor (APS00B) integrated circuit with dual analog voltage outputs. A pair of linear amplifiers, based on Analog Devices AD623, raised the output voltage for each channel with a gain of 25 or 30. A small cube shaped high flux magnetic was attached to the moving parts using epoxy putty and drop of adhesive (refer to Figure 3.1). The electronics were mounted on long then wood sticks, with attached soldered wires, and located in close proximity to the rotating shafts with center alignment for optimal magnetic field sensing. These signals were supplied to a National Instruments Elvis II 16-bit hardware interface featuring 16 channels of analog-to-digital converters (ADC). The host computer executed LabView for real time data logging and Matlab™ for post processing including 4^{th} order low pass Butterworth 250 Hz filter.

Three of these custom fabricated magnetic-amplifier sensors sets (six ADC channels totals) were placed onto the mechanical movement – escape wheel pivot, crutch pivot, and pendulum. For the latter two, the angle of rotation was approximately ±2 degrees. In Figure 2.6, the angular motion of escape wheel, crutch, and pendulum are displayed for a little more than two second interval during normal clock operation. A two second period is observed for pendulum and crutch. The angle of escapement wheel experiences a sudden drop every second which correspond to its engagement with either the left or right pallet for each half period. An escape wheel tooth slides on the given pallet when releasing and catching so its time in free spin is relatively short.

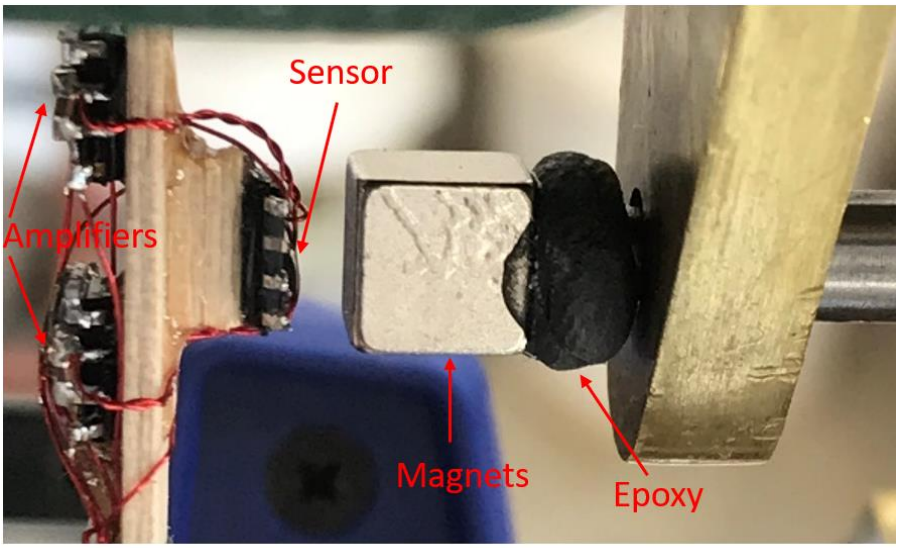

Figure 3.1: Experimental measurement of the crutch arbor angular motion with magnet, sensor, and amplifier.

To evaluate the quality factor, the crutch is removed from the m ovement and the pendulum allowed to freely swing. An initial displacement from vertical of 2.12° is given to the pendulum and then released. A portion of the gradual decay due to aerodynamic drag forces and suspension spring losses is shown in 2.6. The time constant can be measured by determining the elapsed time for the initial amplitude to drop by 63.2% or 0.632*2.12°=1.34°. For this system, the time constant is experimentally determined to be $\tau = 5599$. Hence, the quality factor becomes Q=8,780.

To validate the dynamic model and computer simulation, the pendulum response for normal (weight driven) clock operation has been compared against the experimental results. In Figure 3.2, the agreement between them is within 1% as the pendulum's inertia largely smooths the periodic crutch impulses.

3.5 Optimization Study

An engineering optimization problem provides a rigorous methodology to identify a set of values for the design vector $\bar{x} = \{x_1, x_2, \dots, x_n\}$ when subject to constraints can minimize an objective function $f(x)$ (Geletu, 2007). If the objective function or constraints are not linear functions of the design variables, then it becomes a nonlinear optimization problem of the form

$$\min f(\bar{x}) \tag{3.7a}$$

subject to the constraints

$$\text{boundary: } x_{i,L} \leq x_i \leq x_{i,H}, \ \forall i \in \text{I} \tag{3.7b}$$

$$\text{equality: } g_j(x) = 0, \ \forall j \in \text{J} \tag{3.7c}$$

$$\text{inequality: } h_k(x) \leq 0 \ \forall k \in K \tag{3.7d}$$

For this study, a Simulated Annealing method was applied in the optimization process (Van Larrhoven et al., 1987). Annealing is a heat treatment method used in material science to increase the ductility and reduce the dislocation density of materials. Specifically, materials are heated up and then allowed to slowly air cool. At elevated temperature, particles have sufficient energy to migrate themselves randomly within the lattice. In this manner, particles can arrange themselves into stable sites which have the lowest energy level. The simulated annealing mimics the process of annealing by controlling the rate at which an optimization routine can randomly move to reach a better optimal solution (Wang et al., 2021).

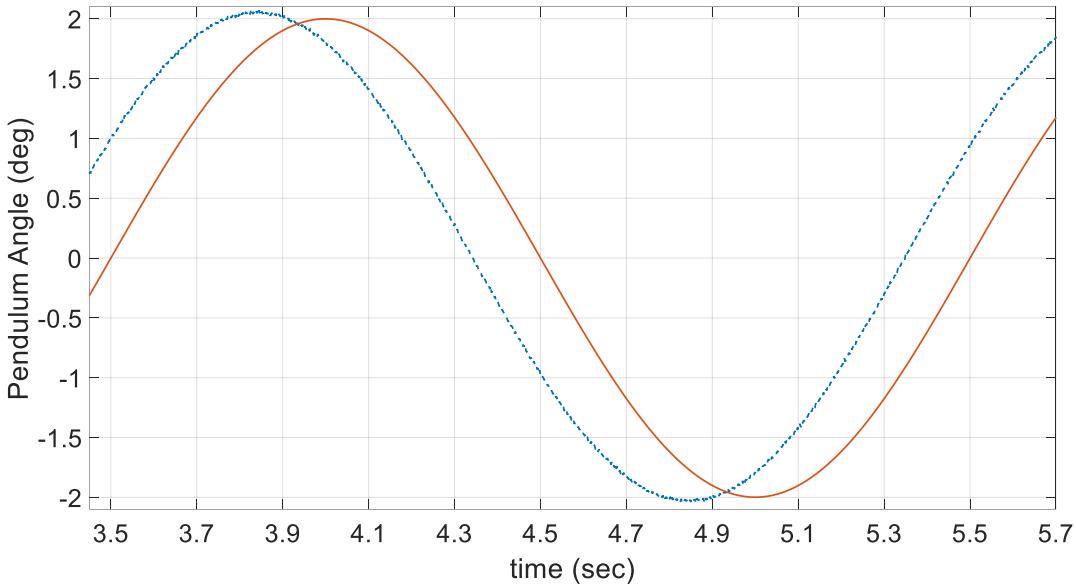

Figure 3.2: Comparison of pendulum angular response for normal clock operation with simulation (solid) and test (dash) results with artificial time-based adjustment to enable signal profiles to be better discerned.

3.6 Case Study – Optimal Design of Pendulum

The mathematical model and simulated annealing strategy will be applied to optimize the mechanical clock's pendulum feature. The design of the pendulum rod and bob was chosen due to the fact that the size and shape influences the weight, quality factor, and accuracy (i.e., period) of the clock. The design vector terms are x_1= L, x_2= R, and x_3= t with upper/lower limits selected based on the general pendulum properties for the target clock.

The objective function is a summation of three parts – weight of the pendulum rod and bob, the quality factor variation from Q_{des}, and accuracy variation from T_{des}.

$$\min (f(x) = \overbrace{k_0(\pi {x_2}^2 x_3 p_{ir} + \mathrm{s} x_1 p_{wo})}^{f_1(x)} + \overbrace{k_1|Q - Q_{des}|}^{f_2(x)} + \underbrace{k_2|T - T_{des}|}_{f_3(x)}) \quad (3.8)$$

Using equation (7), the quality factor and period can be substituted to realize the form where k_0, k_1, k_2 are weighting factors that enable similar magnitudes in the objective function. The step size, X_{st}, was considered based on the design variable box constraints.

The governing equations and optimization algorithm were coded in Matlab™ with a sixth order Runge-Kutta numerical integration method. Two operating scenarios were investigated - (a) Pendulum release from a vertical angle of 2.0° (0.035 rads) which allows the system to experience free oscillation, and (b) Normal clock operation for 10,000 seconds to evaluate accuracy by measuring the period. The study's parameters are listed in Table 3.1.

Symbol	Value	Units	Symbol	Value	Units
A	0.032	m^2	ρ_{ir}	7,800	kg/m^3
B	0.0036	N/rad/s	ρ_{wo}	800	kg/m^3
C_D	1.6	-	Q_{des}	10,000	-
g	9.81	m/s^2	T_0	500	°C
k_0	1	kg^{-1}	T_{des}	2	s
k_1	100	-	T_{end}	66	°C
k_2	0.01	s^{-1}	$x_{1,in}$	0.994	m
N_{A1}	90	teeth	$x_{1,L}$	0.9	m
N_{B1}	18	teeth	$x_{1,H}$	1.1	m
N_{B2}	80	teeth	$x_{2,in}$	0.0825	m
N_{c1}	18	teeth	$x_{2,L}$	0.04	m
Nc_2	96	teeth	$x_{2,H}$	0.15	m
N_{D1}	12	teeth	$x_{3,in}$	0.06	m
N_{D2}	90	teeth	$x_{3,L}$	0.03	m
N_{E1}	12	teeth	$x_{3,H}$	0.15	m
ρ_{ai}	1.225	kg/m^3	x_{st}	[0.005, 0.0005, 0.001]	m

Table 3.1: Summary of model and optimization parameters.

To begin the simulation, the initial annealing temperature was set at T_0 with a design vector of $\bar{x}_1 = \bar{x}_{in} = [x_{1,in}\ x_{2,in}\ x_{3,in}]$ as shown in Figure 3.3. Six neighbors of y_1 or ($[x_{1,in} \pm 0.005\ x_{2,in}\ x_{3,in}]$, $[x_{1,in},\ x_{2,in} \pm 0.001, x_{3,in}]$, $[x_{1,in}\ x_{2,in}\ x_{3,in} \pm 0.001]$) were created based on the step size. The algorithm calculated the weight, Q error, and accuracy error in the objective function, $f(\bar{x}_1)$. Next, a new set of design variables, y_2, was randomly selected among these neighbors and then calculated for the new value of the cost function, $f(\bar{x}_2)$. If $f(\bar{x}_2) < f(\bar{x}_1)$, which corresponds to the new site containing energy that is favorable for the particles, then replace y_1 with y_2 as the next starting point. Otherwise, the chance to accept y_2 is equal to $\exp\left(-\frac{f(\bar{x}_1)-f(\bar{x}_2)}{k_B T_1}\right)$. The reason of possibly accepting a worse answer is to avoid getting struck in a local minimum (Kirkpatrick et al.,

1983). After comparison, the temperature drops to 98% of the initial value. Repeat the above process until the annealing temperature is reached or below the value T_{end}.

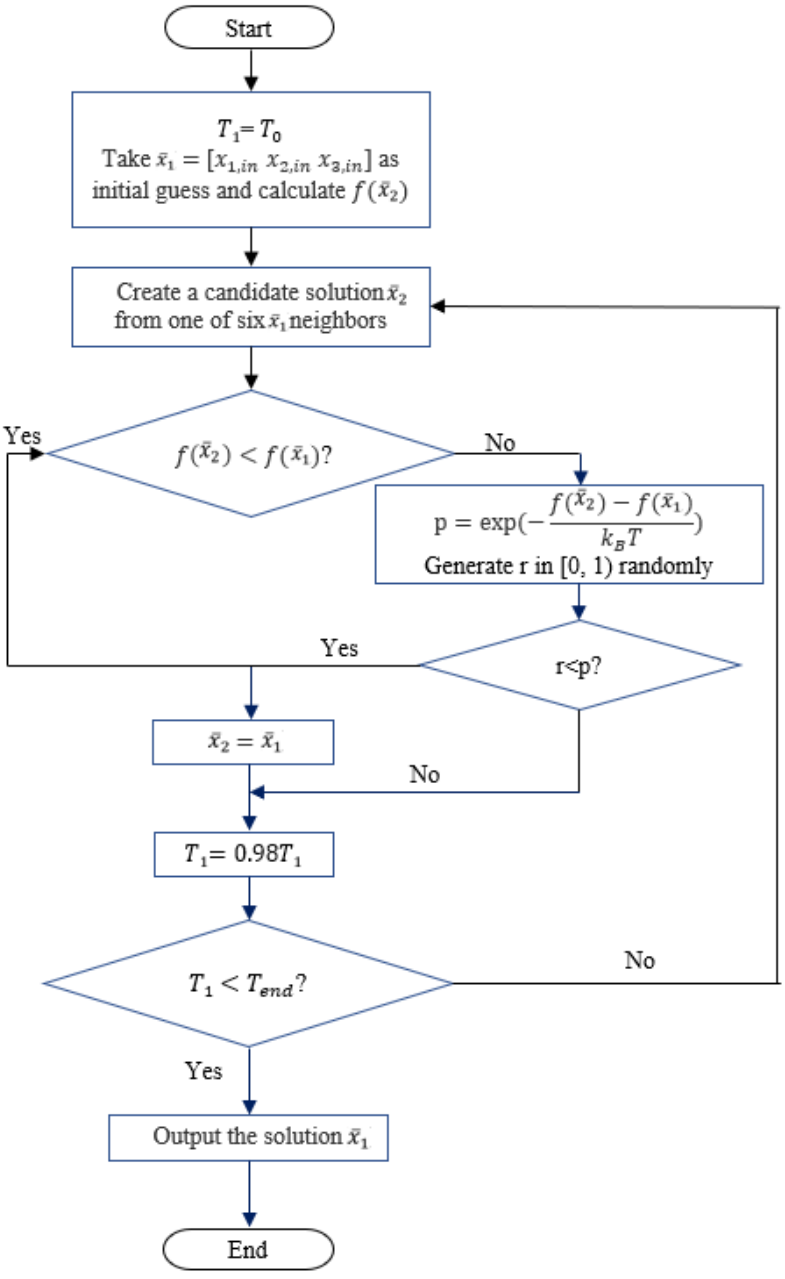

Figure 3.3: Flow chart of simulated annealing algorithm used in the optimization study.

The design study results from the simulated annealing optimization strategy will now be evaluated and discussed. As shown in Figure 3.4, the cost function value drops sharply as the optimization progresses. The quality factor approaches the target of 10,000 gradually while the clock period maintains a constant profile about the desired 2.0 seconds. During the optimization, the design variables x_2= R and x_3= t varied dramatically while x_1= L was relatively constant. This was most evident in Figure 3.4(a). For some iterations the value of cost function increased when the simulated annealing accepted a worse answer. At the end of optimization, the cost function value was $f(x)$ =13.0401 and the three design variables are $\bar{x}_f$= [0.989, 0.0865, 0.063]. Compared to the initial design vector value, $\bar{x}_{in}$= [0.994, 0.0825, 0.06] as measured directly from the E. Howard clock, the final design values differ by [-0.5%, +4.8%, +5.0%]. Specifically, the pendulum bob mass increased by 15% from 10.31 kg to 11.86 kg. On the other hand, the optimized quality factor and clock period equals to 10,015, and 2 seconds, respectively, which are very close to the desired values. The heavier bob enables the pendulum to store more potential energy thus having a higher Q value. Clearly, a tradeoff exists between the mass and the quality factor, this result was also verified by running optimization with different starting points as shown in table 3.2. The production cost of this time piece which must be evaluated by the design engineer and management.

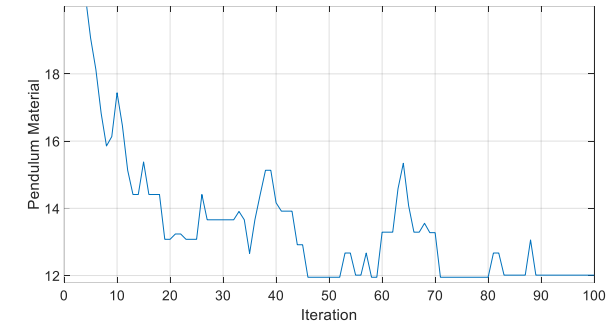

(a)

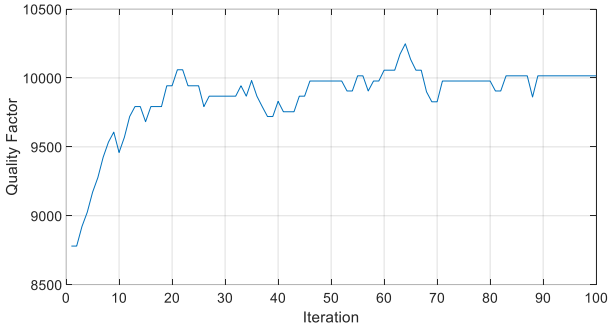

(b)

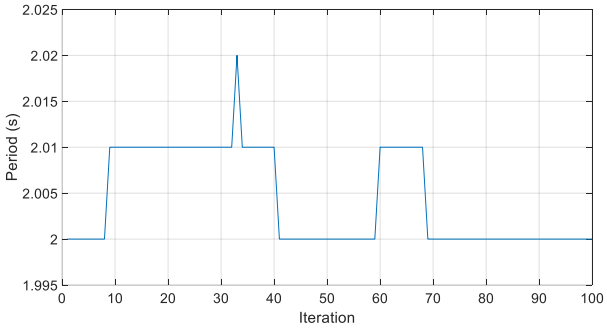

(c)

Figure 3.4: Optimization objective functions verse iteration - (a) $f_1(x)$: Weight, (b) $f_2(x)$: Quality factor, and (c) $f_3(x)$: Accuracy.

Case	Starting Point	Destination	Objective functions Value
A	[0.994, 0.0825, 0.06]	[0.989, 0.0885, 0.06]	11.8883
B	[1.0, 0.095, 0.09]	[0.985,0.079,0.076]	12.1142
C	[0.95,0.06.0.05]	[0.985,0.078,0.078]	12.1828

Table 3.2: Summary of simulated annealing results from different staring points

3.7 Conclusion

In this article, the working principle of a classical mechanical clock with pendulum has been reviewed. A lumped parameter mathematical model has been derived and validated in laboratory testing. To achieve optimum pendulum subsystem mass, quality factor, and clock accuracy, a simulated annealing optimization method has been applied. The numerical results demonstrate that the desired quality factor and period can be achieved with a modest increase in the pendulum bob mass. This study effectively combines dynamic system analysis, modeling, experimental testing, and optimization method in the design of a pendulum clock.

CHAPTER FOUR

MULTI-OBJECTIVE OPTIMIZATION AND TRADESPACE ANALYSIS PF A MECHANICAL CLOCK MOVEMENT DESGIN

Pendulum clocks were the prevalent time keeping standard for centuries to regulate commerce and public activities. These mechanical movements were the most accurate timekeepers globally until replaced by electric clocks. Although mainly used for decorative purposes today, the pendulum clock's working principles and mechanical behavior can serve to demonstrate fundamental science and engineering concepts. The tradeoff between a clock's quality factor, pendulum properties, and period can best be explored with multiple objective optimization and tradespace analysis methods. In this project, a Multi-Objective Genetic Algorithm (MOGA-II) and a Multi-Objective Simulated Annealing (MOSA) optimization approaches are applied to evaluate a Graham escapement street clock for pendulum mass and time accuracy with a range of the period. These clock designs vary the pendulum length, pendulum bob radius, and bob thickness. Horological concepts are used to calculate the overall performance and general utility. The numerical results show a 0.7% increase in the quality factor, and a 0.56% reduction in the mass, while maintaining the designed period by modifying the clock parameters. More importantly, these changes can provide material cost savings in a mass production scenario. Overall, the study highlights the tradeoff designer engineers have considered for decades which can now be visualized using computer tools for greater insight.

4.1 Introduction

A mechanical clock converts potential energy into impulsed oscillating pendulum or balance wheel motion that can be harnessed to display the passage of time. The typical clock uses a hanging weight or coiled spring as the power source to drive the gear train, dial hands, escapement, and pendulum (Wagner et al., 2010). The escapement engages symmetrically with a multi-toothed escape wheel through dual pallets and a crutch to discretize rotational motion into pendulum swing (Penman., 2002). In this manner, the pendulum, usually a round or cylindrical weight on a wooden rod, maintains periodic oscillations. The pendulum's period primarily depends on the rod length with a nominal small-angle of swing. A thin steel suspension spring vertically holds the pendulum while the crutch provides impulsive forces to the rod based on the escapement dynamics. The time display (minutes, hours) is driven by the gear train with a 12:1 motion work ratio for the hours. The innovative design of pendulum clocks served as the global time keeping standard until they were replaced by electric clocks (Denny., 2002). The assorted components within the movement provide a platform to explore design tradeoffs and evaluation of the original factory product using optimization and tradespace analysis methods (Wanger et al., 2008).

The design of a clock movement requires the consideration of various factors including overall size, material selection, timekeeping accuracy, and escapement type. Further, these factors may be influenced by each other. In this study, three fundamental characteristics will be explored – timekeeping accuracy, pendulum mass, and clock period deviation from the reference setpoint. The pendulum clock's accuracy is proportional to its

quality factor, Q, as shown in Figure 4.1 (Matthys., 2004). The quality factor is a dimensionless parameter defined as the ratio of the energy stored to the energy lost in one period (Feinstein., 2006) (Nawrodt., 2008). Therefore, designers may want to maximize Q for better accuracy, which generally corresponds to less system resistance. The pendulum's mass is another essential factor that must be considered in the design phase. In most cases, a small, lightweight pendulum clock is desired by manufacturers as it consumes fewer materials and is easier to ship; however, the energy stored is a function of mass. The period difference from the ideal value contributes to established the daily accuracy. For the target street clock, a 2.0-second period is desired. These three characteristics are directly related to the geometry of the pendulum clock, and tradeoffs exist amongst them. Therefore, a method of determining the best design with optimal overall performance is necessary.

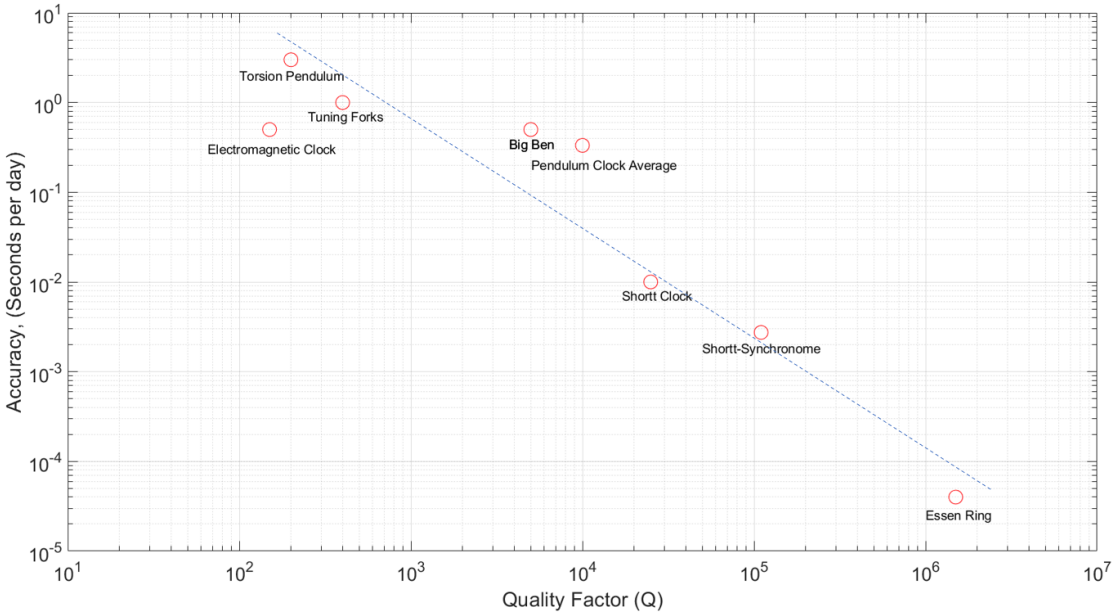

Figure 4.1: Accuracy verse quality factor for mechanical clocks and oscillators

To evaluate these different design criteria, a Multiple Objective Optimization (MOO) method and Tradespace analysis will be applied. In general, engineering problems have conflicting objectives. Specifically, optimizing one objective often results in unacceptable results concerning the others (Burke et al., 2014). Therefore, MOO methods are essential to determine solutions that satisfy all objectives at an acceptable level; such solutions are called optimal solutions [9]. Although single objective optimization offers a unique optimal solution, MOO may provide multiple optimal (Pareto) solutions. Pareto solutions are characterized in that an improvement in one objective will adversely impact at least one of the other objectives. MOO seeks to find the best Pareto solution. One approach is to begin by identifying all of the Pareto solutions and then selecting between them. However, full enumeration of the tradespace of Pareto solutions is usually computationally expensive at best and prohibitive in many cases. Thus, choosing an algorithm to find a subset of desirable Pareto solutions that represent the whole set is vital for MOO (Konak et al., 2006). In this project, Multi-Objective Genetic Algorithm (MOGA-II) and Multi-Objective Simulated Annealing (MOSA) MOO algorithm are utilized. By comparing these results with an iterative approach, the MOO method's effectiveness may be explored in finding optimal solutions. Finally, a tradespace analysis method was applied by determining the highest utility design with a fixed cost to visually investigate the design space.

The optimal design of a pendulum clock with a MOO algorithm and tradespace analysis method will be investigated using a model-based approach with experimental validation. The remainder of the paper is organized as follows: Section 4.2 introduces the

fundamentals of MOO and two algorithms. Tradespace analysis methods will be presented in Section 4.3. In Section 4.4, the mathematical model for a pendulum clock, including escapement, is developed with experimental validation on a street clock. Representative numerical results are discussed to explore the various designs. The summary is contained in Section 4.5.

4.2 Multiple Objective Optimization

Engineering design problems often require the simultaneous optimization of multiple, often conflicting, objectives. A MOO problem can be solved by identifying the design variables, x_i, which are assembled into the design vector, $\bar{x} = (x_1, x_2, \dots, x_n)$, which are subject to the constraints (Geletu et al., 2007)

$$\text{boundary:} \quad x_{i,L} \leq x_i \leq x_{i,H}, \ \forall i \in \text{I} \tag{4.1a}$$

$$\text{equality:} \quad h_j(\bar{x}) = 0, \ \forall j \in \text{J} \tag{4.1b}$$

$$\text{inequality:} \quad g_k(\bar{x}) \leq 0, \forall k \in K \tag{4.1c}$$

to minimize the multiple objective functions, $f_L(\bar{x})$, given as

$$\min \ f_L(\bar{x}) \ \forall l \in \text{L} \tag{4.1d}$$

The individual objective functions usually do not have their minimum value at the same set of design variables. Thus, the tradeoff may need to consider conflicting objectives. A general approach to MOO problems is a Pareto solution, $\bar{x}_p = (x_{p1}, x_{p2}, \dots, x_{pn})$, such that no other solution can dominate it, i.e., a solution does not exist in which the objective functions' values are smaller than $f_i(\bar{x}_p)$. All the Pareto solutions form a set called the

Pareto Frontier. Therefore, the goal is to identify a set of solutions that are as close as possible to, and uniformly distributed over the true Pareto frontier (Konak et al., 2005).

4.2.1 Genetic Algorithm

Genetic algorithms (GA) are popular in finding Pareto solutions for MOO by encoding potential solutions using a "chromosome-like" data structure (Whiley., 1994). The process of natural selection has inspired the GA codes. In natural selection theory, a specie that carries genes fitting the environment has a higher chance of surviving and passing its genes to offspring. Therefore, their genes become increasingly dominant within their population. In some cases, random mutations occur and may change a portion of an individual's genes. If such mutations help individuals survive in the environment, then the new genes will be inherited by further generations. Otherwise, the mutated individual will be eliminated by the natural selection process. GA emulate this process, so each design variable set is called an "individual", and a collection of individuals is called a "population". Individuals consist of genes that are represented by binary strings. An encoding process is required to convert the design variables into such binary strings (Konak., 2006).

Pareto solutions may be achieved by repeating the "crossover" and "mutation" scenario for each iteration in the GA. In the crossover, two individuals (i.e., parents) who were selected based on the fitness of the population are combined to form a new individual (i.e., offspring). The crossover process may randomly select one or more crossover points to cut the genetic sequence into several pieces and swipe them afterward to recombine the sequence for the children. An offspring is expected to inherit the advantages of both of its parents and, therefore, has better fitness. The population will eventually converge by

repeating this process, which means a single design variable set dominates it. Since the crossover leads to similar design variable sets, the mutation step must be included to ensure the diversity of the Pareto solutions. Mutation occurs at the gene level and alters one bit in the genetic sequence from its original state. Thus, new individuals were created that differ from the population.

The MOGA-II algorithm, based on the GA principle, was selected to solve the MOO problem. Although the MOGA-II approach is similar for each GA stage, it uses a directional crossover along with selection crossover and mutation as the MOGA-ii operators. When an individual, In_i, is subject to directional crossover it will create a new individual, In_{i+1}, with two other same generation individuals, $In_{i+2}\ and\ In_{i+3}$, by moving in a randomly weighted direction. These two individuals, $In_{i+2}\ and\ In_{i+3}$, are the best fitness individuals from the two pools, which were created by random walks from the initial individual, In_i. The research shows that directional crossover can achieve better optimization results than the classical crossover (Poles., 2003).

The process of MOGA-II may be described as follows:

1. Generate a pre-set number, N_{in}, of design vectors to form the first-generation P with an empty elite set E $(i.e., E \epsilon Null)$.
2. For each generation, assign a new set with $P' = P \cup E$.
3. Randomly remove individuals in P' until the population of P' is equal to P.
4. Select one of four MOGA-ii operators (e.g., selection, crossover, mutation, directional crossover) based on the set possibilities for each individual of P' to generate the offspring generation P''.

5. Determine the fitness of all individuals in P'' where the fitness is related to the objective functions values.
6. Copy and store all optimal designs into E; remove both non-optimal and duplicate designs.
7. Randomly remove designs in the E if the population of E exceeds P.
8. Set $P''= P$; return to step two.
9. Repeat steps 2-8 until the pre-set iteration number, N_{it}, is reached or other stop criteria is meet.

4.2.2 Multi-Objective Simulated Annealing (MOSA)

MOSA is a randomized search algorithm for approximating the global optimum of multiple objective functions (Amine., 2019). Annealing is a heat treatment method used in material science to increase the ductility, and reduce the dislocation density, of metals. Specifically, materials are heated up and then allowed to air cool slowly. At elevated temperatures, particles may experience random perturbations thus orientating themselves randomly within the lattice. As the temperature goes down the particles are more reluctant to move to the location with higher energy level due to the energy barrier. In this manner, particles can arrange themselves into stable sites with the lowest energy level (Regoni., 2003).

A MOSA algorithm mimics the annealing process by controlling the "cooling rate" at which an optimization routine can randomly move along a direction with a perturbation length, l_{per}, to reach a better optimal solution. At the beginning of the optimization process, select the current annealing temperature as $T_a = T_i$ where T_i is the initial

temperature. A number of solutions, N_{MO}, with $P_1, P_2, \dots, P_n \ and \ P \in R^{nx1}$ were created randomly to form the first starting point. A perturbation may be applied to every element of P to generate additional n individuals as $P_1', P_2', \dots, P_n'$. Afterward, a rank, r_i, was assigned to each of the 2n solutions, from 0 the highest-ranking (i.e., not dominated by any other solutions) to the possible lowest ranking 2n-1 (i.e., dominated by all other 2n-1 solutions). The quantized energy, E_i, is assigned to every solution based on their rank as

$$E_i = \frac{r_i}{2n-1} \tag{4.2}$$

To check whether the P_i perturbation pair, P_i', will replace it as the next starting point, the following condition applies

$$\begin{cases} P_{acc_i} = 1 & if\ \Delta E_i \leq 0, \\ P_{acc_i} = e^{\left(-\frac{\Delta E_i}{T_a}\right)} & if\ \Delta E_i > 0 \end{cases} \tag{4.3}$$

where P_{acc_i} is the chance that P_i will be replaced by its perturbation pair, P_i'. The variable $\Delta E_i = E_{p_{i'}} - E_{p_i}$ is defined as the energy difference between them. When $\Delta E_i \leq 0$, which means the perturbation state is energy favorable and the new state will be accepted as the next starting point. Otherwise, the chance to accept the perturbation state is equal to $e^{\left(-\frac{\Delta E_i}{T_a}\right)}$. The possible acceptance of a worse answer occurs when the designers may be concerned about becoming stuck in a local minimum.

The temperature T_a was modified according to the set rule. In MOSA, the temperature profile (as shown in Figure 4.2) was separated into two phases with

$$T_a = \begin{cases} \left(1 - \frac{N}{N_{hot}}\right)^2 T_i & ;\mathrm{N} < N_{hot} \\ 0 & ;Otherwise \end{cases} \tag{4.4}$$

where N is the current iteration number, and N_{hot} is the hot iteration number. The temperature profile starts with the hot phase, N<N_{hot}, which is followed by a cold phase, $N \geq N_{hot}$. When the total phase iteration number, N_{tot}, was reached, the optimization stops. In the hot phase, $T_a > 0$ and $P_{acc_i} > 0$. Thus, it is possible to accept a worse solution. As the temperature drops, P_{acc_i} also decreases with $\Delta E_i > 0$. Eventually, in the cold phase, $T = 0$, and no worse solution will be accepted, leading to final convergence (Rigoni., 2003).

The perturbation direction and length are controlled separately. The perturbation direction is random and uniformly distributed. The length of the perturbation vector is a random value that follows the Gaussian distribution with a null mean value and unity standard deviation. It is scaled with the perturbation length parameter, $l_{per} \in [0, 1]$. The perturbation length is the fraction of the diagonal of a unitary hypercube in the N-dimensional variable space, and it is governed by the perturbation length scheduler with

$$l_{per} = \begin{cases} (l_i - l_{min})\left(1 - \frac{N}{N_{hot}}\right)^2 + l_{min}; & \mathrm{N} < N_{hot} \\ l_{min} \quad ; & Otherwise \end{cases} \tag{4.5}$$

where l_i is the initial perturbation length. Similar to temperature, the value of l_{per} gradually decreases after each iteration in the hot phase until reaching the minimum perturbation direction, l_{min}, at the end of the hot phase. It maintains this value during the cold phase (Rigoni., 2003).

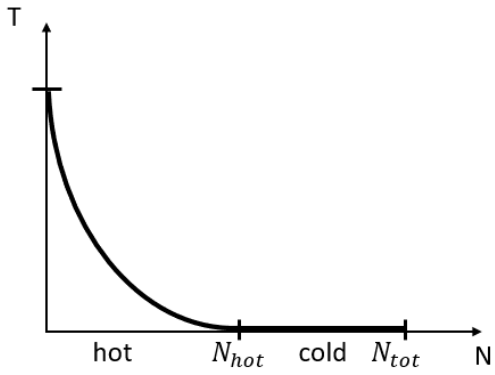

Figure 4.2: MOSA temperature scheduler.

4.3 Tradespace Analysis

The tradespace analysis is a visual process that enables design engineers to recognize capabilities, gaps, and potential tradeoffs that facilitate the meeting of system performance objectives (Spero et al., 2014). Models are developed to simulate the attributes of a product based on its user's preferences and further guide the design choice. These choices are then varied systematically to produce tradespace representation. Tradespace is the space of possible design options with a given set of design variables viewed in the performance objective space. Simply put, in tradespace analysis, performance capabilities are visualized.

The attributes define the system completely, which means by naming their values, people can understand how well the system reaches its overall objectives. These attributes are then aggregated into a single utility function, u_{tot}. The utility function, is a dimensionless variable that measures relative gratification by allocating the resources of an attribute. The total utility function allows the comparison of different system practicality by assigning weighting factors to every attribute. Finally, a cost model will be applied to

provide a metric to compare the estimated expense for each design. These actions enable a utility-cost plot to be created to help find the highest utility for a fixed cost (Ross et al., 2005). Similar to the MOO, the optimal design Pareto Frontier can be identified through design variable variation. Utility variables usually range from zero (minimal acceptable) to one (most desirable). Consequently, a size rule was applied to calculate the proposed system attribute. The system designs were then evaluated in consideration of the utility magnitudes to understand which design best satisfies the needs.

4.4. Case Study

The classical E. Howard Model 00 street clock movement from 1905 features an external weight driven gear train, escapement, and large pendulum. A mathematic model will be developed followed by experimental validation and optimization of the pendulum subsystem.

4.4.1 Mathematic Model

The pendulum clock with escapement provides an opportunity to derive a nonlinear dynamic system model. The hanging mass, M, acts on the winding drum of radius R_A to provide a torque $T_w = MgR_A$ that drives the movement. The gear train features five shafts or arbors, shown in Figure 2.3 and 2.4, that significantly reduces the torque that acts on the escapement. For this clock, the train ratio, R_t, can be expressed as (2.2)

The torque acting on the escape wheel, T_e, becomes $T_e = \frac{1}{R_t} T_w$.

The escapement provides energy to the pendulum to overcome the losses due to friction and aerodynamic forces. The escapement model was developed based on the following four assumptions:

A1.The escapement engages and disengages with the pendulum at the pendulum swing angle of $\pm\theta_e$ which is a specification for the target clock movement.

A2. The impulsive torque accelerates the pendulum to maintain oscillatory motion.

A3. The angular motion of the pendulum, θ, is symmetric.

A4. The system maybe considered stable in a dynamic sense when the angular amplitude of the pendulum's oscillation, θ, ends between $0.7\theta_e < \theta < 1.5\theta_e$.

The torque, T_A, applied by the escapement anchor to the pendulum crutch becomes

$$T_A = S_1 S_2 T_e \tag{4.6}$$

where $S_1 and\ S_2$ are relational digital variables that control the impulse sign based on the pendulum's angle such as

$$S_1 = \begin{cases} 1; & if\ \dot{\theta} > 0 \\ 0; & if\ \dot{\theta} = 0 \\ -1; & if\ \dot{\theta} < 0 \end{cases} \qquad S_2 = \begin{cases} 1;\ if\ -\theta_e \leq \theta \leq \theta_e \\ 0;\ otherwise \end{cases} \tag{4.7}$$

In this manner, the pendulum swings back and forth at a fixed period with regular impulses.

The dynamic model for the pendulum oscillation angle, θ, becomes

$$J\ddot{\theta} + B\dot{\theta} + mgLsin\theta + LF_{ai} = T_A \tag{4.8}$$

where $J = mL^2$ is the pendulum's moment of inertia which assumes a point mass, and B is the damping coefficient. The impulsive torque, T_A, arises every half-period due to the escape wheel and crutch drive torque. An aerodynamic drag force, F_{ai}, primarily acts on

the pendulum bob to dissipate energy as it swings through the air. This force requires the drag coefficient, C_D, the surface area of the bob (and rod) acted on by the air, A, the air density, ρ_{ai}, and the translational velocity of the bob, $L\dot{\theta}$, to calculate as

$$F_{ai} = \frac{1}{2} C_D A \rho_{ai} (L\dot{\theta})^2 \tag{4.9}$$

The design of the pendulum system, refer to Figure 3(a), was explored given its importance for clock precision. For this subsystem, the total pendulum mass, m, depends on the radius of the bob, R, the thickness of the bob, h, the rod length, L, and the rod radius, r, so that

$$m = (\pi R^2) h \rho_i + (\pi r^2) L \rho_w \tag{4.10}$$

where ρ_i and ρ_w are the density of the cast iron and the wood, respectively. The minimum, m_L, and maximum, m_u, pendulum mass values to maintain the system motion are define a priori given the design space operating limitations.

4.4.2 Experimental Validation of Mathematical Model

To validate the tower clock mathematical model, the E. Howard clock movement was experimentally investigated. Three cube-shaped high flux magnets were attached to the escape wheel pivot, crutch pivot, and pendulum using epoxy putty and a drop of adhesive. A high resolution magnetic field angular position sensor (Honeywell APS00B) with a pair of linear amplifiers (Analog Device AD623) was placed on a stick opposite each magnet as shown in Figure 3.1. These magnetic signals were converted to digital signals and supplied to the National Instrument ELVIS™ data acquisition system. The host laptop procured the data files using LabView™ and Matlab™. During the experimental testing, the crutch was also removed and the pendulum was released from an angular

position of 2.12°. The time constant ,τ, was measured by determining the elapsed time for the initial amplitude to drop by 63.2% or 0.632*2.12°=1.34°. The time constant for this E. Howard tower clock movement was experimentally determined to be $\tau = 5599$ seconds. A portion of the pendulum's angle vs. time is shown in Figure 2.5 which offers the time constant free response. The operation of the escapement was also recorded and used to validate the mathematical model. Further, the various system parameters were carefully measured using a caliper and other laboratory tools.

4.4.3 Optimization Problem

The optimization problem was explored using MOO with MOGA-II and MOSA algorithms. The mechanical clock's overall accuracy was investigated with the design of the pendulum system's mass, Quality Factor, and period. In a pendulum system, a higher Q value tends to be more accurate due to the lower rate of energy loss. For an oscillatory system, the quality factor can be calculated as

$$Q = \pi f_0 \tau \tag{4.11}$$

where f_0 is the system's natural frequency, and τ is the exponential time constant. For a small pendulum swing, the period, $T = 1/f_0$, can be expressed as

$$T = 2\pi\sqrt{L/g} \tag{4.12}$$

so that equation (12) becomes

$$Q = \frac{\tau}{2}\sqrt{\frac{g}{L}} \tag{4.13}$$

Three clock parameters, $x_1 = L$, $x_2 = R$, and $x_3 = h$, were selected as the design variables. The optimization problem may be stated as

$$\min \ (f_1(x): \pi x_2^2 x_3 \rho_i + \ \pi r^2 x_1 \rho_w) \tag{4.14a}$$

$$\min \ (f_2(x) = -Q) \tag{4.14b}$$

$$\min \ (f_3(x) = |T - T_{des}|) \tag{4.14c}$$

Subject to:

$$x_{i,L} \leq x_i \leq x_{i,H} \tag{4.14d}$$

For this study, the system and optimization parameters are listed in Table 4.1. The other MOGA-ii and MOSA parameters that have not been included in Table 1 were set at default values. Overall, 2500 solutions were created during the MOGA-ii and MOSA optimization process. For comparison, the iterative method also generated 2500 solutions between the upper and lower limit of design variables.

Symbol	Value	Units	Symb	Value	Units	Symbol	Value	Units
A	0.032	m^2	N_{A1}	90	teeth	T_{des}	2.0	s
a_1	-0.035	-	N_{B1}	18	teeth	T_i	0.1	-
a_2	$4 * 10^{-5}$	-	N_{B2}	80	teeth	T_o	2.0	s
a_3	-5	-	N_{c1}	18	teeth	T_{des}	2.0	s
B	0.0036	N/rad/s	Nc_2	96	teeth	$x_{1,L}$	0.9	m
b_1	1.175	-	N_{D1}	12	teeth	$x_{1,o}$	0.994	m
b_2	0.125	-	N_{D2}	90	teeth	$x_{1,U}$	1.1	m
b_3	1	-	N_{E1}	12	teeth	$x_{2,L}$	0.06	m
C_D	1.6	-	N_{hot}	25	-	$x_{2,o}$	0.0825	m
C_{ir}	10.68	€/kg	N_{in}	50	-	$x_{2,U}$	0.12	m
C_o	14.24	€/m	N_{it}	50	-	$x_{3,L}$	0.04	m
g	9.81	m/s^2	N_{MO}	50	-	$x_{3,o}$	0.06	m
l_{min}	0.05	-	N_{tot}	50	-	$x_{3,U}$	0.08	m
M	13.6	kg	Q_o	8,783		ρ_{ai}	1.225	kg/m^3
m_L	5	kg	R_A	0.0762	m	ρ_i	7,800	kg/m^3
m_o	10.316	kg	R_t	1333.33		ρ_w	800	kg/m^3
m_U	25	kg	r	0.011	m	θ_e	0.02	rad

Table 4.1: Summary of model and optimization parameters.

The governing equations and MOO were coded in MATLAB™ and a two steps process followed. First, the pendulum was released from a vertical angle of θ = 2.0° (0.035 rads), allowing the system to experience free oscillation. The time constant, τ, was calculated by determining the elapsed time for the initial amplitude to drop by 63.2% or 0.632*2°=1.264°. The variables m and Q were computed for every solution. Second, the pendulum received an impulsive torque, T_A, (i.e., engage and disengage with the pendulum rod every half period) due to the clock escapement. The period was calculated after the clock was operating for 600s. Afterwards, the results were supplied to the

modeFRONTIER® tool where the multi-objective optimization process was performed. The simulation and optimization process has been displayed in Figure 4.3.

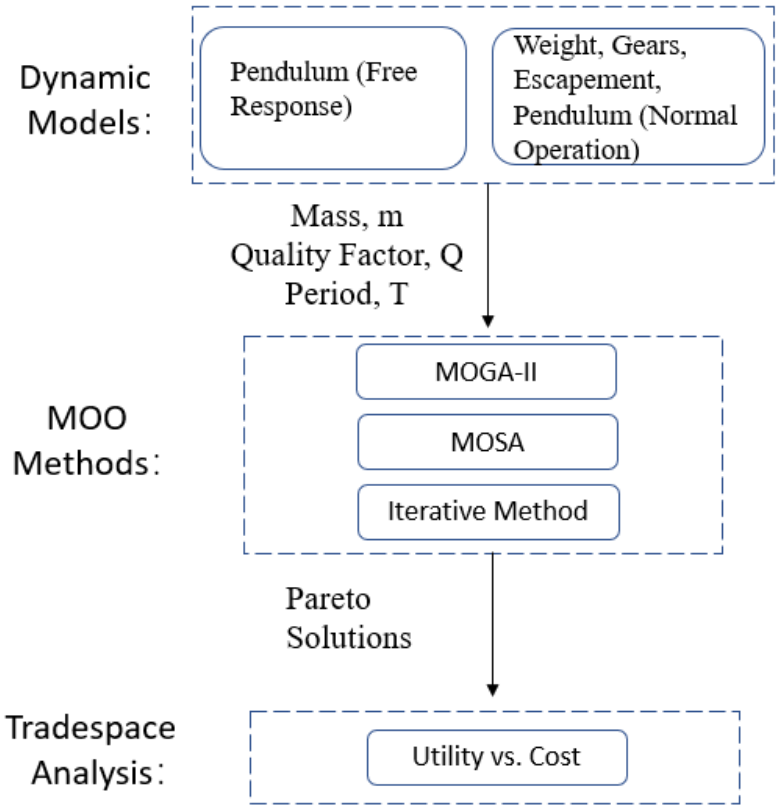

Figure 4.3: Summary of the simulation and optimization process

4.4.4 Optimization Results

All of three MOO methods are supposed to generate Pareto solutions, however, the number of feasible and Pareto solutions is an indicator of the effectiveness of the MOO method. Three groups of 2500 solutions were collected and further analyzed in MATLAB™ and modeFRONTIER® to obtain the feasible and Pareto solutions. The high level results are summarized in Table 4.2. It may be observed that the MOSA, MOGA-II

and iterative method all reach the real Pareto-frontier and preserve the computations in the feasible region.

No.	Method	Total Solutions	Feasible Solutions	Pareto Solutions
1	MOSA	2500	2469	1149
2	MOGA-II	2500	2467	1162
3	Iterative method	2500	2410	1105

Table 4.2. Summary of MOO methods results

To offer insight into the design process, the MOGA-II method (o) Pareto solutions and the original E. Howard clock's design (Δ) are shown in Figure 4.4. The optimal design was dominated by the Pareto solution, $\bar{x}$ = [1.002,0.089,0.051], which corresponds to a mass of 10.258 kg, a quality factor of 8843, and a period of 2.0 s. The original 1905 design was $\bar{x}_o$= [0.994, 0.0825, 0.06] as measured directly from the E. Howard clock. When comparing these two solutions, the optimal design values differ by $\Delta\bar{x}$ = [+0.8%, +7.9%, -15%]. In terms of the objective functions, the differences are a 0.56% reduction in the mass, a 0.7% increment in the Quality Factor, and a value of similar period.

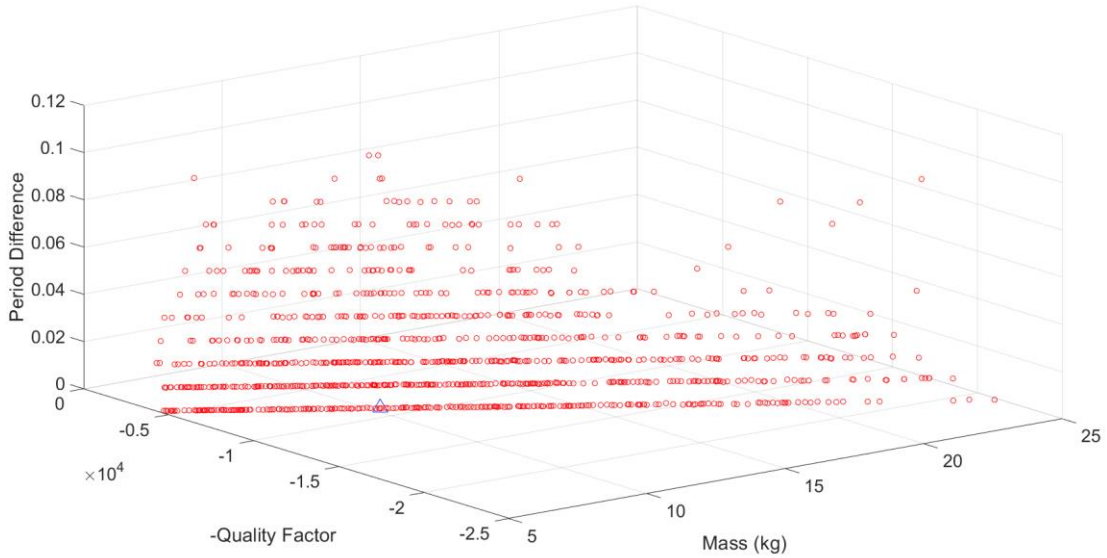

Figure 4.4: MOGA-II Pareto solutions (o) and original design (Δ) for the tower clock

4.4.5 Tradespace Analysis

Tradesapce analysis enables the investigation of the design with the highest utility at a fixed cost among the MOO-based Pareto solution. The pendulum subsystem features were translated into a single linear utility function, u_{tot}, given as

$$u_{tot} = w_m v_m + w_Q v_Q + w_{\Delta T} v_{\Delta T} \tag{4.15}$$

where w_i is the weighting factor that allows emphasis of different aspects as shown in Table 4.3.

Design Aspect	Description	Weighting		
		w_m	w_Q	$w_{\Delta T}$
A	Smaller Mass	0.6	0.3	0.1
B	Higher Accuracy	0.3	0.6	0.1
C	Nominal Design	0.4	0.4	0.2

Table 4.3: Proposed weighting factors for design aspects A-C in mechanical clock study

The clock pendulum financial cost was estimated based on the mass of the materials used in the design excluding manufacturing. A typical pendulum was made of cast iron, ρ_i, for the bob; and wood, ρ_w, for the rod. For the bob and the rod shape materials, the prices of the cast iron C_{ir}, and the oak, C_o, were assigned per the current market values. The minimum and maximum values of the MOO Pareto solutions are listed in Table 4.1. A linear utility relationship has been assumed between the mass, the Quality factor, and the period difference so that

$$v_m = a_1 m + b_1 \tag{4.16a}$$

$$v_Q = a_2 Q + b_2 \tag{4.16b}$$

$$v_p = a_3 |T - 2| + b_3 \tag{4.16c}$$

To explore the utility function, one of the tower clock design aspects will be presented with comparisons to the original design. Figure 4.5(a) displays the tradespace analysis for Design Aspect B (Higher accuracy) with utility vs. cost; each point represents an optimal solution obtained by the MOGA-II method. In Figure 4.5(b), a clear Pareto Frontier, which indicates desirable designs, can be extracted. The original design of the pendulum clock is also shown on this plot with a Δ symbol. It can be observed that the original design is slightly off the Pareto Frontier which means that the total utility of original design could be enhanced further without a price increase. The tradespace results of other Design Aspects can be found in appendix G.

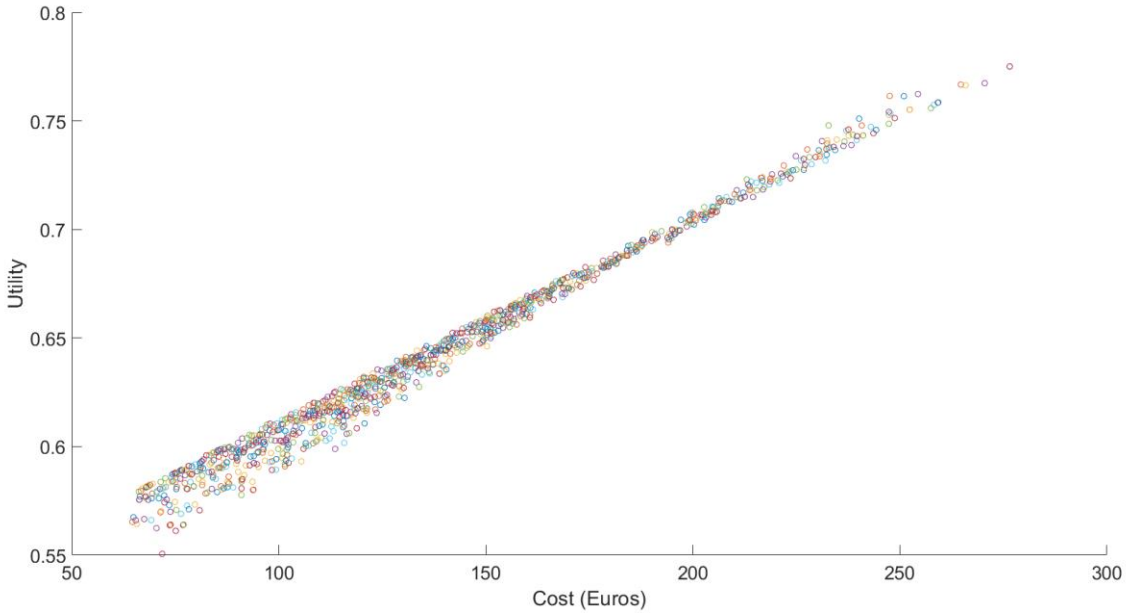

(a)

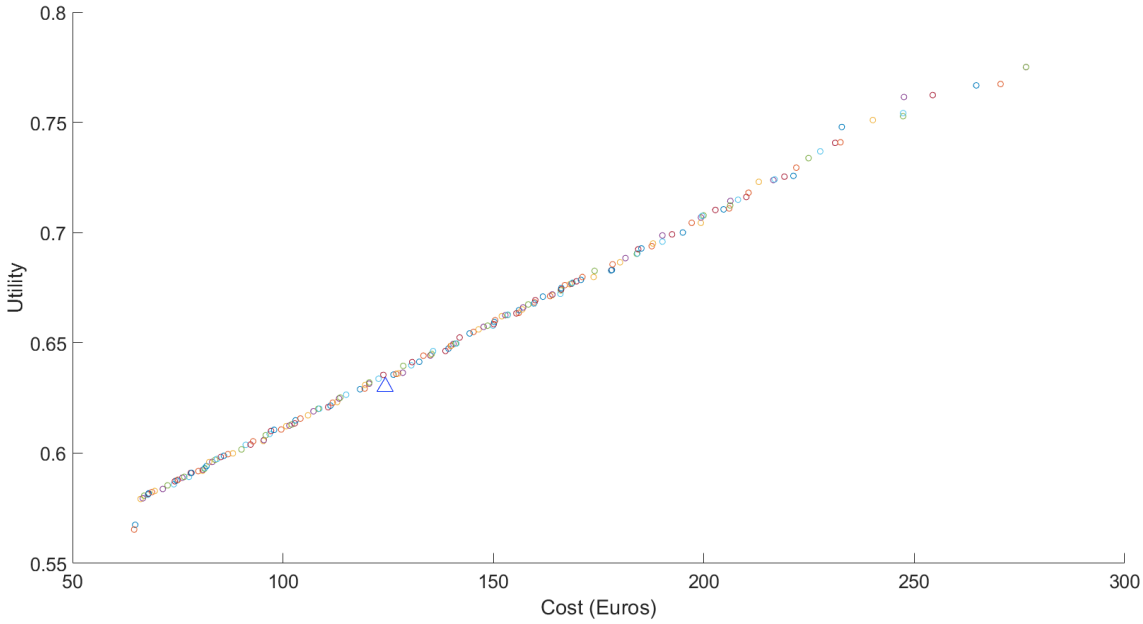

(b)

Figure 4.5. Optimization study results - (a) Tradespace analysis result for Design Aspect B, and (b) Selected optimal designs with original E. Howard design shown in the Δ symbol.

4.5 Conclusion

The working principle of a classical pendulum mechanical clock and three system parameter design, the MOO, and the tradespace analysis method has been reviewed. A lumped parameter mathematical model of the pendulum clock has been developed. To achieve optimum pendulum design, its mass, quality factor, and clock accuracy have been explained with two MOO methods. The MOGA-II/MOSA algorithm is efficient in finding the Pareto optimal solutions compared to an iterative method. The MOO results also demonstrate that a better quality factor lightweight design can be achieved without changing the original period. The tradespace result further expands the possible design option for the pendulum clock.

CHAPTER FIVE

CONCLUSION

This research shows how virtual engineering design plays an essential role in modern design. With the aid of virtual engineering, the development of a physical model is no longer required. Thus, the cost and complexity have been reduced compared to the traditional design process. Furthermore, many potential pendulum designs have been generated and evaluated with appropriate models and optimization algorithms. In this manner, the tedious iterative process has been skipped as well. With the application of the virtual engineering design technique on the E. Howard Model 00 pendulum clock, we proved that compared to its original design, an optimum design with better accuracy, a lower mass, and the desired period existed.

5.1 Research Summary

Design and optimization are two core concepts of engineering disciplines. This thesis has discussed the formulation of these two concepts in detail. Engineering design is an iterative process, usually repeating the same process to modify the current design and compare this design with the initial design. The whole process may be tedious. By applying optimization, the iterative process can be largely removed and evaluate all alternative designs simultaneously. Therefore, optimization expedites the process of engineering.

Mathematic model creation is the essential step of simulation in this research; good models are supposed to have the same or very similar behavior and performance as the system. In this research, two models representing the pendulum and escapement subsystem have been built. The pendulum subsystem has been used to simulate the free response of

the pendulum, and the Quality Factor can be obtained by implementing this model. And the escapement subsystem has been used to simulate the clock's regular running to get the pendulum's period for different designs. The experiments have been conducted to validate these two models. During the experiments, magnetic sensors and amplifiers were used to record the movement of the pendulum and escapement, which were attached by magnets. And the Quality Factor of E. Howard Model 00 is also determined in this manner. Experiments were conducted to validate all the models could represent the corresponding subsystems.

A total of three optimization algorithms have been applied in this research: simulated annealing, MOGA-ii, and MOSA. Their ideas have been discussed extensively in the thesis. The simulated annealing algorithm mimics the annealing process to approach a global optimum solution which is achieved by setting a possibility of accepting a worse answer with progressively decreasing as the optimization proceeds. MOGA-ii algorithm is based on the genetic algorithm; potential solutions with the highest fitness were selected to crossover and mutation to form new solutions. By repeating this process, the solution becomes convergence eventually. MOSA is similar to the simulated annealing algorithm, except it is applied to the MOO problem. All of these algorithms were implemented under the same geometry constraints.

By using Simulated Annealing in SOO, we confirmed the desired Quality Factor could be achieved by modifying the pendulum rod length and the pendulum bob's radius and thickness. Such geometry modification results in a 15% increment in the mass without a change in the clock's period. This result also proves a tradeoff between the pendulum's

mass and its Quality Factor. In other words, the increment of accuracy can be achieved by sacrificing the lightweight of the pendulum clock and vice versa.

With the application of MOGA-II and MOSA, two MOO algorithms, we explored the optimized designs for the same movement with lightweight accuracy and desire period as objective functions. The MOO results show a 0.7% increase in the quality factor and a 0.56% reduction in the mass while maintaining the designed period by modifying the clock parameters. It proved that the original design of the E. Howard Model 00 still has room for improvement in terms of lightweight and accuracy at the same time. By further analyzing the MOO result, it was evident these two MOO algorithm is efficient in finding the Pareto optimal solutions compared to an iterative method.

A relatively new concept, tradespace analysis, has been discussed in this thesis; it enabled us to consider economic factors when designing a pendulum clock. With tradespace analysis based on the results of MOO, we can identify a number of optimum designs with the highest utility at a fixed cost or lowest cost for a fixed utility. These results are promising in material cost savings in a mass production scenario. Table 5.1 summarizes the simulation and experiments that were completed at all stages of the research.

	Models	Single Optimization	Multiple Optimization	Trade Space Analysis	Experiments
	(A) Pendulum (free Response) (B) Escapement, Weight, Gears, Pendulum	(i) Simulated Annealing	(I) MOGA (II) MOSA (III) Random Solution	(1) ModeFrontier® with Tradespace Analysis	(A) Pendulum Subsystem Validation (B) Escapement Subsystem Validation (*)
Chapter 3	A&B	(i)			A&B
Chapter 4	A&B		(I),(II),(III)	(1)	A&B

Table 5.1: Summary of simulation and optimization in the research

(*Supplemental experiments results can be found in Appendix E)

This research applied computational tools extensively, including building a three-dimensional model of the E. Howard Model 00 in SolidWork™ software package and a two-dimensional schematic diagram of the clock's time train in Inventor™. Those two models help visually illustrate the pendulum clock's working principle. Matlab™ was used

to implement the mathematic model and conduct SOO optimization. Two MOO algorithm have been performed in Modefrontier^{TM} combined with Matlab^{TM}. Furthermore, all the data was also processed and analyzed by Matlab^{TM}. It is evident that computational skills are increasingly necessary for modern research.

The design and working principle of the pendulum clock has been reviewed, and the importance of the Quality Factor was discussed. A literature review concluded that Quality Factor is proportional to the accuracy of the pendulum clock and other oscillators and thus must be considered in engineering design.

5.2 List of Recommendations

The following work is recommended for future study:

A. Extend the research to other street and tower clocks to explore the optimized parameters of different mechanical systems. This research provides methods that could be applied to any clocks with escapement and pendulum system, only minor changes to the codes are required.

B. Implement MOO by selecting different objective functions, for example, the manufacturing cost can be optimized if the information of the unit manufacturing cost of the pendulum rod and bob can be acquired.

C. Develop mathematical models for different subsystems of the pendulum clock (e.g., gear trains) and conduct corresponding experiments to validate the models. If the friction between gears and between gears and arbors can be experimentally measured, the mathematical model can also be developed.

D. Incorporate the design of gears (number of teeth, materials of the gears) into the optimization and tradespace analysis. After the gear train subsystem is developed, the MOO could include this model to explore the mechanical behaviors of gears of different designs and select the optimized design.

E. Develop codes to automate the engineering design cycle fully. After developing and validating all major subsystems of the pendulum clock. All the parameters of the pendulum can be automatically optimized by running the optimization code.

The completion of optimization may establish a standard for the pendulum clock and its subsystem design for mass production. And the whole process of optimization of this pendulum clock can serve as a case study for a graduate level design and optimization course. Students are expected to have a better understanding of design concepts through this practical example. Finally, complete optimization of this classical mechanical model will provide insight into other complex and advanced systems designs, for example, micro or nano-sized machines.

APPENDICES

Appendix A

Numerical Integration

The gerenal form of the Runge-Kutta method may be stated as

$$x(t+h) = x(t) + \frac{16}{135}k_1 + \frac{6656}{12825}k_3 + \frac{28561}{56430}k_4 - \frac{9}{50}k_5 + \frac{2}{55}k_6 \quad \text{(A.1)}$$

where h is step size and the individual k_i terms are

$$k_1 = h * f(t, x) \quad \text{(A.2)}$$

$$k_2 = h * f\left(t + \frac{1}{4}h, x + \frac{1}{4}k_1\right) \quad \text{(A.3)}$$

$$k_3 = h * f\left(t + \frac{3}{8}h, x + \frac{3}{32}k_1 + \frac{9}{32}k_2\right) \quad \text{(A.4)}$$

$$k_4 = h * f\left(t + \frac{12}{13}h, x + \frac{1932}{2197}k_1 - \frac{7200}{2197}k_2 + \frac{7296}{2197}k_3\right) \quad \text{(A.5)}$$

$$k_5 = h * f(t + h, x + \frac{439}{216}k_1 - 8k_2 + \frac{3680}{513}k_3 - \frac{845}{4104}k_4) \quad \text{(A.6)}$$

$$k_6 = h * f(t + \frac{1}{2}h, x - \frac{8}{27}k_1 + 2k_2 + \frac{3544}{2565}k_3 + \frac{1859}{4104}k_4 - \frac{1}{5}k_5) \quad \text{(A.7)}$$

Appendix B

MATLAB Code for Chapter Three

B.1 SOO Simulated Annealling Code

```
% This code intends to optimize design varibables in SOO by using simulated
% anealing method
clear all
initial = [0.994 0.0825 0.06]; %set current initial value of design
cost_initial = 22.5097; % run runge-kutta method with initial value to get initial cost
Quality_initial=8780;
Period_initial = 2;
lb = [0.9,0.04,0.03];
ub = [1.1,0.15,0.15];
stepSize = [0.005, 0.0005, 0.001];
A.position = initial;
A.cost     = cost_initial;
A.Quality  = Quality_initial;
A.Period   = Period_initial;

T0=1;       % Initial Temp.
T=T0;
alpha=0.99;     % Cooling factor
maxIteration = 100;

for iter = 1: maxIteration
   trajectory(iter).position = A.position;
   trajectory(iter).cost = A.cost;
   trajectory(iter).Quality= A.Quality;
   trajectory(iter).Period= A.Period;

   [B,Quality,Per] = generateNeighbours4SA(A , stepSize, lb, ub);
   % generate a random point through function

   Delta = A.cost - B.cost;
   if Delta > 0  % downhill move (good move)
      A.cost = B.cost;
      A.position = B.position;
      A.Quality= B.Quality;
      A.Period= B.Period;
   else         % uphill move (bad move)
      P=exp(Delta/(T*1));
      if rand<=P
```

```
            A.cost = B.cost;
            A.position = B.position;
            A.Quality= B.Quality;
            A.Period= B.Period;
        end
    end

    % Update Temp.
    T=alpha*T;
end
subplot(3,1,1);
plot([trajectory.cost]);
xlabel('Iteration')
ylabel('Cost')
set(gca,'FontSize',30)
yticks ([12:2:18])
ylim([12 20])

subplot(3,1,2);
plot([trajectory.Quality]);
xlabel('Iteration')
ylabel('Q')
set(gca,'FontSize',30)

subplot(3,1,3);
plot([trajectory.Period]);
xlabel('Iteration')
ylabel('Period (s)')
set(gca,'FontSize',30)
```

B.1.1 Objectivefunction

```
% This code define the objective function and is called by simulatedAnneal
function[o]= objectiveFunction(v,t0,Per)
o= (pi.*v(2).^2.*v(3).*7800+3.8795e-04.*v(1).*800)+0.01*abs(1/2*(9.81/v(1)).^0.5*t0-
10000)+100*abs(Per-2);
end
```

B.1.2 generateNeighbours4SA

```
% This code define the neibour of current solution and is called by simulatedAnneal
function [Neighbour,Quality,Per] = generateNeighbours4SA(currentSolution , stepSize,
lb, ub)
nVar = 3;
idx = 0;
```

```
    for j = 1 : nVar
        idx = idx + 1;
        stepVector = zeros(1,nVar);
        stepVector(j) = stepSize(j);
        Neighbours(idx).position = currentSolution.position + stepVector;
        if Neighbours(idx).position(j) > ub(j)
            Neighbours(idx).position(j) = ub(j);
        end
        if Neighbours(idx).position(j) < lb(j)
            Neighbours(idx).position(j) = lb(j);
        end
        idx = idx + 1;
        stepVector = zeros(1,nVar);
        stepVector(j) = stepSize(j);
        Neighbours(idx).position = currentSolution.position - stepVector;
        if Neighbours(idx).position(j) > ub(j)
            Neighbours(idx).position(j) = ub(j);
        end
        if Neighbours(idx).position(j) < lb(j)
            Neighbours(idx).position(j) = lb(j);
        end
    end

    idx = floor(length(Neighbours)* rand() + 1); % randomly select one point from six
generated points
    RKFsolver % call Runge-kutta-Fehlberg method to calculate t0 value
    Neighbours(idx).cost = objectiveFunction(Neighbours(idx).position,t0,Per);
    Neighbours(idx).Quality=Quality;
    Neighbours(idx).Period=Per;
    Neighbour = Neighbours(idx);
```

B.1.2.1 RKFsolver

```
% This code intends to solve 2st order ODE by using Runge-kutta-Fehlberg method and
is called by generateNeighbours4SA
l=Neighbours(idx).position(1);
R=Neighbours(idx).position(2);
T=Neighbours(idx).position(3);

g = 9.81;
c = 0.00165;                % damping force coefficient in n/rad/s
Cd = 1.6;                   % the drag coefficient of the pendulum          system
dimensionless
pa = 1.225;                 % the density of air in kg/m^3
```

```
s  = pi*(0.022225/2)^2;          % the area of rod in m^2
p1 = 800;                    % the density of oak im kg/m^3
m1 = s*l*p1;                   % the mass of rod in kg
p2 = 7800;                   % the density of bob in kg/m^3
m2  = p2*pi*R.^2*T;             % the mass of bob in kg
m = m1+m2;                    % the mass of entire pendulum in kg
A1 =l*(0.02225);               % the area of rod in meter^2
A2 = 2*R*T;                   % the are of bob in meter^2
A = A1+A2;                    % the total reference area of pendulum in meter^2

% Inputs and Declaration
h = 0.01; % solution stepsize
% Function declaration x=theta y=d(theta)/dt
% f1: dx/dt=y;
% f2: dy/dt=[-c/(ml^2)](dx/dt)+(g/l)*x-1/2*Cd*A*p_air*r^2*(dx/dt)^2
f1 = @(t,x,y) y;
f2 = @(t,x,y) -c/(m*l.^2)*y-g/l*x-0.5*Cd*A*pa*R.^2*y.^2;
t(1) = 0;        %time start from 0S
x(1) = 0.0349;   %initial state angle = 0.0349rad/2 degree
y(1) = 0;        %initla velocity = 0
tfinal=10000;    %final time at 10000s

N=ceil((tfinal-t(1))/h);
for i = 1:N
t(i+1)=t(i)+h;
k1x = h*f1(t(i),x(i),y(i));
k1y = h*f2(t(i),x(i),y(i));

k2x = h*f1(t(i)+h/4,x(i)+k1x/4, y(i)+k1y/4);
k2y = h*f2(t(i)+h/4,x(i)+k1x/4, y(i)+k1y/4);

k3x = h*f1(t(i)+3/8*h,x(i)+3/32*k1x+9/32*k2x, y(i)+3/32*k1y+9/32*k2y);
k3y = h*f2(t(i)+3/8*h,x(i)+3/32*k1x+9/32*k2x, y(i)+3/32*k1y+9/32*k2y);

k4x = h*f1(t(i)+12/13*h,x(i)+1932/2197*k1x-7200/2197*k2x+7296/2197*k3x,
y(i)+1932/2197*k1y-7200/2197*k2y+7296/2197*k3y);
k4y = h*f2(t(i)+12/13*h,x(i)+1932/2197*k1x-7200/2197*k2x+7296/2197*k3x,
y(i)+1932/2197*k1y-7200/2197*k2y+7296/2197*k3y);

k5x = h*f1(t(i)+h, x(i)+439/216*k1x-8*k2x+3680/513*k3x-845/4104*k4x,
y(i)+439/216*k1y-8*k2y+3680/513*k3y-845/4104*k4y);
k5y = h*f2(t(i)+h, x(i)+439/216*k1x-8*k2x+3680/513*k3x-845/4104*k4x,
y(i)+439/216*k1y-8*k2y+3680/513*k3y-845/4104*k4y);
```

```
k6x = h*f1(t(i)+h/2, x(i)-8/27*k1x+2*k2x-3544/2565*k3x+1859/4104*k4x-11/40*k5x,
y(i)-8/27*k1y+2*k2y-3544/2565*k3y+1859/4104*k4y-11/40*k5y);
k6y = h*f2(t(i)+h/2, x(i)-8/27*k1x+2*k2x-3544/2565*k3x+1859/4104*k4x-11/40*k5x,
y(i)-8/27*k1y+2*k2y-3544/2565*k3y+1859/4104*k4y-11/40*k5y);

x(i+1)=x(i)+(16/135*k1x+0*k2x+6656/12825*k3x+28561/56430*k4x-
9/50*k5x+2/55*k6x);
y(i+1)=y(i)+(16/135*k1y+0*k2y+6656/12825*k3y+28561/56430*k4y-
9/50*k5y+2/55*k6y);
end
%find time t0 when amlpitude drops to 63.2% of 0.0349rad (0.022)
for i=2:N-1
   if x(i)>x(i+1) & x(i)> x(i-1)
      if x(i)-0.022<0.0002 || x(i)<0.022
         t0=i*h;
      break
      end
   end
end
% find period (T)
% we know 1s=100h and period = 2s/200h so we find the amplitude at
for i=(N-600):N-1
   if  x(i)>x(i+1) & x(i)> x(i-1)
      break
   end
end
T1=i*h;
for j=i+2:N-1
   if  x(j)>x(j+1) & x(j)> x(j-1)
      T2=j*h;
      break
   end
end
%period is the difference between the two highest point at the end
Per=T2-T1;
Quality = 1/2*(9.81/l).^0.5*t0;
%f=1/(2*pi*(l/g).^0.5);
disp('Quality Factor=');
disp(Quality);
```

Appendix C

MATLAB Code and Simulink Model for Chapter Four

C.1 MOO_INPUT

```
% This code intends to set MOO environment and input parameter too ModeFrontier
%<fmiModelDescription fmiVersion="2.1" modelName="MyScript" guid="">
   %<ModelVariables>
      %<Variable name="l" valueReference="0" causality="parameter">
         %<Real/>
      %</Variable>

      %<Variable name="R" valueReference="1" causality="parameter">
         %<Real/>
      %</Variable>

      %<Variable name="T" valueReference="2" causality="parameter">
         %<Real/>
      %</Variable>

      %<Variable name="o1" valueReference="3" causality="output">
         %<Real/>
      %</Variable>

      %<Variable name="o2" valueReference="4" causality="output">
         %<Real/>
      %</Variable>

      %<Variable name="o3" valueReference="5" causality="output">
         %<Real/>
      %</Variable>
 %</ModelVariables>

 %<ModelStructure>
      %<Outputs>
         %<Unknown index="3"/>
         %<Unknown index="4"/>
         %<Unknown index="5"/>
      %</Outputs>
   %</ModelStructure>
%</fmiModelDescription>
g = 9.81;
c = 0.0036;                 % damping force coefficient in n/rad/s
```

```
Cd = 1.6;                  % the drag coefficient of the pendulum system dimensionless
p = 1.225;                 % the density of air in kg/m^3
s  = pi*(0.022225/2)^2;        % the area of rod in m^2
P1 = 800;                  % the density of oak im kg/m^3
m1 = s*l*P1;                 % the mass of rod in kg
p2 = 7800;                 % the density of bob in kg/m^3
m2  = p2*pi*R.^2*T;            % the mass of bob in kg
m = m1+m2;                   % the mass of entire pendulum in kg
A1 =(l)*(0.02225);           % the area of rod in meter^2
A2 = 2*R*T;                % the are of bob in meter^2
A = A1+A2;                 % the total reference area of pendulum in meter^2

% Inputs and Declaration
h = 0.01; % solution stepsize
% Function declaration x=theta y=d(theta)/dt
% f1: dx/dt=y;
% f2: dy/dt=[-c/(ml^2)](dx/dt)+(g/l)*x-1/2*Cd*A*p_air*r^2*(dx/dt)^2
f1 = @(t,x,y) y;
f2 = @(t,x,y) -c/(m*l.^2)*y-g/l*x-(0.5*Cd*A*p*l.^2*y.^2)/(m*l);
t(1) = 0;       %time start from 0S
x(1) = 0.0349;   %initial state angle = 0.035
y(1) = 0;       %initla velocity = 0
tfinal=30000;      %final time at 30000s

N=ceil((tfinal-t(1))/h);
for i = 1:N
t(i+1)=t(i)+h;
k1x = h*f1(t(i),x(i),y(i));
k1y = h*f2(t(i),x(i),y(i));

k2x = h*f1(t(i)+h/4,x(i)+k1x/4, y(i)+k1y/4);
k2y = h*f2(t(i)+h/4,x(i)+k1x/4, y(i)+k1y/4);

k3x = h*f1(t(i)+3/8*h,x(i)+3/32*k1x+9/32*k2x, y(i)+3/32*k1y+9/32*k2y);
k3y = h*f2(t(i)+3/8*h,x(i)+3/32*k1x+9/32*k2x, y(i)+3/32*k1y+9/32*k2y);

k4x = h*f1(t(i)+12/13*h,x(i)+1932/2197*k1x-7200/2197*k2x+7296/2197*k3x,
y(i)+1932/2197*k1y-7200/2197*k2y+7296/2197*k3y);
k4y = h*f2(t(i)+12/13*h,x(i)+1932/2197*k1x-7200/2197*k2x+7296/2197*k3x,
y(i)+1932/2197*k1y-7200/2197*k2y+7296/2197*k3y);

k5x = h*f1(t(i)+h, x(i)+439/216*k1x-8*k2x+3680/513*k3x-845/4104*k4x,
y(i)+439/216*k1y-8*k2y+3680/513*k3y-845/4104*k4y);
```

```
k5y = h*f2(t(i)+h, x(i)+439/216*k1x-8*k2x+3680/513*k3x-845/4104*k4x,
y(i)+439/216*k1y-8*k2y+3680/513*k3y-845/4104*k4y);

k6x = h*f1(t(i)+h/2, x(i)-8/27*k1x+2*k2x-3544/2565*k3x+1859/4104*k4x-11/40*k5x,
y(i)-8/27*k1y+2*k2y-3544/2565*k3y+1859/4104*k4y-11/40*k5y);
k6y = h*f2(t(i)+h/2, x(i)-8/27*k1x+2*k2x-3544/2565*k3x+1859/4104*k4x-11/40*k5x,
y(i)-8/27*k1y+2*k2y-3544/2565*k3y+1859/4104*k4y-11/40*k5y);

x(i+1)=x(i)+(16/135*k1x+0*k2x+6656/12825*k3x+28561/56430*k4x-
9/50*k5x+2/55*k6x);
y(i+1)=y(i)+(16/135*k1y+0*k2y+6656/12825*k3y+28561/56430*k4y-
9/50*k5y+2/55*k6y);
end

for i=2:N-1
   if x(i)>x(i+1) && x(i)> x(i-1)
      if x(i)-0.0128<0.0002 || x(i)<0.0128
         t0=i*h;
      break
      end
   end
end
o1 = (pi.*R.^2.*T.*7800+3.8795e-04.*l.*800);  %objective function 1 for the weight
o2 = -(1/2*(9.81/l).^0.5*t0);                 %objective function 2 for the quality factor

Air_Resistance=0.5*Cd*A*p*l^2*l/(m*l^2)
dampcoef=0.0036
sim('Clock_Model',600)
for i=(size(simout.time)-6000):N-1
   if  simout.data(i)>simout.data(i+1) && simout.data(i)> simout.data(i-1)
      break
   end
end
T1=i*h;
for j=i+2:N-1
   if  simout.data(j)>simout.data(j+1) && simout.data(j)> simout.data(j-1)
      break
   end
end
T2=j*h;
Period=T2-T1;
o3 = abs(Period-2);             %objective function 3 for the period
```

C.1.1 Escapment Model
%This simulink model intends to simulating the swing behavior escapement of pendulum clock

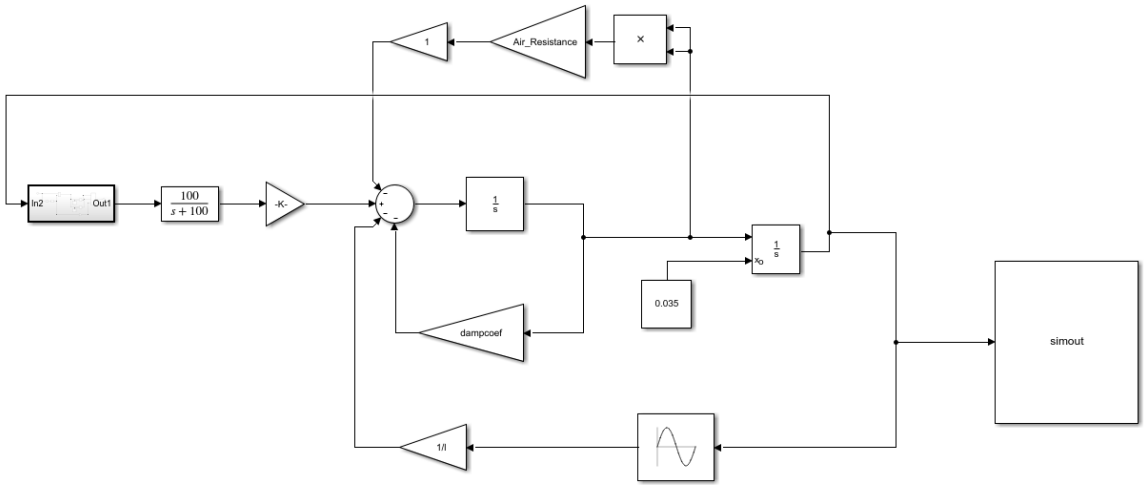

Figure C1: Simulink model of escapement

C.1.1.1 Impusive model
%This simulink model is a sub model of escapement model that intends to simulate the impulsive torque

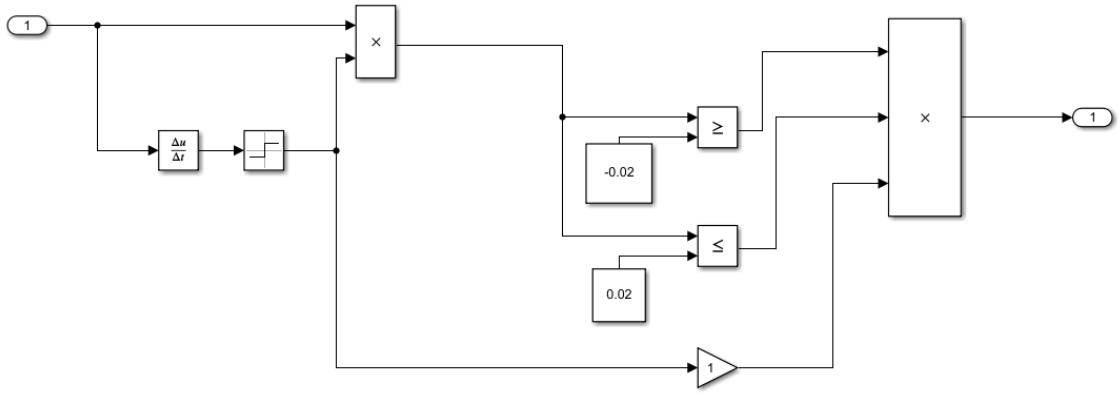

Figure C2: Simulink sub-model to simulate impulsive torque

C.2.1 Figure_1.3
%This code is used to created figure 1.3 with input data from measurement

```
clear all
load final_run2
ts=-.16;
interval=11.6+[0 2.25];
fs=13;
```

```
subplot(211),plot(t+ts,esc-1770,'m','linewidth',2)
set(gca,'fontsize',fs,'ytick',[-6:2:6],'xtick',11.1:.2:13.9)
fgg,xlim(interval+ts), ylim([-6 7])
xlabel('Time (sec)'), ylabel('Escape Wheel Angle (deg)')
subplot(212),plot(t+ts,pend,'--','linewidth',2)
hold on
subplot(212),plot(t+ts,-crutch-0.05,'linewidth',2)
hold off
set(gca,'fontsize',fs,'xtick',11.1:.2:13.9)
fgg,xlim(interval+ts),ylim([-2.2 2.2])
xlabel('Time (sec)'), ylabel('Pendulum and Crutch Angle (deg)')
```

B.2.2 MOO-result-analysis

```
%This code is used to created Figure 3.3 with MOO result as input
clear all;
Matrix = readmatrix('MOGA_Pareto.xls');
[m,n]=size(Matrix);
for i=1:m
   Mass = Matrix(i,8)
   Quality = Matrix(i,9)
   Period = Matrix(i,10)
   plot3 (Mass, Quality, Period, 'ro')
   hold on
end
plot3 (10.3155, -8783, 0 , 'b^','MarkerSize',15)
hold off
xlabel('Mass (kg)')
ylabel('-Quality Factor')
zlabel('Period Difference')
set(gca,'FontSize',20)
```

B.2.3 Tradespace_analysis

```
%This code is used to created Figure 3.4 with MOO Pareto Solutions as input
clear all
Matrix = readmatrix('MOGA_Pareto.xls');
price_iron=10.68;  % eur/kg
price_wood=14.24;   % eur/m^2
[m,n]=size(Matrix);
total_price=[];
total_utility=[];
density_iron=7800; % kg/m^3
Q_utility = [];
M_utility = [];
P_utility = [];
```

```
for i=1:m
   R=Matrix(i,5);
   T=Matrix(i,6);
   l=Matrix(i,7);
   mass_iron=pi*R^2*T*density_iron;
   price = mass_iron*price_iron+l*price_wood;
   total_price(end+1)=price;
   M=Matrix(i,8);
   Q=Matrix(i,9);
   P=Matrix(i,10);
   M_Utility = -0.035*M+1.175;
   Q_Utility = -Q/25000+0.125;
   P_Utility = -5*P+1;

   Q_utility(end+1) =  Q_Utility;
   M_utility(end+1) =  M_Utility;
   P_utility(end+1) =  P_Utility;
   M_Weight = 0.3;
   Q_Weight  = 0.6;
   P_Weight  = 0.1;
   Utility =  M_Utility * M_Weight + Q_Utility *  Q_Weight + P_Utility * P_Weight;
   total_utility(end+1) = Utility;
   scatter (price,Utility)
   hold on
end

hold off
ylabel('Utility')
xlabel('Cost (Euros)')
set(gca,'FontSize',20)
```

B.2.3.1 Tradespace_analysis_Pareto_Solution

```
%This code is used to created Figure 3.5 with tradespace result as input
for iter = 1:1162
   temp = [];
   for iter2=1:1162
      if total_utility(iter)< total_utility(iter2)
         temp(end+1)=iter2;
      end
   end
   [m,n]=size(temp);
   temp2=1;
   while temp2<=n
      if  total_price(iter)>=total_price(temp(temp2))
```

```
            break
        elseif total_price(iter) < total_price(temp(temp2))
            temp2=temp2+1;
        end
    end
    if temp2>n
        scatter(total_price(iter),total_utility(iter))
    end
    hold on
end

Original_Utility = (10.3155*-0.035+1.175)*0.3+(8783/25000+0.125)*0.6+0.1;
Original_Cost = 10.3155*10.68+0.994*14.24
plot (Original_Cost, Original_Utility ,'b^', 'MarkerSize',15)
hold off
ylabel('Utility')
xlabel('Cost (Euros)')
set(gca,'FontSize',20)
```

Appendix D

Photos of Experimental Activities

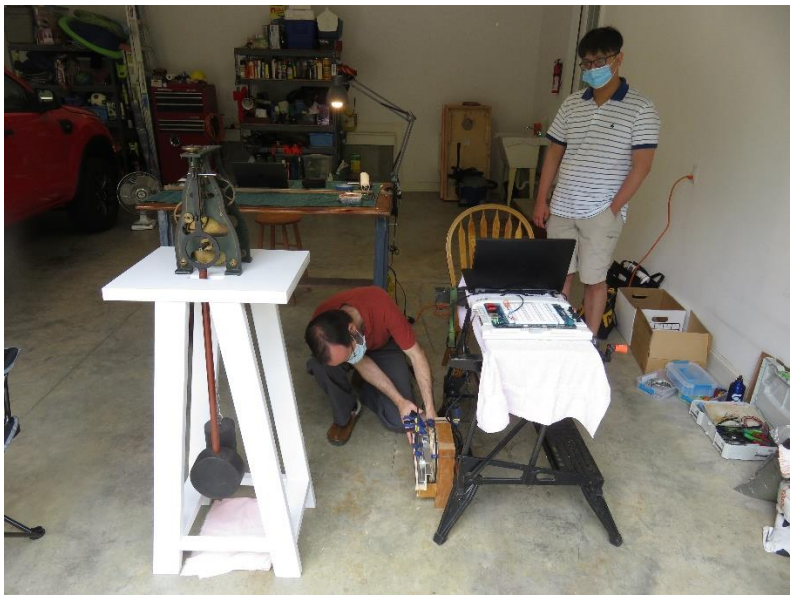

Figure D1: Overview of the experimental site (garage) and equipment

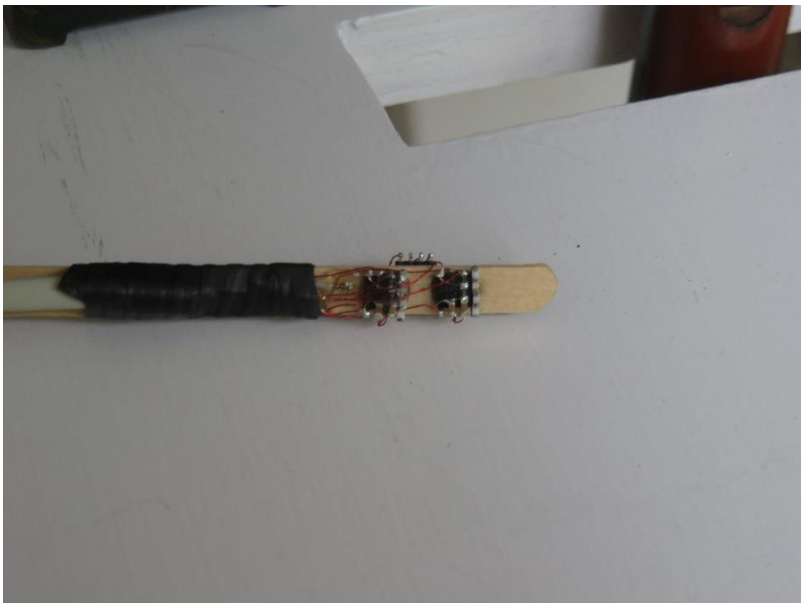

Figure D2: Magnetic sensors and amplifier attached on both sides of a wood stick

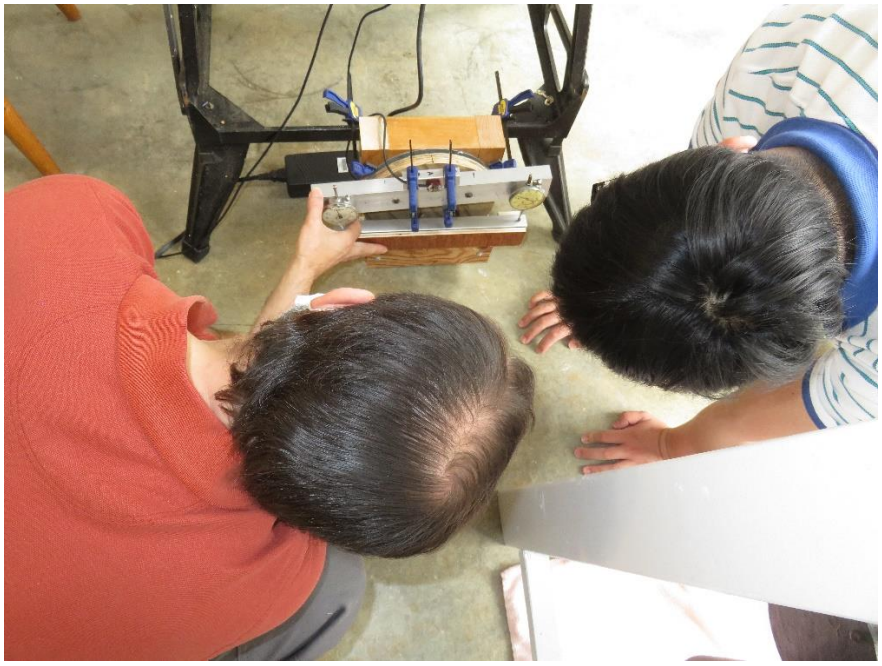

Figure D3: Experimenters are calibrating the substrate of the pendulum clock to ensure it is a horizontal plane

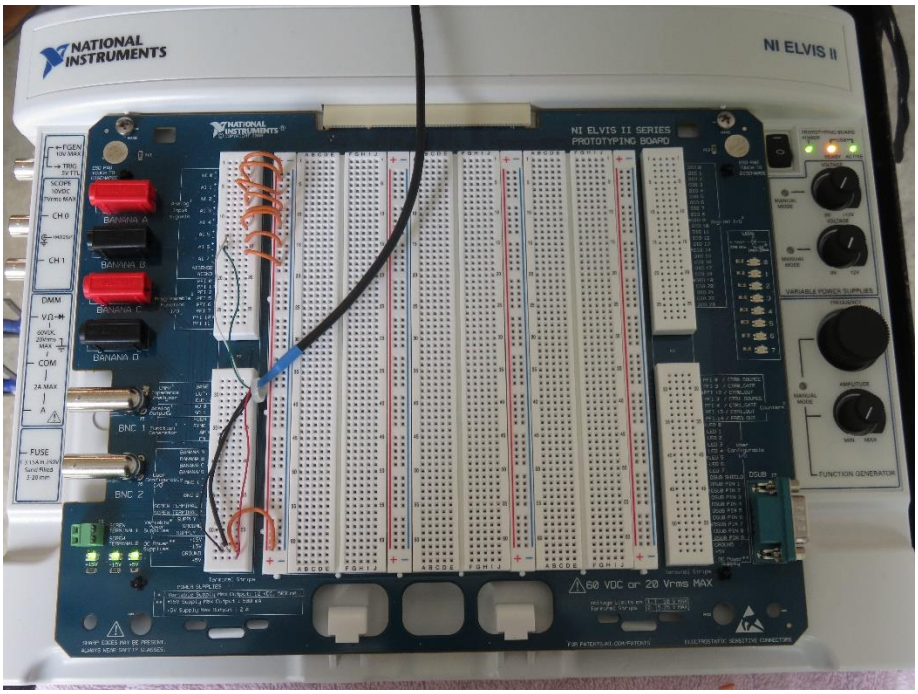

Figure D4: National Instrument ELVIS™ data acquisition system

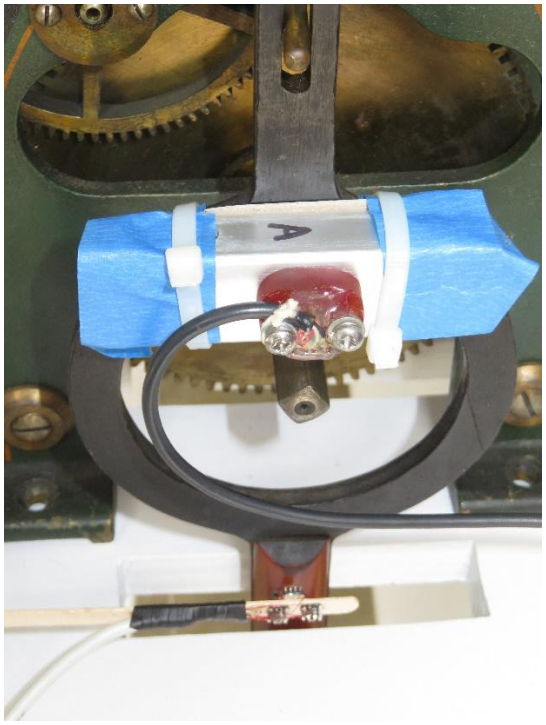

Figure D.5: Experimental setup of Quality Factor measuring

Figure D.6: Real-time processing of measured data

Appendix E

Supplemental Experimental Results

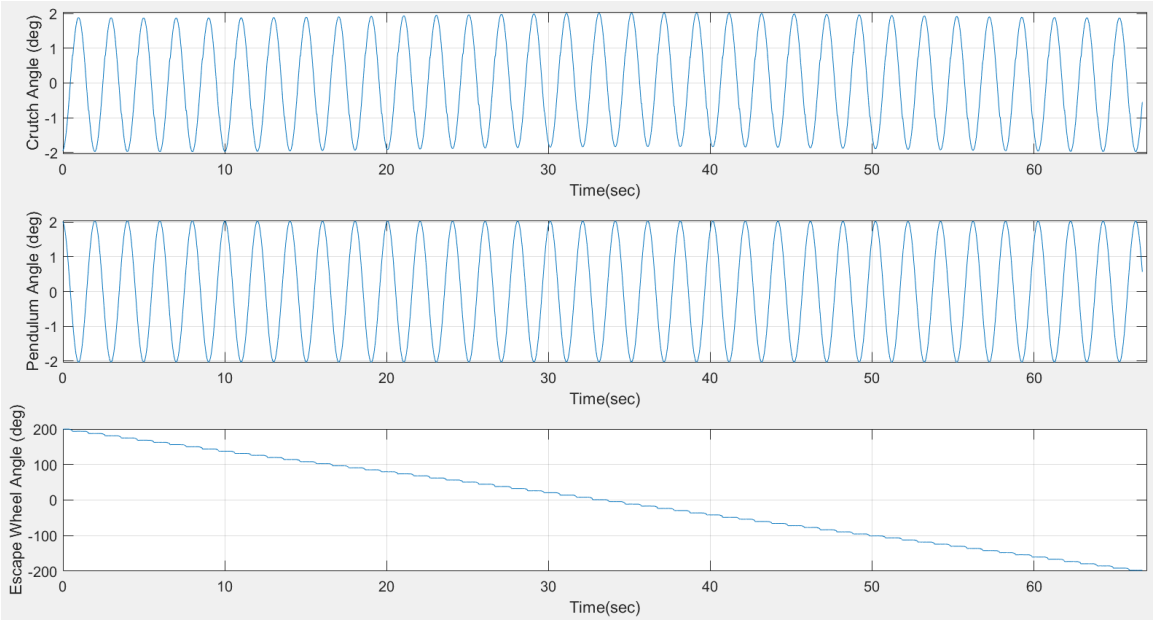

Figure E.1: Full experimental data collected on the E. Howard Model 00 for angles of Crutch (top) Pendulum (middle) and Escape Wheel (bottom), versus time

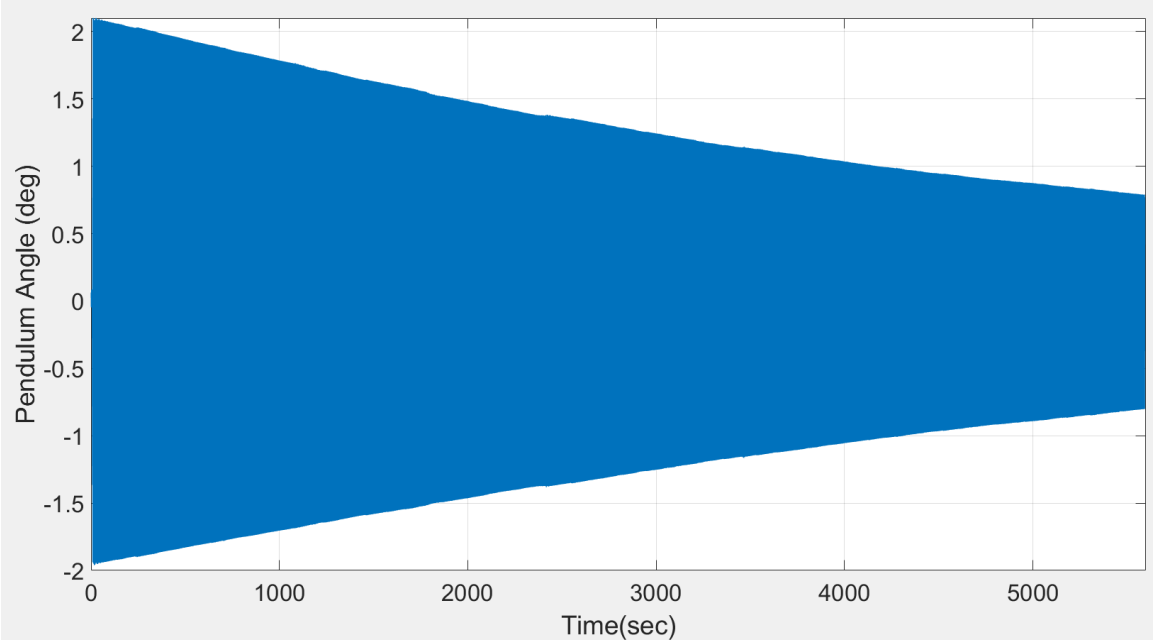

Figure E.2 : Full experimental data for Quality Factor determination by free response of clock pendulum;

Appendix F

Supplemental Computer-Aided-Design Models of Pendulum Components*

*All dimensions were labeled in inch

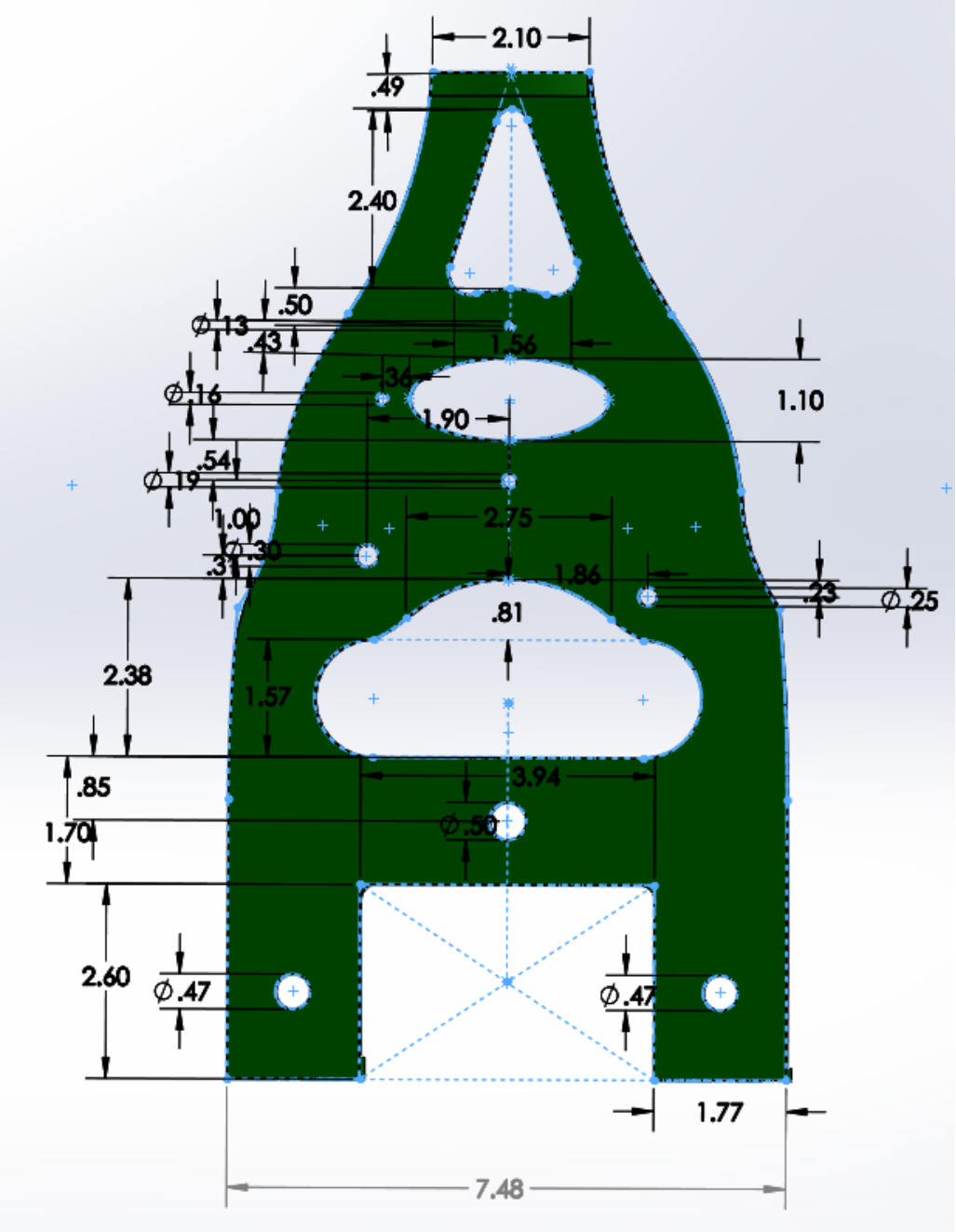

Figure F.1: Computer-aided-design model with dimensions for support frame of E. Howard Model 00 Movement

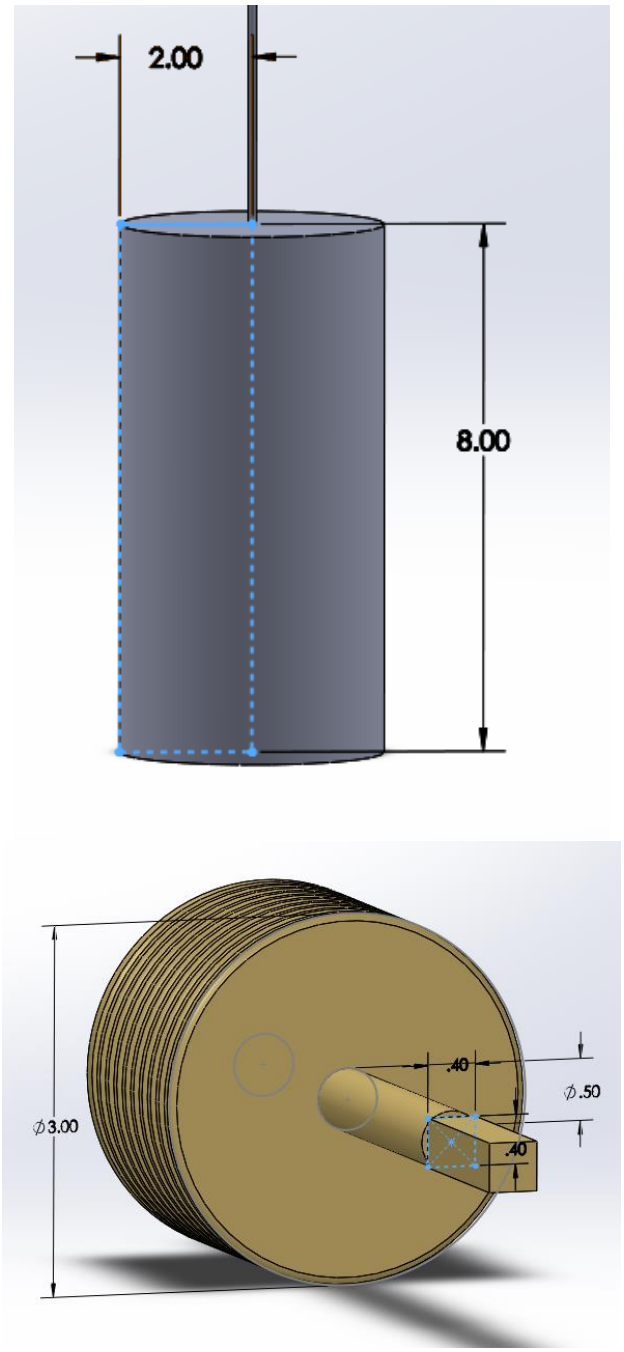

Figure F.2: Computer-aided-design model with dimensions for hanging weight (top) and arbor 1 (bottom) of E. Howard Model 00 Movement

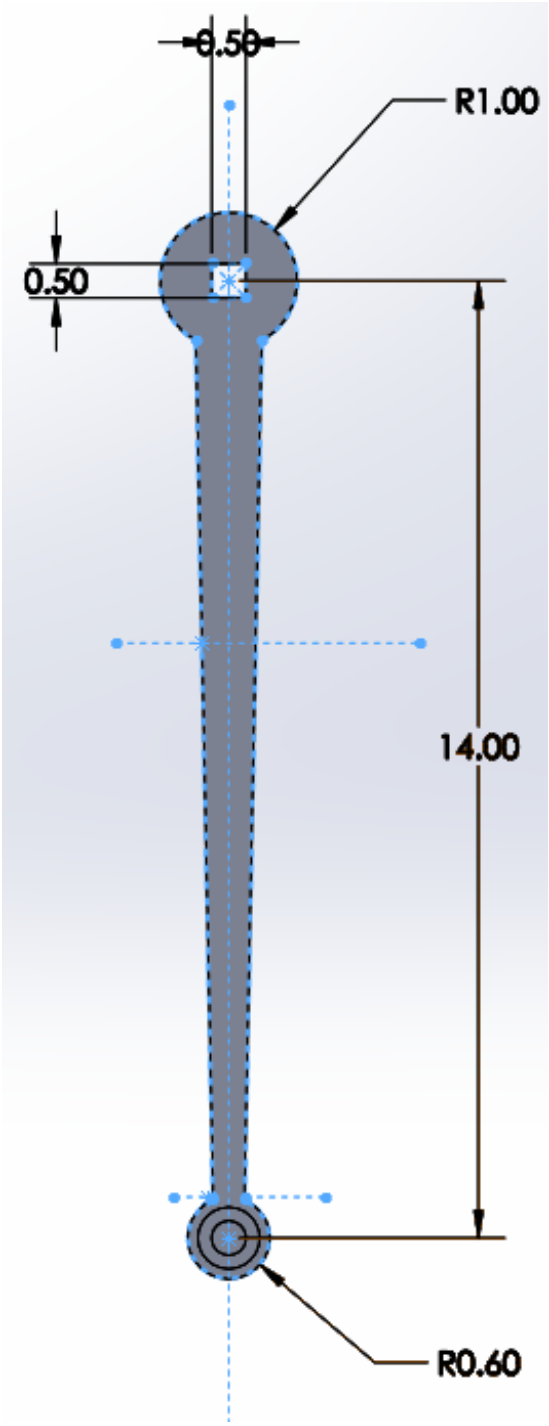

Figure F.3: Computer-aided-design model with dimensions for crutch of E. Howard Model 00 Movement

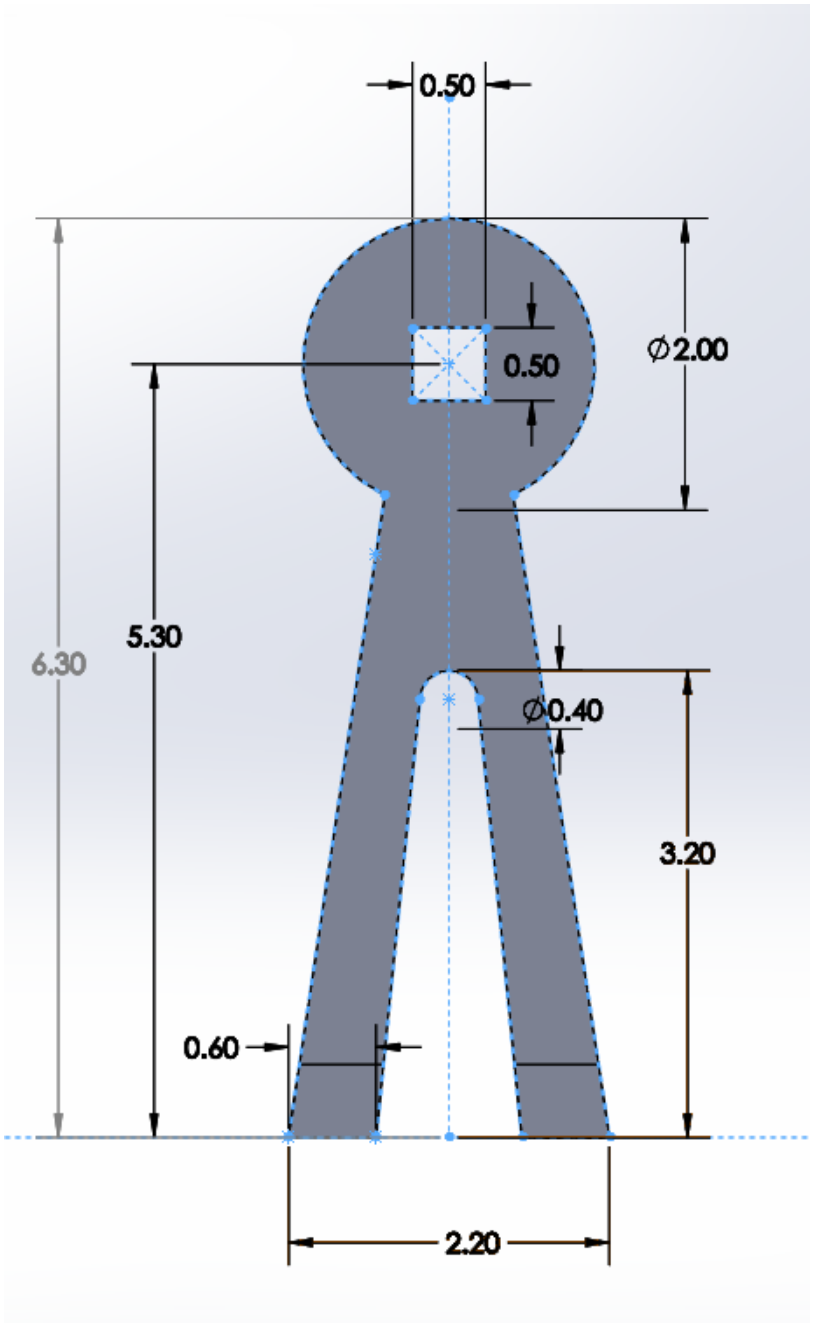

Figure F.4: Computer-aided-design model with dimensions for crutch support of E. Howard Model 00 Movement

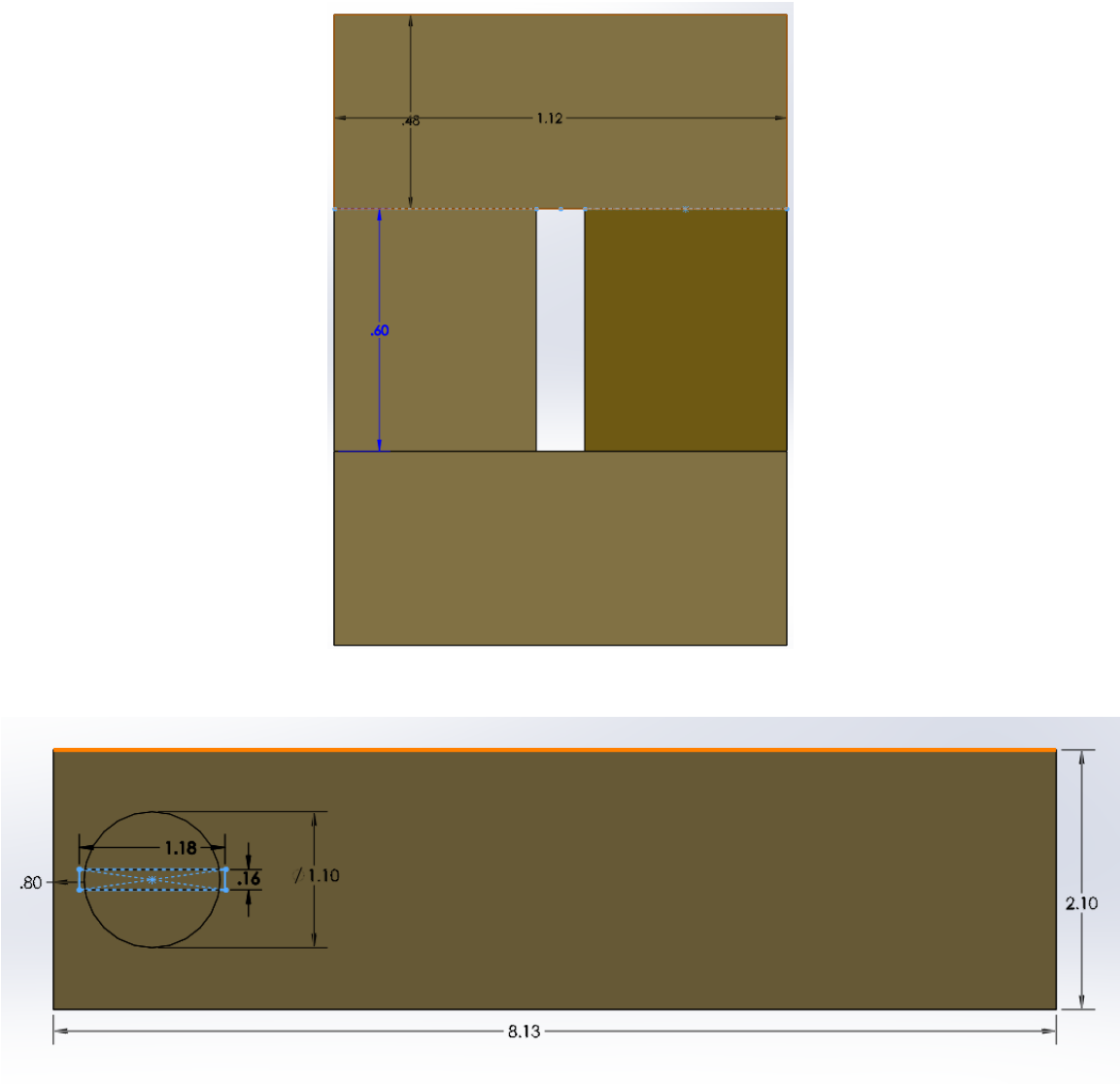

Figure F.5: Computer-aided-design model with dimensions for suspension spring (top) and top plate (bottom) of E. Howard Model 00 Movement

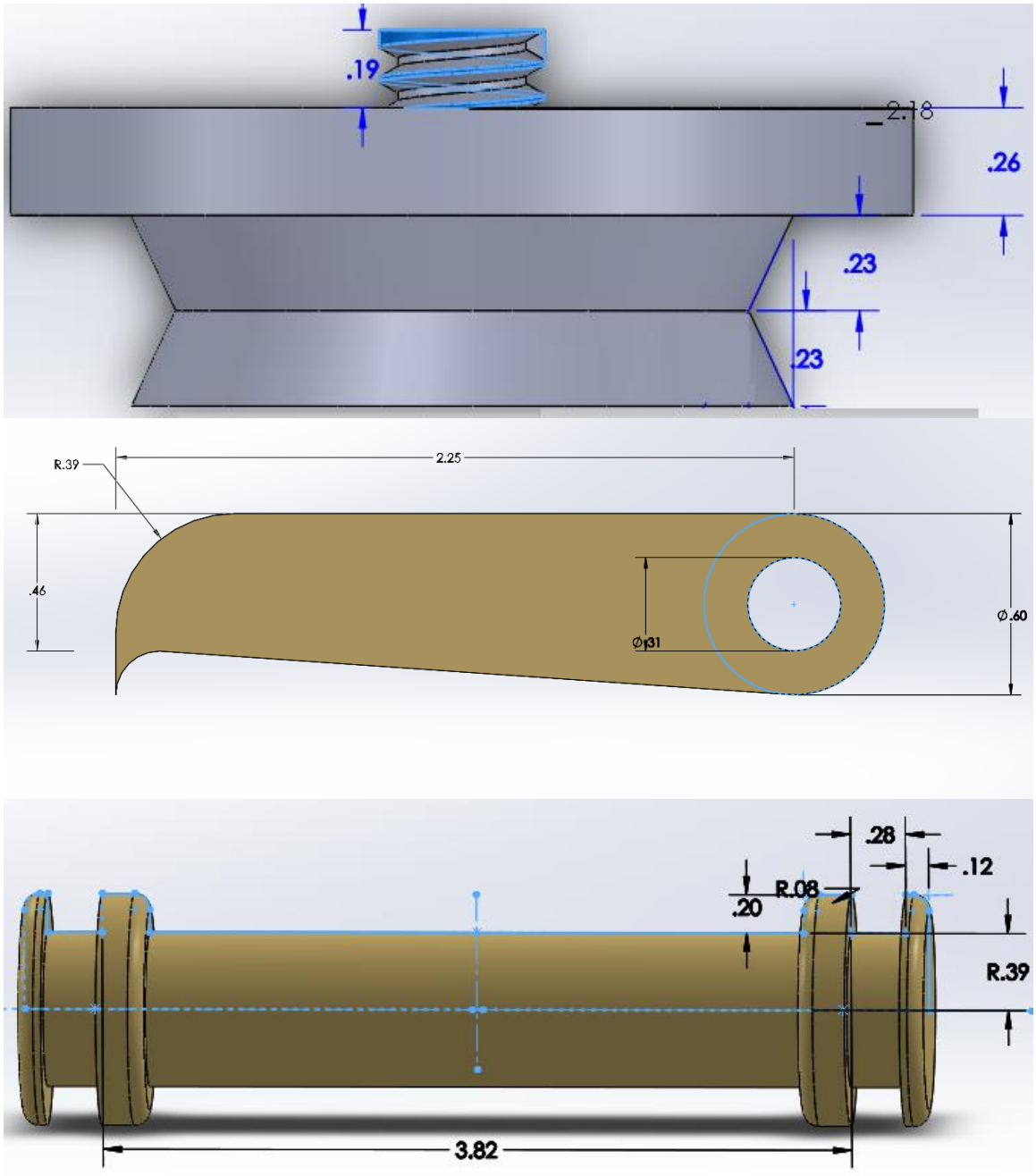

Figure F.6: Computer-aided-design model with dimensions for top bolt (top) pawl (middle) and support bolt (bottom) of E. Howard Model 00 Movement

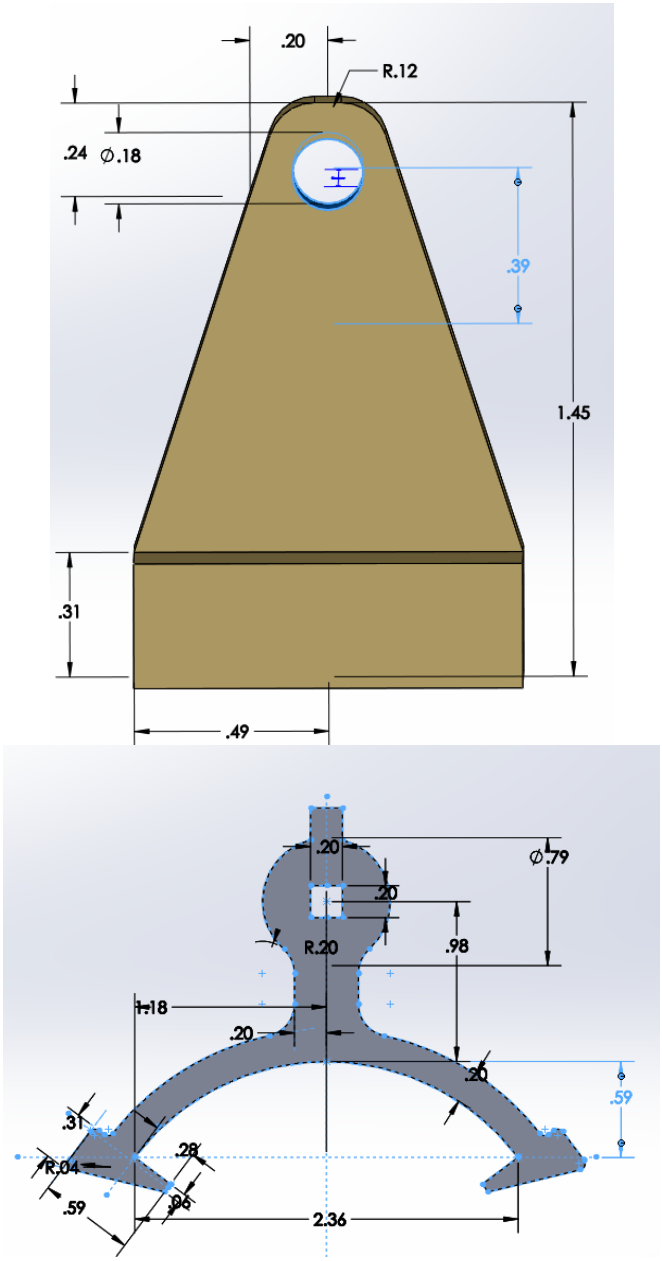

Figure F.7: Computer-aided-design model with dimensions for suspension knob (top) and verge (bottom) of E. Howard Model 00 Movement

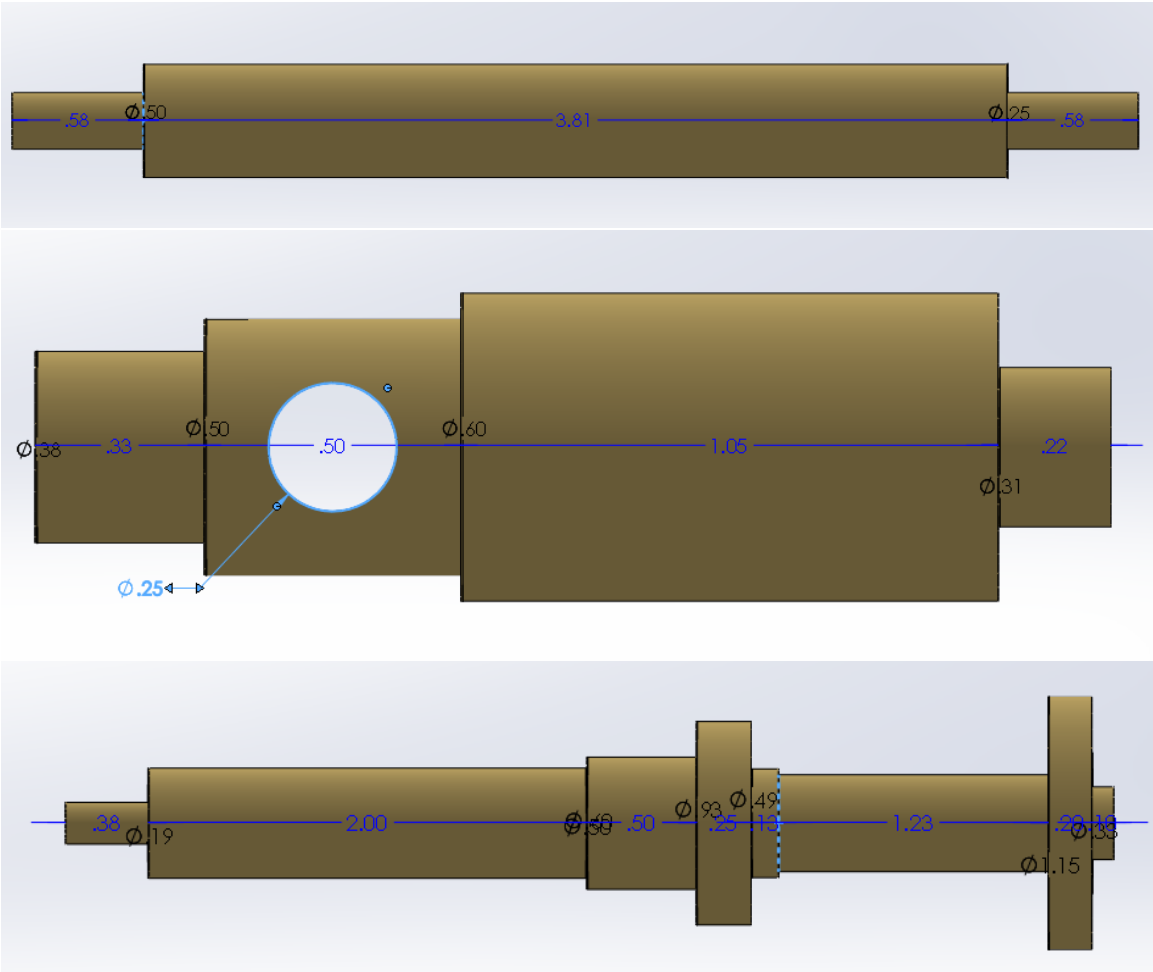

Figure F.8: Computer-aided-design model with dimensions for arbors: B (top), C (middle) and D (bottom) of E. Howard Model 00 Movement

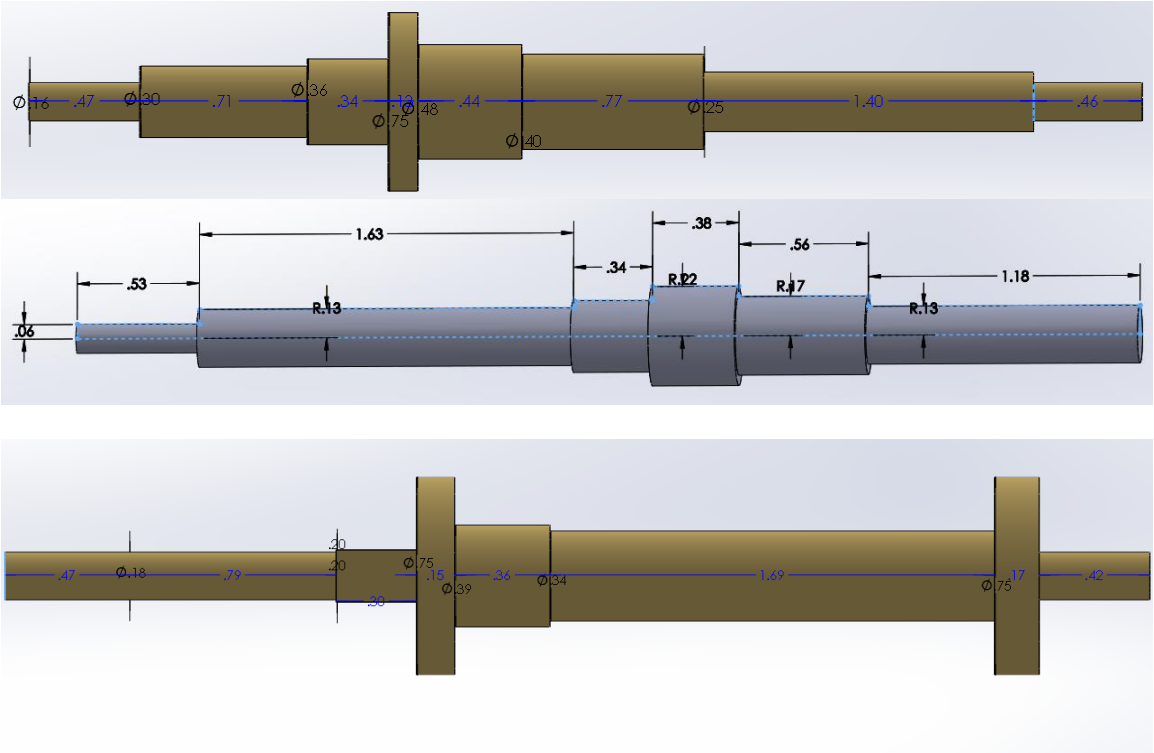

Figure F.9: Computer-aided-design model with dimensions for arbors: E (top), F (middle), Escapement (bottom) of E. Howard Model 00 Movement

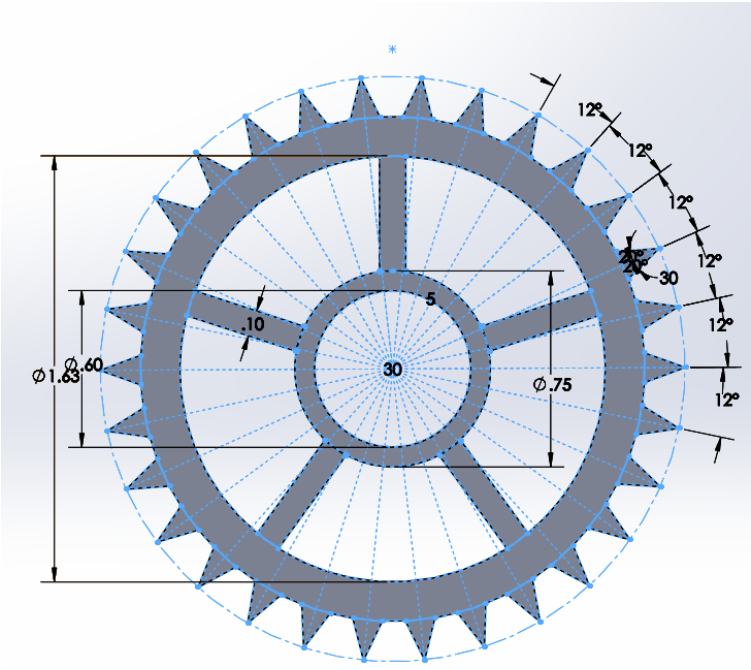

Figure F.10: Computer-aided-design model with dimensions for escape wheel of E. Howard Model 00 Movement

Appendix G

Tradespace Analysis Results for Other Design Aspects

This appendix contains the supplement tradespace results for chapter 4.4.5

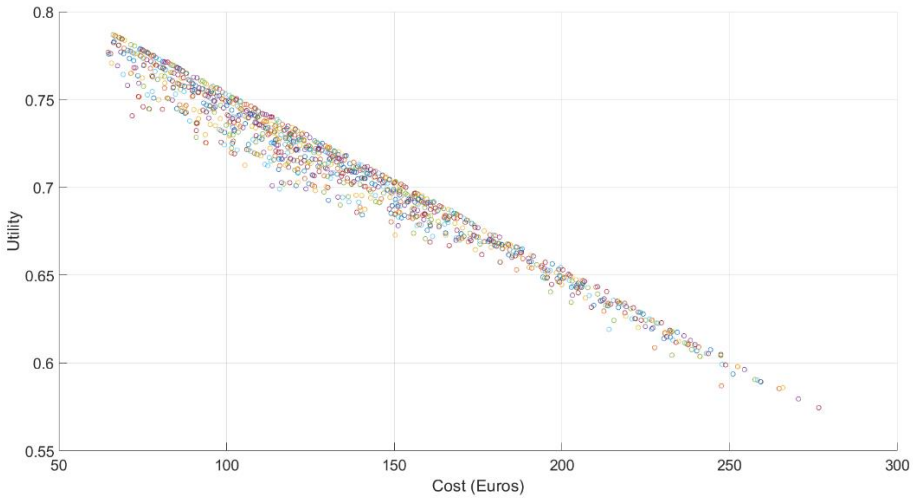

(a)

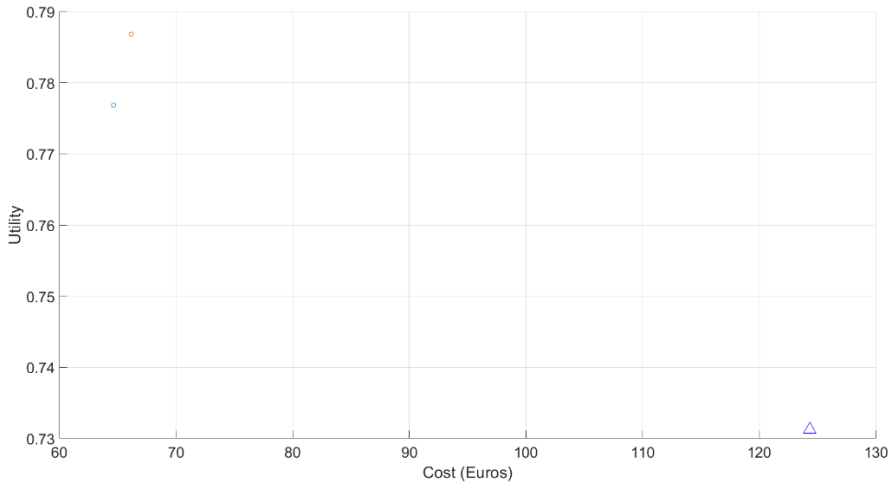

(b)

Figure G.1: (a) Tradespace analysis result for smaller mass Design Aspect, and (b) Selected optimal designs with original E. Howard design shown in the Δ symbol.

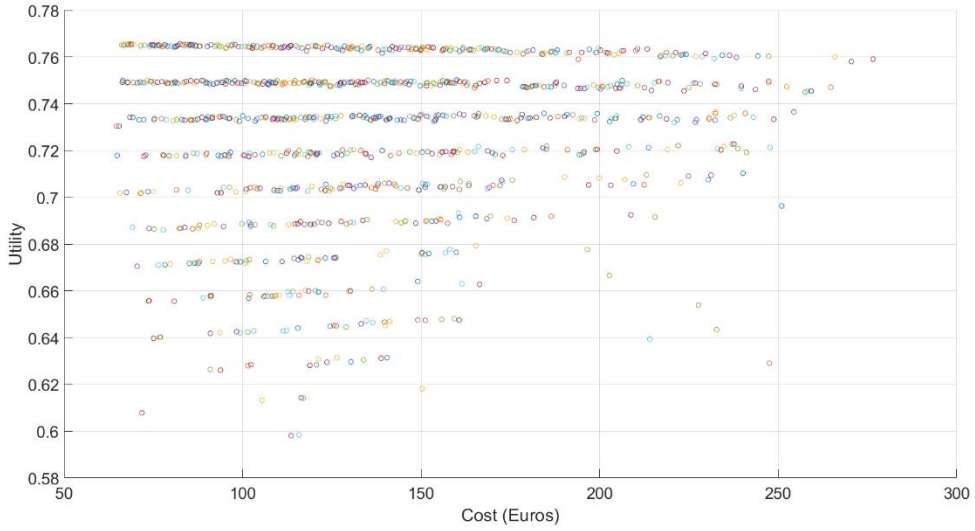

(a)

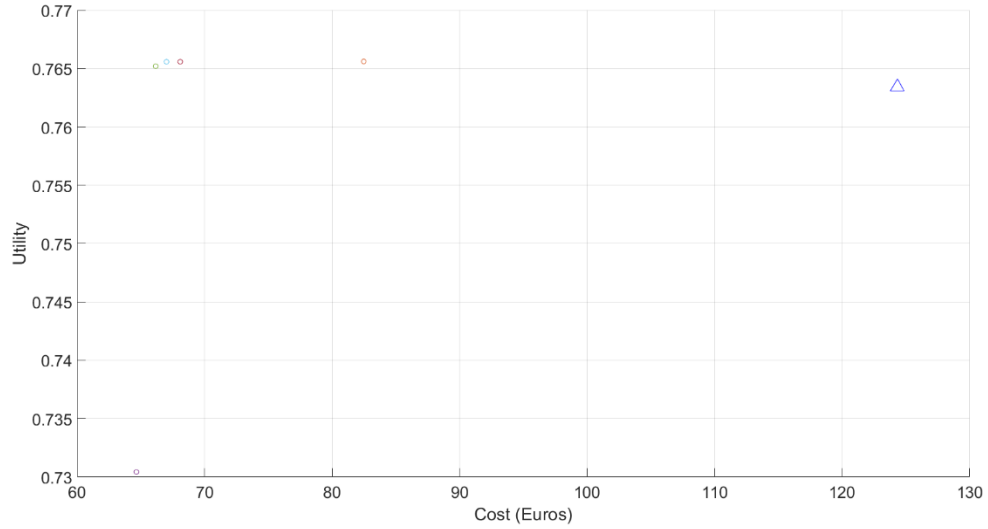

(b)

Figure G.2: (a) Tradespace analysis result for nominal Design Aspect, and (b) Selected optimal designs with original E. Howard design shown in the Δ symbol.

REFERENCES

Amine, K., 2019, "Multi-objective Simulated Annealing: Principles and Algorithm Variants," *Advances in Operations Research* 2019. DOI:10.1155/2019/8134674

Baldick, R., 2009, *Applied Optimization: Formulation and Algorithms for Engineering Systems*, Cambridge, England: Cambridge University Press, ISBN: 9781107394087

Baker, G., and Blackburn, J., 2008, *The pendulum: a case study in physics*, OUP Oxford, ISBN: 9780198567547

Bartky. Ian., 1989, "Railroad Timekeepers," *NAWCC Bulletin*, 31(262), pp. 399-411.

Bernstein, D., 2002, "Feedback control: an invisible thread in the history of technology". *IEEE Control systems magazine*, *22*(2), pp. 53-68. DOI: 10.1109/37.993315

Burke, E. K., and Kendell G., 2014, *Search Methodologies,* Springer, Chap. 15 ISBN: 9781461469391.

Denny, M., 2002, "The Pendulum Clock: A Venerable Dynamical System", *European Journal of Physics*, 23, pp. 449-458. DOI:10.1088/0143-0807/23/4/309.

E. Howard Watch and Clock Company., 1890 "Catalog and Descriptions of Tower Clocks" Boston, MA.

Feinstein, G., 2006, "Impulsing the Pendulum: Escapement Error," *NAWCC Horological Science* 161(3) pp. 569-575.

Geletu, A., 2007 "Solving Optimization Problems using the Matlab Optimization Toolbox-A Tutorial," TU-Ilmenau, Fakultät für Mathematik und Naturwissenschaften. https://www.researchgate.net/publication/255586170_Solving_Optimization_Problems_using_the_Matlab_Optimization_Toolbox_-_a_Tutori

Haik, Y., and Shahin, T., 2015, *Engineering design process*, Cengage Learning, ISBN: 9780495668145

Hatch, M., Ron., E., Bouville, A., Zablotska, L., and Howe, G., 2005, “The Chernobyl Disaster: Cancer following the Accident at the Chernobyl Nuclear Power Plant”, *Epidemiologic reviews*, 27, pp. 56-66. DOI: 10.1093/epirev/mxi012

Hua, C., 2016, *e-Design: computer-aided engineering design.* Academic Press ISBN: 9780123820389

Ly. T., 1995, *American Clocks Volume 2,* Austin, TX: Arlington Book Company. ISBN: 9780930163440

Kirkpatrick, S., Gelatt Jr, C., and Vecchi, M., 1983, "Optimization by simulated annealing," *Science*, 220(4598), pp. 671-680. DOI: 10.1126/science.220.4598.671

Kesteven, M., 1978, "On the mathematical theory of clock escapements," *American Journal of Physics*, *46*(2), pp. 125-129. DOI: 10.1119/1.11369

Konak, A., Coit, D. W., and Smith, A. E., 2006, "Multi-objective Optimization Using Genetic Algorithms: A Tutorial," *Reliability Engineering and System safety*, 91 pp. 992-1007. DOI:10.1016/j.ress.2005.11.018

Marini. R., 2019, "San Antonio's 140-year-old Hertzberg Clock Gets a Makeover," San Antonio Express-News.

Martins, J., and Ning, A., 2021, *Engineering design optimization,* Cambridge University Press. ISBN: 9780495668145

Matthews, M., 2000, *Time for science education: How teaching the history and philosophy of pendulum motion can contribute to science literacy,* Springer Science & Business Media, ISBN: 9780306458804

Matthys, R., 2004 *Accurate Clock Pendulums,* Oxford, Great British: Oxford University, ISBN: 0198529716

Middents. P., 2014, "Howard Tower Clock Model Numbers," *Tower Talk,* 134(20).

Nagourney, T., Cho, J., Shiari, B., Darvishian, A., and Najafi, K., 2017, "259 second ring-down time and 4.45 million quality factor in 5.5 kHz fused silica birdbath shell resonator" *19th International Conference on Solid-State Sensors, Actuators and Microsystems (TRANSDUCERS)* pp. 790-793. DOI: 10.1109/TRANSDUCERS.2017.7994167

Nawrodt, R., et al., 2008, "High Mechanical Q-factor Measurements on Silicon Bulk Samples," J. Phys.: Conf. Ser. 122 012008. DOI:10.1088/1742-6596/122/1/012008

Nawrod, R., Zimmer, A., Nietzsche, S.,Thurk, M., Vodel, W., and Seidel, P., 2006 "A New Apparatus for Mechanical Q-Factor Measurements Between 5 and 300 K", *Cryogenics*, 46, pp. 718-723. DOI:10.1016/j.cryogenics.2006.06.001

Ngatchou, P., Zarei, A., and El-Sharkawi, M. A., 2005 "Pareto Multi Objective Optimization," *Proceeding of the 13th International Conference.* 6-10 pp. 84-91. DOI: 10.1109/ISAP.2005.1599245

Pahl, G., Beitz, W., Feldhusen, J and Grote, K., 2007, *Engineering design: a systematic approach*, London, England: Springer London, ISBN:9781846283185

Palm III. W., 2007, *Mechanical Vibration,* Hoboken, NJ: John Wiley & Sons. ISBN: 9780471345558

Penman, L., *Practical Clock Escapements,* Vitoria, Spain: Mayfield Books, 2002. ISBN: 9780952327042

Poles, S., 2003, "MOGA-II: An improved Multi-objective Genetic Algorithm, "Technical Report No. 2003-006 Esteco, Trieste.

Rawlings. A., 1993, *The Science of Clocks & Watches*, Upton, England: British Horological Institute. ISBN: 9780950962139

Rigoni, E., 2003, "MOSA Multi Objective Simulated Annealing" Technical Report No. 2003-003 Esteco, Trieste.

Ross, A. M., and Hasting. D, E., 2005, "The Tradespace Exploration Paradigm," In *INCOSE International Symposium* 15(1) pp. 1706-1718. DOI:10.1002/j.2334-5837.2005.tb00783.x

Schwartz, C., and Gran, R., 2001, "Describing function analysis using MATLAB and Simulink," *IEEE Control Systems Magazine*, 21(4), pp. 19-26. DOI: 10.1109/37.939940

Shaw. R., 2016 "E. Howard Tower Clock Restoration," *NAWCC Watch & Clock Bulletin*, 58(420), pp. 161-163.

Shelley, F., 1999, *Early American Tower Clocks: Surviving American Tower Clocks from 1726 to 1870,* Lathrop. D., eds., Columbia, PA: National Association of Watch & Clock. Collectors ISBN: 9780966886900

Spero, E., Avera, M., Valdez P., and Goerger, S., 2014, "Tradespace Exploration for the Engineering of Resilient Systems," *Procedia Computer Science* 28 pp 591-600. DOI:10.1016/j.procs.2014.03.072

Van Laarhoven, P., and Aarts, E., 1987, *Simulated annealing. In Simulated annealing: Theory and applications*, Springer, Dordrecht. ISBN: 978-9027725134

Wagner, J., Huey, C., and Knaub, K., 2008, "Clock Mechanism Fundamentals for Education: Modeling and Analysis, "*ASME Dynamics Systems and Control Conference*, pp. 1-8. DOI:10.1115/DSCC2008-2100

Wagner, J., Knaub, H. K., Volk, E., and Jagarwal, A., 2010, "Modeling and Analysis of a Weight Driven Mechanical Tower Clock," *American Control Conference*, pp. 634–639. DOI: 10.1109/ACC.2010.5531093

Wang, Y., Li, Y., Zhang, D., and Xie, Y., 2021, "Aerodynamic optimization of a SCO2 radial-inflow turbine based on an improved simulated annealing algorithm," *Proceedings of the Institution of Mechanical Engineers, Part A: Journal of Power and Energy*," 235(5), pp. 1039-1052. DOI:10.1177/0957650920976666

Whiley, D., 1994, "A genetic Algorithm Tutorial," *Statistics and Computing* 4 pp. 65-85. DOI:10.1007/BF00175354